How neuronal SKN-1B acts to control appetite in *C. elegans*

-

James Evans

Master of Research: Genetics

Submitted for examination:

07.10.2021

Abstract

The number of people suffering from obesity and its related complications (cancer; cardiovascular disease; type II diabetes) are increasing worldwide, leading to consequences in health, with an increased financial cost for managing these pathologies. Better understanding of food-related behaviours at the cellular and molecular level is needed to uncover potential treatments for pathological eating to halt these related complications. The nematode worm *Caenorhabditis elegans* is a suitable model for study, as it has food-related behaviours similar to mammals, is quick and cheap to use, genetically tractable, has a completely mapped nervous system, and with~75% of its genes homologous to humans, it overall offers advantages other model organisms do not.

SKN-1 is a transcription factor in *C. elegans*, homologous to human Nrf. Recently, the neuronal SKN-1 isoform, SKN-1B, which is expressed in the sensory ASI neurons, akin to the hypothalamus, has been shown to have a role in food-related exploratory behaviour, i.e. looking for food, eating and stopping food intake, similar to aspects of appetite control in humans. Yet, many aspects of SKN-1B functionality were still unknown, and so three areas were investigated.

1) It was unknown how SKN-1B signals from ASI neurons to the nervous system, but through using neurotransmitter mutants, it revealed tyramine, released from RIM moto/interneurons, is likely part of the neural circuit needed for SKN-1B food-related exploration behaviour.

2) *C. elegans* have both hermaphrodite and male sexes, but it was unknown if there were sex-specific differences in SKN-1B functionality. Using male *skn-1b* mutants and microscopy, it was found unlike hermaphrodites, male adults did not need SKN-1B for food-related exploration. However, males still expressed SKN-1B in ASI neurons, but also had male-specific expression of SKN-1B in the VA11 motoneuron, indicating SKN-1B has yet unexplored roles in the male.

3) Genes needed for SKN-1B-related exploration behaviour was unknown, and so an RNAi screen with the genes upregulated and downregulated in a *skn-1b* mutant was performed to understand if any of these genes contributed to SKN-1B-related exploration. The screen revealed no obvious

exploratory function, yet bioinformatic analysis of these genes indicated SKN-1B may have roles outside of food-related exploration e.g. immunity.

Overall, SKN-1B needs tyramine for food-related exploration, whilst adult male exploration does not need SKN-1B, yet what genes contribute to SKN-1B-related exploration is still unclear. As SKN-1B is conserved in humans, further investigation of Nrfs in the mammalian brain may give insight into the regulation of eating behaviours in mammals and offer a potential drug target for eating pathologies.

Contents Page

Abbreviations

Abbreviation	Full name	Description
5-HT	Serotonin	Biogenic neurotransmitter
C. elegans	*Caenorhabditis elegans*	Nematode worm model organism
CeNGEN	*Caenorhabditis elegans* Neuronal Gene Expression Network	*C. elegans* single cell RNA-Seq (scRNA-Seq) nervous system project
DCVs	Dense core vesicles	Vesicles that package neuropeptides and biogenic amines
D1	Day 1 adult	
DA	Dopamine	Biogenic neurotransmitter
Egl	Egg laying defective	Reduced egg laying phenotype in *C. elegans*
FDR	False discovery rate	
IIS	Insulin/IGF-1 signalling	Insulin signalling pathway in *C. elegans*
GI	Gastro-intestinal	
LB	Luria Broth	
modENCODE	model organism ENCyclopedia Of DNA Elements	Database that includes binding site data of transcription factors
N2	N2 CGCM or wild-type/WT	Bristol *C. elegans* strain used as a wild-type control
NPY/AgRP	Neuropeptide Y/agouti-related protein (NPY/AgRP)	Released from neurons that stimulate food seeking in mammals
O.N.	Overnight	
OA	Octopamine	Biogenic neurotransmitter
POMC	Pro-opiomelanocortin	Released from neurons that reduce eating in mammals
ROS	Radical oxygen species	
SIQ	Satiety-induced quiescence	A sleep state induced after eating food when previously starved in *C. elegans*
skn-1	*skinhead-1*	Gene
TA	Tyramine	Biogenic neurotransmitter
TPR	True positive rate	
Unc	Uncoordinated	Reduced movement phenotype in *C. elegans*
UPR^{ER}	ER-mediated unfolded protein response	
UPR^{mt}	Mitochondrial-mediated unfolded protein response	
VA	Ventral-A	Type of motoneuron

Introduction

Obesity and pathological eating behaviours

A third of the world is classed as overweight, with >85% of American adults projected to be overweight or obese by 2030, alongside increasing overweight or obesity rates in China, Europe, and Mexico. Obesity increases risk of disease e.g. type 2 diabetes; cardiovascular disease and cancer, with obese children at increased risk in adulthood [1]. Therefore, obesity needs effective management and treatment at all ages. Understanding the biological regulation of eating behaviour may help uncover potential treatments for pathological eating e.g. overeating but also undereating in disorders such as anorexia nervosa.

Hunger initiates eating, with satiety being the feeling of fullness whilst eating and knowing when to stop eating, therefore controlling meal size. This behaviour is repeated as satiation signals decrease and hunger signals increase [2, 3]. In mammals, this behaviour is controlled by the gastro-intestinal (GI) tract and adipose signalling, which are integrated to control feeding behaviours via the hypothalamus [4]. The arcuate nucleus of the hypothalamus has two distinct neurons that control eating behaviour: neuropeptide Y/agouti-related protein (NPY/AgRP)-expressing neurons and pro-opiomelanocortin (POMC)-expressing neurons [5]. These sets of neurons are co-ordinated via a complex signalling network of neurotransmitters and hormonal neuropeptides.

NPY/AgRP-expressing neurons are activated under energy deficit (e.g. sensing increased ghrelin from the GI tract [6]), releasing the neuropeptide NPY/AgRP and neurotransmitter GABA to stimulate food seeking and increase eating [5]. Only NPY is needed to sustain hunger whilst eating, not AgRP or GABA [7]. Opposingly, POMC-expressing neurons are activated by sensing increased levels of the hormones insulin and/or leptin [8] in energy surplus [5], causing POMC release to reduce eating. When either POMC or NPY/AgRP-expressing neurons are activated, the opposing neuron is inhibited i.e. NPY/AgRP-expressing neurons inhibit POMC-expressing neurons, but AgRP-expressing neurons are inhibited upon seeing and/or smelling [9] food, allowing POMC-expressing neurons to be active and

reduce eating [8, 10]. These neurons can bind to various non-brain proteins in the circulation due to lack of blood brain barrier [6], allowing real-time monitoring of hormone and nutrient concentration (and food availability) to adjust to changes in nutritional state [5]. Lesions (in rats) destroying NPY/AgRP-expressing neurons or POMC-expressing neurons cause overeating or undereating, respectively [11], with insulin or leptin deficiencies cause overeating, as they can no longer activate POMC-expressing neurons to supress eating [8]. In addition, tanycytes (glial-like cells) found in the 3rd ventricle of the brain within the hypothalamus have also been shown to control weight and energy balance [12], including triggering acute overeating via the arcuate neuronal network [13].

The nematode *Caenorhabditis elegans* (*C. elegans*) is a good model to study eating behaviour

From the literature in mammals, it is clear a wide variety of sensory (sight and smell) and metabolic (adipose and GI) signalling pathways integrate and communicate to the hypothalamus of the brain which uses neurotransmitters and neuropeptides to control food-related behaviours. Studying these mammalian behaviours in cellular and molecular detail is complex, so a cheaper, quicker, and more genetically tractable organism is needed.

The nematode worm, *Caenorhabditis elegans* (*C. elegans*), takes 3 days to develop, with the developmental cycle broken down into 6 stages: embryo, L1, L2, L3, L4 and adult [14], and in starvation can enter an alternative larval state known as dauer [15]. The rate of this life cycle is dependent on temperature and food source. Lower temperatures (15°C) slow life cycle with 25°C increasing life cycle speed. 20°C is the normal temperature for raising worms which takes ~3 days from embryo to adult [16]. This developmental speed, alongside a ~2-3 week lifespan [17], and low maintenance cost allows many experiments to be performed much quicker than with other higher organisms. Alongside these benefits, *C. elegans* are an androdioecious species, meaning the main population are hermaphrodites with few males. Hermaphrodites are diploid and have 5 autosomes and 1 sex chromosome (XX), and generate both sperm and oocytes for self-fertilisation and maintenance of the population [18]. Opposingly, males are rare (~1:500) and arise from spontaneous

loss of one X chromosome (XO), making it diploid for autosomes, but haploid for its sex chromosome [18–20]. Having both hermaphrodite and male sexes allow for sex-specific differences to be studied e.g. in food behaviour.

C. elegans have four types of locomotion that generally make up its food-related and sex-related behaviours: 1) forward locomotion, 2) backward locomotion (reversals), including changing direction (omega turns), 3) postural changes and 4) pausing/stopping locomotion [21]. These types of locomotion are needed for the worms similar eating behaviours (Fig. 1), with their time divided between three states: roaming (foraging i.e. active movement in looking for food), dwelling (staying in the same place of food and consuming it [22]) and quiescence, the gradual stopping of both movement and food intake [4], the latter similar to mammalian post-prandial sleep [23]. Quiescence can also occur in starved conditions, known as fasting quiescence, or after fasting then refeeding, known as satiety-induced quiescence (SIQ). Quiescence should not be confused with other quiescence/sleep-like states unrelated to satiety, including lethargus [24–27], and stress-induced quiescence [28, 29]. These behaviours can be automatically quantified using computer-based worm tracking software [30], allowing high-throughput (and unbiased) investigation, or as used in this project, imaging and counting the tracks of the worm in a defined time period to give an overall readout of exploration behaviour, rather than specific time periods entered for all 3 behaviours.

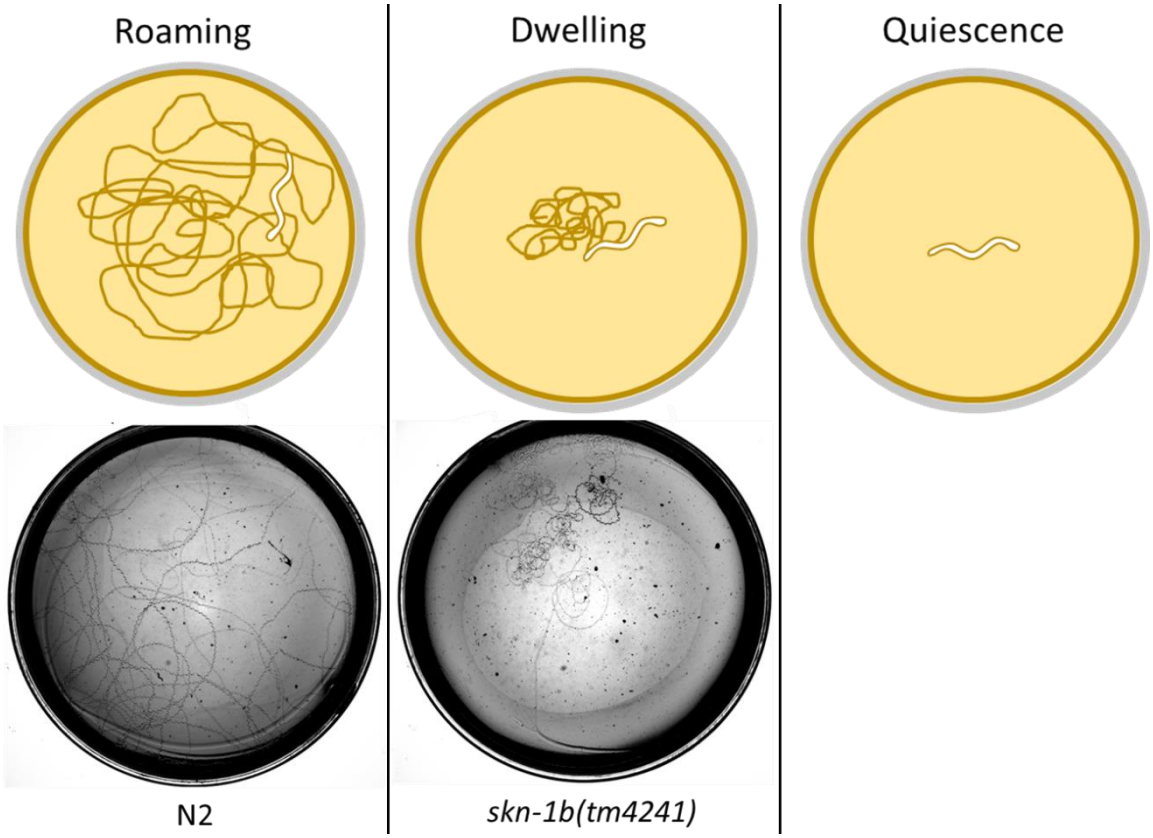

Figure 1. Food-related exploratory behaviours in *C. elegans*. The 3 stages of food-related behaviours in *C. elegans*: roaming has long tracks as the worm is looking for food (as seen in the wildtype (N2) worm example); dwelling has circular, back and forth tracks close together where the worm has found food and eating it (seen in the *skn-1b(tm4241)* mutant, where increase dwelling tracks are seen), whilst quiescence is the lack of eating and movement (no real life image to show, as no tracks would be seen).

C. elegans also have other food behaviours, specifically when removed from food, worms undergo a behaviour known as local search (area-restricted search), wherein worms search for 10-20 minutes in the local (small) area for food, similar in locomotive pattern to dwelling, but without eating. If food is not found in the local area, a second behaviour takes over, global search (dispersal), wherein worms search for food in a wider area, similar to roaming in locomotive pattern but with no turns [21]. Male *C. elegans* have a specific-sex behaviour, mate searching, wherein males will leave food to find hermaphrodites to mate with, with the presence of hermaphrodites overriding food seeking behaviour. Mate searching is reduced upon starvation, indicating food and mate-finding drives are regulated in tandem [21, 31].

All of these behaviours are controlled by the nervous system, and the *C. elegans* nervous system is completely mapped (302 neurons [32] and 56 glia [33] in hermaphrodites, 387 neurons and 60 glia in

males [34]), and every cell is known in the adult hermaphrodite and male (959 cells and 1031 cells, respectively [35]), allowing specific behaviours to be attributed to individual neurons. *C. elegans* genes are also highly homologous with humans (83% of its 18,452 genes have human homologs) [36] and can be genetically manipulated [37] by using RNAi [38], specific genome mutations and transgenic expression of fluorescent reporters, the latter with a unique advantage in *C. elegans* in that it has a transparent cuticle allowing for easy live *in vivo* imaging. This, alongside neuronal ablation (laser; genetic; photo and optogenetic), can all be used to modulate and understand neuronal activity, therefore, behaviours at a genetic level. Overall, experimental investigation using *C. elegans* allows study of how eating behaviours are controlled at the cellular and cell to cell circuitry level in both sexes.

Given the prevalence of obesity, there is interest in finding new genetic modulators of appetite. Recently, the Tullet lab identified a new appetite regulator called SKN-1B, a neuronal isoform of transcription factor SKN-1, which controls both exploratory and satiety behaviours [39].

The transcription factor SKN-1

SKN-1 is a *C. elegans* transcription factor, homologous to mammalian NF-E2-related factors e.g. NRF1; -2; -3 and p45 NF-E2 [40], unrelated to nuclear respiratory factor transcription factors [41]. SKN-1 has 3 isoforms (A; B; C) confirmed *in vivo*, with a possible forth isoform (SKN-1D) [42] (Fig. 2). SKN-1 (likely SKN-1A/C) is needed in embryogenesis for establishing fates of endomesodermal precursor cells, with *skn-1 a/c* mutants embryonic lethal [43]. After embryogenesis, SKN-1 has many functions e.g. oxidative stress resistance, mitochondrial biogenesis; innate immunity; extracellular matrix (ECM) remodelling; unfolded protein response (UPR^{ER}) and lifespan [41].

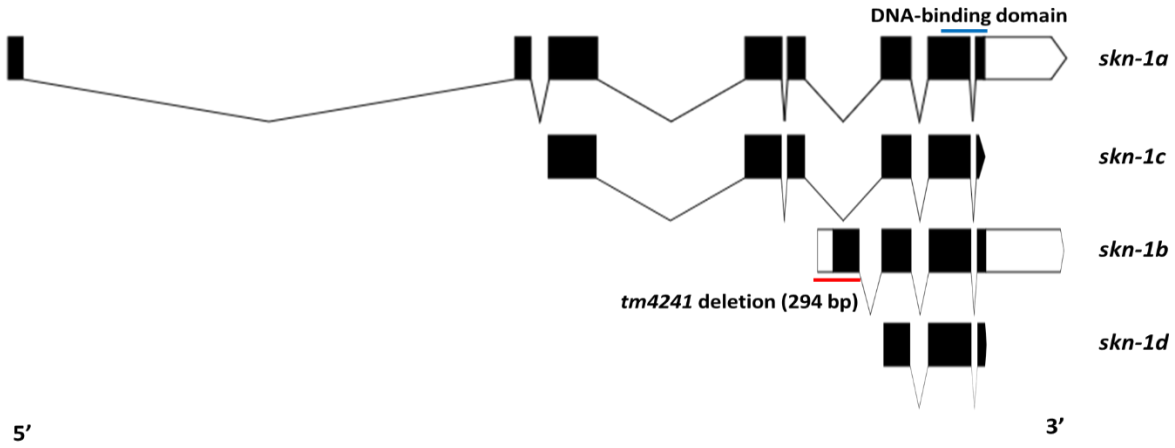

Figure 2. **Graphical representation of the 4 *skn-1* isoforms.** The blue line represents the Cap'n'Collar DNA-binding domain in all isoforms. Note the *tm4241* mutation (represented by a red line) is in an exon for *skn-1b*, whereas it is an intron and spliced out in *skn-1a/c/d*. Black squares are exons. Black lines indicate introns. White squares are UTRs. Note *skn-1a* only has a 3' UTR predicted, whilst *skn-1b* has both 5' UTR and 3' UTR. *skn-1c* and *skn-1d* have no UTR predictions. Diagram made using Exon-Intron graphic maker (http://wormweb.org/exonintron).

To function as transcription factors, all SKN-1 isoforms have a Cap'n'Collar DNA-binding domain (Fig. 2). SKN-1A and SKN-1C also have the DIDLID motif that contributes to transcriptional activity, whilst SKN-1B does not have this motif. However, SKN-1B still likely has transcriptional activity, as even on loss of the DIDLID motif, transcriptional activity is still retained, albeit, in a reduced capacity [41, 44].

SKN-1C is the most widely studied isoform and is expressed in the intestine [45]. SKN-1C is required for many biological processes including the oxidative stress response [46] and for longevity [47]. SKN-1A is widely expressed in *C. elegans* [45] as it is bound to the ER to monitor and maintain the proteosome [48, 49]. SKN-1A is also found on the outer mitochondrial membrane to possibly regulate metabolism and adapt to starvation [50]. SKN-1B (the focus of this thesis) is expressed exclusively in the ASI neurons of the hermaphrodite in fed conditions (and ADL in starved), and has lately been revealed to have functions in both exploratory and food-related behaviours [39].

Recently, SKN-1B functionality has been characterised using a *skn-1b(tm4241)* mutant, finding *skn-1b* mutants have reduced exploration in hermaphrodites, but not males, with tracks resembling a dwelling phenotype (Fig. 1), unlike SKN-1A/C, which have normal exploration [39]. Note the term 'reduced exploration' will be attributed to *skn-1b(tm4241)* mutants when discussed, as *skn-1b*

mutants have not been quantitatively measured for all three behavioural states (roaming; dwelling; quiescence), so it cannot be stated that *skn-1b* mutants dwell more, although this is likely true. The reduced exploration of *skn-1b* mutants is purely due to its role in food-related behaviours, as *skn-1b* mutants develop normally, as no defects in embryogenesis, body wall muscle, ASI neurons (*skn-1(zu135)* mutants with all isoforms removed have normal ASI morphology [46]) or egg laying [39] occurs that would influence exploration behaviour.

SKN-1B acts to control these behaviours through cGMP (DAF-11), TGF-β (DAF-7) and insulin signalling (IIS)/DAF-16, with all 3 pathways needed for normal exploration [51]. DAF-11, DAF-7 and DAF-16 are all needed to promote fasting quiescence, whilst SKN-1B represses it (but promotes it in fed conditions). SKN-1B supresses DAF-7 in fed conditions, but both SKN-1B and DAF-7 expression are increased upon starvation and refeeding, yet DAF-7 can now promote fasting quiescence. This is similar to IIS, which is needed for normal exploration, but is downregulated upon fasting and re-feeding [39], causing DAF-16 (which is inhibited by IIS) to be active. DAF-16 reduces exploration and promotes fasting quiescence, which is SKN-1B-dependent. This is juxtaposing, as SKN-1B represses fasting quiescence, yet is needed to promote DAF-16-dependent fasting quiescence. This indicates these pathways that interact with SKN-1B would have to be active at different time scales, as if only fasting quiescence occurred, the worm would never be able to enter roaming to find new food or enter dwelling to feed and replenish food stores after starvation.

An unexpected role with SKN-1B was that it is involved in promoting mitochondrial fission. Mitochondria morphology is dependent on nutrient availability, with mitochondrial fusion occurring in nutrient-poor conditions which maintain less energy efficient mitochondria, compared to nutrient-rich conditions, which maintain more energy efficient fissioned mitochondria [52]. The role of SKN-1B and mitochondrial morphology was found to be directly related to food exploratory behaviour, as *skn-1b* mutants have fused mitochondria within its body wall muscle like starved N2 worms, indicating *skn-1b* mutants, internally, are starved. Upon *eat-3* and *fzo-1* RNAi which inhibit

mitochondrial fusion, the mitochondria and exploration of *skn-1b* mutants were rescued to N2 levels, indicating SKN-1B possibly promotes mitochondrial fission to control food behaviour. This would also indicate SKN-1B also has cell non-autonomous effects in muscle due to signalling only from ASI neurons.

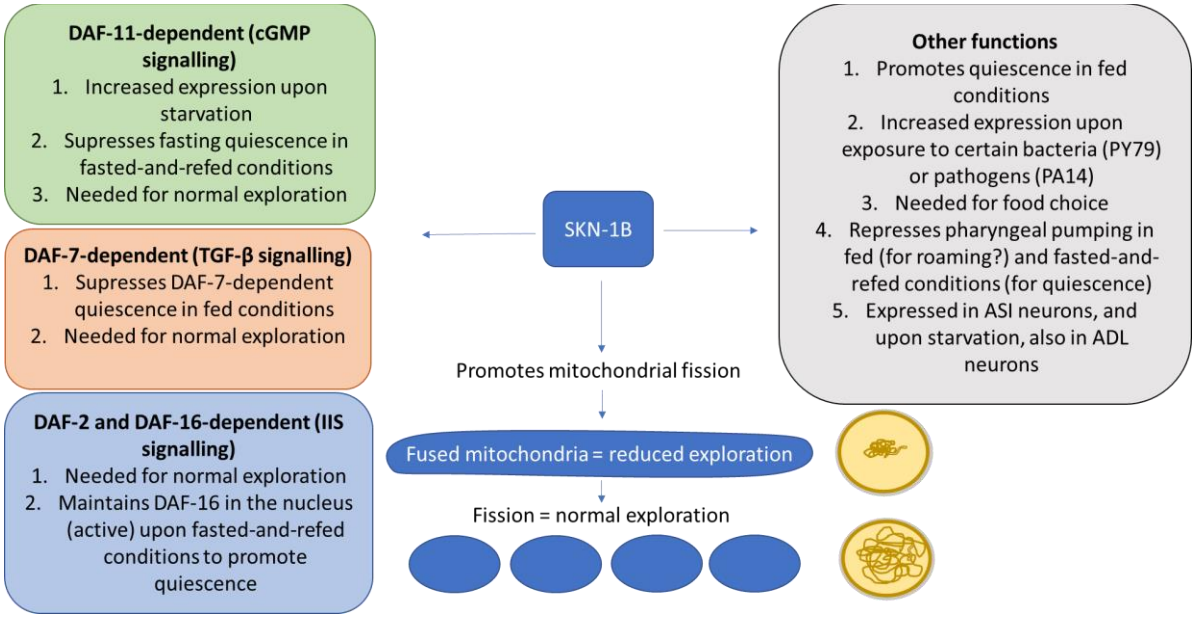

Figure 3. SKN-1B signals via cGMP, TGF-β and IIS signalling pathways to promote or inhibit food-related behaviours [39]**.** SKN-1B and all 3 pathways are needed for normal exploration, with the pathways promoting fasting quiescence, whilst SKN-1B inhibits it (yet promotes it in fed conditions). SKN-1B is also needed to promote mitochondrial fission, which is needed for normal exploratory behaviour, as fused mitochondria reduce exploration. SKN-1B also has other functions not (yet) associated with the 3 pathways, which includes food choice preference e.g. prefer food source A over food source B, and represses pharyngeal pumping in fed and fasted and refed conditions. SKN-1B expression increases with environmental changes e.g. exposure to pathogen *Pseudomonas aeruginosa* (PA14) and in starvation (where ADL neurons then express SKN-1B).

Overall SKN-1B communicates with cGMP, TGF-β and IIS signalling pathways to promote exploration behaviour in both fed and fasted conditions, alongside other functions including food preference, pharyngeal pumping, and mitochondrial fission (Fig. 3). As SKN-1B is expressed in ASI neurons, understanding the general function of ASI neurons, and how it interacts with other neurons and the whole organism would give better insight to how SKN-1B plays a role in these behaviours.

ASI neurons are peptidergic and respond to the environment

ASI neurons are a pair of ciliated amphid sensory neurons located in the head, with dendritic endings open to the outside to detect stimuli [32]. ASI neurons, among other amphid neurons, have AMso and

AMsh glia associations, but specific ASI neuron interactions are not documented [53]. ASI neurons are involved in a variety of other functions, including responding to ascarosides (ASI ascaroside receptor SRX-43 binds icas#9 to promote dwelling) [54]; thermotaxis [55]; preventing dauer formation [56]; repressing DAF-7 in ASI to allow dauer entry [57]; repressing male sexual behaviour in hermaphrodites via DAF-7 [58]; repressing insulin-like peptide (ILP) DAF-28 secretion via EXP-2 voltage-gated K^+ channel [59]; the innate immune response [60] and triggering global search (dispersal) behaviour if food cannot be found after an area-restricted search [61]. Also, relevant to this project, ASIs control satiety-related behaviour, acting like parts of the hypothalamus. Together with other neurons, ASIs can respond and promote the three main satiety-related behaviours (roaming, dwelling and quiescence) [23, 62, 63], allowing worms to respond to their environmental conditions.

ASI neurons are involved in roaming: for example when NSM and HSN neurons release serotonin (5-HT), it binds to the inhibitory receptor MOD-1 on ASI, AIY and RIF neurons, inhibiting these neurons and promote dwelling, as without inhibition, roaming occurs [62]. ASI neurons can also promote fat breakdown and dwelling (Fig. 4).

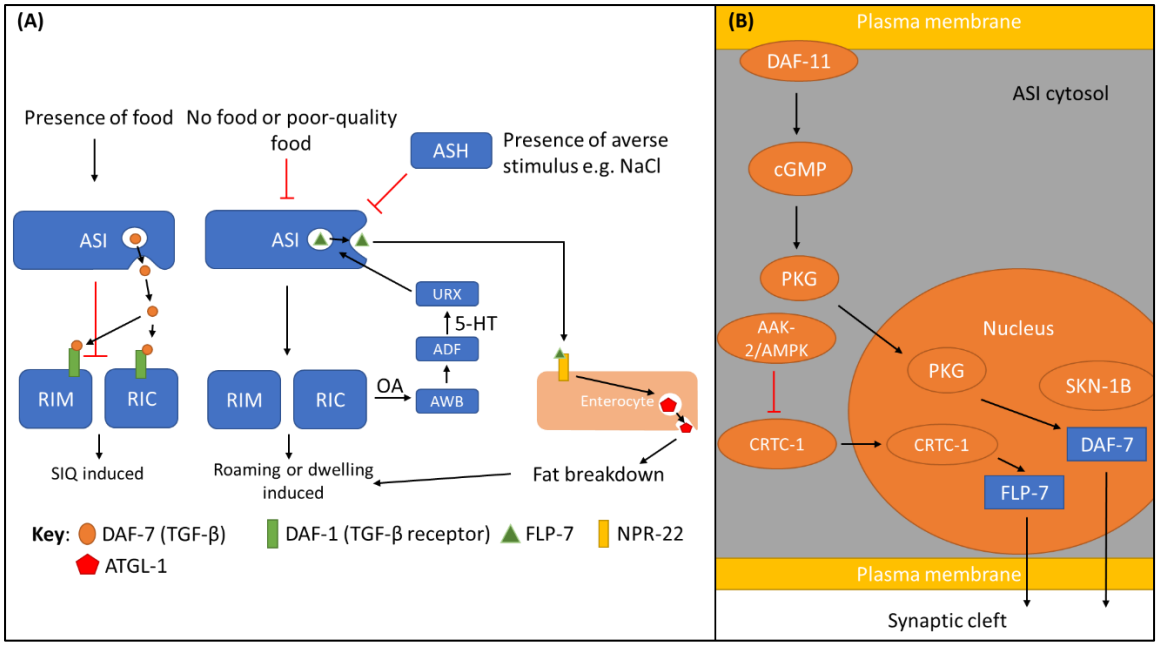

Figure 4. *C. elegans* neuronal control of feeding behaviour. (A) ASI neurons are activated in the presence of food, triggering DAF-7/TGF-β release from ASI, and binding to DAF-1/TGF-β receptors on RIC and RIM neurons, inactivating the neurons and promoting SIQ. In no food or poor-quality food, ASI neurons are not activated, allowing RIC and RIM to be active, which supress SIQ and promote roaming or dwelling behaviour [23]. ASI neurons are also inhibited by ASH neurons if there is an adverse stimulus present to promote roaming away from the stimulus [64]. RIC signals with OA to AWB; AWB signals to ADF which secretes 5-HT. 5-HT binds to URX and URX signals to ASI neurons to release FLP-7. FLP-7 binds to NPR-22 in the intestine which induces secretion of ATGL-1 to induce fat breakdown, inducing dwelling. Downstream of 5-HT signalling are ASG and BAG neurons which use ETS-5 to promote roaming and inhibiting SIQ, and downstream of ETS-5 are PDFR-1 and EGL-4, which promote roaming and SIQ, respectively (not shown) [63, 65]. **(B)** In ASI neurons, DAF-7 and FLP-7 transcription is controlled by the DAF-11 [23] and AMPK pathway, respectively. AAK-2/AMPK inhibits (phosphorylates) CRTC-1 under low energy conditions (high AMP:ATP ratio), but high nutritional states, CRTC-1 is activated, and transcribes FLP-7 which is then secreted via UNC-31/CAPS through dense core vesicles (not shown) [63]. SKN-1B is constitutively nuclear and supresses SIQ [39].

Alongside roaming and dwelling, ASI neurons can promote quiescence and inhibit the switch to dwelling [23], whereas ASH neurons antagonises this behaviour. Quiescence is regulated by variety of cell signalling pathways (Fig. 3, 4 and Table 1). DAF-11 (guanylyl cyclase) is found in ASI neurons (alongside other amphid neurons) [51] and is needed for *daf-7* to be expressed in ASI neurons [66]. In the presence of food, TGF-β (DAF-7) is released from ASI to promote quiescence by binding to DAF-1 on RIC and RIM neurons [23]. But when ASIs are inhibited i.e. under lack of food, so no longer secrete DAF-7, downstream neurons RIM and RIC become active and inhibit quiescence (likely just RIM, as exogenous octopamine does not inhibit quiescence, and octopamine is only made by RIC) [23].

Table 1. Mutants that have reduced-to-no SIQ or increased SIQ compared to N2 worms. *tax-4* mutants could not be tested as mutants would stray away from food [4]. Other mutants that have increased or reduced exploration can be found in Flavell *et al.,* 2013 [62].

Reduced SIQ		
Strain	**Mutant**	**Protein**
CB1370	*daf-2(e1370)* [4]	IIS receptor
DR1942	*daf-2(e979ts)* [4]	
CB1372	*daf-7(e1372ts)* [4]	TGF-β
DR40	*daf-1(m40ts)* [4]	TGF-β receptor type I homolog
CB1364	*daf-4(e1364ts)* [4]	TGF-β receptor type II homolog
JT195	*daf-11(sa195ts)* [4]	Guanylyl cyclase
DR47	*daf-11(m47ts)* [39]	
PR671	*tax-2(p671)* [4]	cGMP-gated channel (made with tax-2 (β subunit) and tax-4 (α subunit)
PR694	*tax-2(p694)* [4]	
FK234	*egl-4(ks62)* [4]	Protein kinase G (PKG)
KP2018	*egl-21(n476)* [4]	Carboxypeptidase E
KP1873	*egl-3(nu349)* [4]	Proprotein convertase
VC461	*egl-3(gk238)* [4]	
GR1328	*egl-3(nr2090)* [4]	
MT1541	*egl-3(n729)* [4]	
DA509	*unc-31(e928)* [4]	Calcium-dependent activator protein for secretion (CAPS)
GR1321	*tph-1(mg280)* [4]	Tryptophan hydroxylase
IN2043	*act-5(dt2017sd) III / eT1(III); + / eT1(V)* [4]	Microvillus-specific actin
Increased SIQ		
Strain	**Mutant**	**Protein**
RJP235	*ets-5(tm1734)* [67]	E twenty-six transcription factor
VC2609	*pdfr-1(ok3425)* [67]	PDF-neuropeptide receptor
DA521	*egl-4(ad450sd)* – gain of function [4]	Protein kinase G (PKG)
BR1671	*gar-2(by124)* [4]	G-protein-linked acetylcholine receptor
GA1058	*skn-1b(tm4241)* [39]	NF-E2 related transcription factor

Overall, ASI neurons are involved in roaming, but are also needed to switch from dwelling to quiescence [62] and induce quiescence in fed conditions [23], with ablation reducing exploration [62] and increasing dwelling [64]. This matches the *skn-1b* mutant phenotype, with reduced exploration, and dwelling tracks seen, indicating ASI and *skn-1b* are linked in their food-related functions (Fig. 3).

For ASI neurons to respond and cause these discussed SKN-1B related behaviours and other functions, neuronal signalling needs to occur. ASI neurons likely signal using only neuropeptides (peptidergic), as ASI neurons do not synthesise classical or biogenic amine neurotransmitters (a neurotransmitter orphan) [68–70], and contain dense/dark core vesicles (DCVs) [32], which only package neuropeptides and/or biogenic amines [71]. ASI neurons need UNC-31 to release neuropeptides [63], as worms with ASI neurons that have reduced neurotransmitter and neuropeptide release (via

tetanus toxin light chain expression to cleave synaptobrevin) have reduced exploration [72]. It has been shown ASI has small, clear synaptic vesicles which may allow the use of unclassified neurotransmitters [69], but this has not been investigated.

Overall, this shows satiety-related behaviour is dependent on the interaction between neurons and other non-neuronal tissues, neurotransmitters, neuropeptides, and other molecules, with receptor type and location crucial for modulating the behaviour with the same ligand. Understanding how ASI neurons and SKN-1B interact with these molecules, the nervous system, and the entire organism as a whole, is key to understanding eating behaviours further on a neural circuitry level, but also how SKN-1B can affect non-neuronal tissues e.g. body wall muscle mitochondria.

Neurotransmitters, specifically biogenic amines, and neuropeptides, are required for the control of appetite behaviours

As the nervous system is needed for food-related behaviour, the neurotransmitters and neuropeptides needed for these behaviours needs to be understood. The advantage of *C. elegans* is that the nervous system is mapped in both hermaphrodites and males, allowing study of these behaviours in neuron-specific detail between the sexes. In *C. elegans*, there are 3 main neuronal types as in mammals: sensory, interneuron and motor (with polymodal neurons classed as having more than one of these types e.g. M3 neurons in the pharynx have both sensory and motor functionality). Sensory neurons 'sense' the external environment to then trigger a response, these can then synapse to interneurons which relay the information to other neuronal types, including motoneurons, which then innervate muscle to contract or not contract, to allow the worm to respond to the stimulus via movement e.g. pharyngeal pumping, locomotion or egg laying [32, 73]. Sensory neurons (sensilla) are subdivided into 7 types: outer and inner labials; anterior and posterior deirids; phasmids; cephalics and amphids, the latter which make up most of the sensory neurons (12 pairs) e.g. SKN-1B-expressing ASI neurons [32, 73].

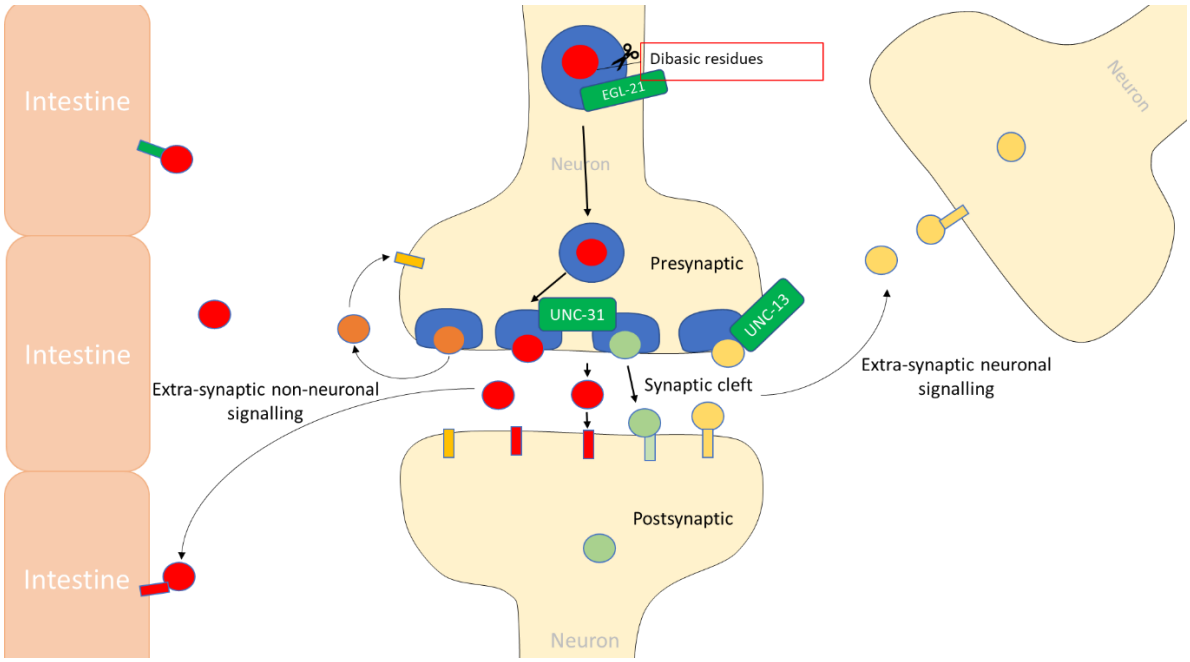

Figure 5. Neurotransmitters and neuropeptides can signal directly to other neurons, and/or indirectly to other neurons and non-neuronal tissues. Signalling can occur using different neurotransmitters or neuropeptides from the same neuron (most neurons only use one neurotransmitter, but some have the potential to use two e.g. RIM [74]). Proneuropeptides are processed into a mature form before use with a variety of enzymes, including EGL-21, which cleaves dibasic residues from the C-terminus [75]. Both neuropeptides and neurotransmitters are released from the plasma membrane with UNC-31 and UNC-13 (classical neurotransmitters only). VMAT (*cat-1*) is also required for all biogenic amines to be loaded into synaptic vesicles [76] (not shown). Signalling can be direct, where two neurons are close enough to each other to synapse, but autocrine (signalling to the cell that has secreted the molecule for self-regulation) and extra-synaptic (paracrine) signalling can also occur, where both neurotransmitter or neuropeptides can signal to non-directly to neurons and non-neuronal cells (example in the figure is the intestine). These molecules can bind to a variety of receptors to modulate the physiological outcome. Neurons can also signal using gap junctions, which are not shown.

C. elegans primarily use 2 classes of neurotransmitters: classical and biogenic amines. Classical neurotransmitters are made up of acetylcholine (ACh), γ-aminobutyric acid (GABA) and glutamate. These are transported from the cell body in small, clear synaptic vesicles and released into the synaptic cleft using protein UNC-13, a protein needed for synaptic vesicle fusion [71, 77]. These bind post-synaptic ionotropic receptors and are needed for fast transmission [78]. These neurotransmitters are involved in eating behaviour, but typically in relation to motoneuron function e.g. controlling body wall muscle to allow locomotion or pharyngeal muscle [79, 80] for eating. Most mutants of classical neurotransmitters, and *unc-13*, have an uncoordinated phenotype, and due to the assay

used in this project to measure food-related exploratory behaviour, analysing these behaviours was not feasible (further discussed in Chapter 2), so shall not be introduced further.

The neurotransmitters relevant to this project are the four biogenic amines: serotonin (5-HT), dopamine (DA), tyramine (TA) and octopamine (OA), which all have different roles in satiety-related behaviours in *C. elegans*. They differ to classical neurotransmitters in that they are packaged into large, dense core vesicles (DCVs), tethered then docked to the plasma membrane using UNC-31 (homolog of human CAPS (calcium-dependent activator protein for secretion), similar to UNC-13. DVCs then fuse to the plasma membrane to release both biogenic amines (and neuropeptides) [71, 81] (Fig. 5). In mammals, 5-HT regulates food intake, with increased and decreased 5-HT inversely reducing and increasing food intake, respectively, whereas DA is released upon wanting and eating palatable/pleasurable food, and makes up part of the major reward pathway in the brain [82]. TA and OA are generally seen as the counterparts to mammalian noradrenaline and adrenaline [63, 83], which are less characterised in mammalian eating behaviours compared to 5-HT and DA.

Table 2. Biogenic amines: expression, receptors and function. At least one receptor for all neurotransmitters were expressed in egg-laying neurons and egg-laying muscles (except the latter for glutamate and GABA) [84]. *For SRX-34 and SRX-44 receptors, ascaroside icas#9 which contains OA binds to these receptors, rather than purely OA itself as a neurotransmitter [72].

Neurotransmitter	Neurotransmitter expression	Receptor	Receptor expression	Receptor function
Serotonin (5-HT)	***tph-1*:** NSM; ADF; AIM; RIH; hermaphrodite-specific: HSN; male-specific: CP0-CP06; R1B; R3B; R9B [70, 85]	SER-1	HSN [84] ASI [86].	5-HIAA inhibits egg laying via SER-1 [87]. promotes fast pharyngeal pumping [88]
		SER-4	?	maintains a high pharyngeal pumping rate [88]
		SER-5	HSN [84]	Pharyngeal pumping [88]
		SER-7	HSN, VC4, -5; vm-1, -2; um1, -2[84]; MC; M2 to M5; vulva muscle [89].	Stimulates pharyngeal pumping and egg laying [89]
		MOD-1	URX [63] AIY; ASI; RIF [62, 90]	AIY, ASI and RIF: promote dwelling [62, 90]
		LGC-40 [91]	?	?
Dopamine (DA)	***cat-2*:** ADE; PDE; CEPD/V Male-specific: R5A; R7A; R9A [92]	DOP-1 [93]	?	Antagonises DOP-3 in cholinergic neurons [93]
		DOP-2 [93]	SIA	Stops OA triggering roaming [94]
		DOP-3 [93]	SIA; RIC	Slows locomotion [93]; stops OA triggering roaming [94]; supresses OA signalling [95]
		DOP-4 [96]	?	?
		DOP-5 [97]	?	Uncharacterised [97]
		DOP-6 [97]	?	Uncharacterised [97]
		LGC-53 [91]	?	?
Tyramine (TA)	***tdc-1*:** RIM; RIC Non-neuronal cells: UV1; gonadal sheath cells [83]	SER-2[98]	RME; BDU; AIY; AVH; AIZ; ALN; RIC; RIM; RIA; PDA Non-neuronal: pharyngeal muscle (pm1; pm6) [99]; uterine toroid cells (ut1; ut2) [98]	Stops head movements for foraging; inhibits pharyngeal pumping [98]; RIC and RIM: activate XBP-1 decreasing food leaving behaviour [100]
		TYRA-2 [101]	MC; NSM; ASE; ASG; ASH; ASI; AVM; ALM; PVM; ALN; PLM [101]	Possibly inhibits head movements (ALM) [101]; detect ascaroside osas#9 (contains OA) [102]; inhibit AIM to reduce pharyngeal pumping [103]

		TYRA-3 [104]	ASI [86]; ASK; RIC; AIM; AVA; BAG; CEP; OLQ; SDQR; ADL [105]; AUA; ADF; AWC Non-neuronal: spermatheca; distal tip cell [104]	ASI: triggers neuropeptide release to inhibit AIA, ADL and ASER, eventually inhibiting ASH neurons [105] ASK: promotes food leaving [104]
		LGC-55 [91]	Direct synaptic input from RIM: AVB; RMD; SMDD/V [106] No direct synaptic input from RIM: IL1D/V; SDQ; HSN; ALN [106] – likely activated extrasynaptically Non-neuronal cells: GLR glia-like cells [91]; neck muscle; UV1; tail muscle [106]	RMD, SMD and neck muscles: inhibits head movements [106] AVB: inhibits locomotion [106]
		OCTR-1 [107]	?	?
Octopamine (OA)	***tbh-1*:** RIC; Non-neuronal: gonadal sheath cells	OCTR-1	ASI, ASH, AIY, ADE; CEP Non-neuronal: spermatheca; uterine toroid cell [107].	ASI; ASH: supress innate immunity [108]
		SER-3	SIA [109]	SIA: Promotes CREB transcription and roaming in starvation [90]
		SER-6	ASI [86]; SIA [109]; AWB [63]	SIA: Promotes CREB transcription and roaming in starvation [90]; AWB: promotes dwelling [63]
		SRX-43*	ASI [72]	Promotes roaming via ASI [72]
		SRX-44*	ASJ; ADL [72]	Promotes roaming via ASJ; inhibits roaming via ADL [72]

Serotonin (5-HT) controls dwelling behaviour in *C. elegans*

To control dwelling behaviour, 5-HT carries out several key roles. It controls speed and maintenance of pharyngeal pumping, whilst supressing long pauses between pumping [88] to ensure maximum food intake. Opposingly, in starvation, it can either promote roaming [90], or slow (and even stop) starved worms from leaving food [110], showing 5-HT can control different eating behaviours dependent on the availability of food.

In *C. elegans*, 5-HT is synthesised from tryptophan using tryptophan hydroxylase (TPH-1), making 5-hydroxy-tryptophan (5-HTP) [85] in 8-10 neurons (Table 2). This process requires GTP cyclohydrolase I

(CAT-4) to occur [111] with 5-HT synthesised from 5-HTP using BAS-1 [112]. 5-HT is transported into cells using the 5-HT reuptake transporter (SERT) MOD-5 [113] and is broken down into 5-hydroxyindole acetic acid (5-HIAA) using the monoamine oxidase AMX-2 [87].

5-HT has 6 receptors (Table 2), with these receptor genes needed for pharyngeal pumping, as when mutated, pharyngeal pumping rates are reduced [88] (except *ser-7*, although it can still stimulate pharyngeal pumping [89]; LGC-40 was not studied). SER-1 promotes fast pumping whilst SER-4 maintains the high pumping rate, and supresses long pauses, therefore 5-HT is needed for dwelling (eating). NSM and HSN neurons release 5-HT for these behaviours [88], including inhibiting AIY, ASI and RIF neurons to promote dwelling via MOD-1 [62, 90] whilst 5-HT can stimulate lipid breakdown to promote dwelling [63] (Fig. 4) as previously discussed. Yet in starved conditions when the worm needs to roam for food, 5-HT released by ADF neurons binds SER-5 in body wall muscle and neurons, supressing quiescence and promoting roaming.

In summary, 5-HT promotes opposing satiety-related behaviours through promoting dwelling in fed worms, but roaming in starvation, showing 5-HT signalling is dependent on receptor and nutritional status.

Dopamine (DA) keeps *C. elegans* on food and once depleted, triggers searching for new food

Whilst 5-HT can trigger dwelling, worms need a signal to keep them on food. Dopamine (DA) acts to keep worms on food (basal slowing response) and inhibit roaming [110]. However, if food is depleted, DA can act to promote roaming. DA is synthesised from tyrosine by tyrosine hydroxylase (CAT-2) into L-DOPA in 8 neurons [92, 114] (Table 2). This process likely requires GTP cyclohydrolase I (CAT-4) to occur [111], with L-DOPA converted to DA likely by BAS-1 [112]. DA is transported into cells using the DA transporter DAT-1 [115], but it is yet unknown if monoamine oxidase AMX-2 can breakdown DA.

For dopamine to control the basal slowing response (slowing down of locomotion), of DAs 5-7 receptors (Table 2), DOP-3 is needed for this slowing of locomotion, but is appropriately regulated by DOP-1 which antagonises DOP-3 in cholinergic neurons [93]. Crosstalk between DA and

octopamine (OA) signalling pathways occurs, as DA can stop OA from triggering roaming by binding to DOP-2 in SIA neurons and DOP-3 in SIA and RIC neurons [94]. DOP-3 also negatively regulates body size without affecting food intake or development through supressing OA GPCRs SER-4 and SER-6 [95]. DA also acts on glutamatergic neurons to increase high-angled turns for area-restricted search (ARS), as previously mentioned, a type of foraging behaviour to find new food after the original source has been exhausted/used up [116]. In summary, DA keeps worms on food, but promotes food searching upon depletion, and inhibits OA-induced roaming.

Tyramine (TA) inhibits roaming and promotes dwelling

Tyramine (TA), similar in structure to mammalian noradrenaline and adrenaline [117], can control locomotive reversal behaviour, but also inhibit egg laying, head movements and pharyngeal pumping [98]. This indicates TA release can occur in low food in order to conserve energy (stop egg laying) and find new food (increase reversal behaviour; stop head movements and pharyngeal pumping) [106]. Opposingly, exogenous TA inhibits roaming and promotes dwelling, opposite of octopamine which promotes roaming and inhibits quiescence [90].

TA is synthesised from tyrosine using tyrosine decarboxylase (*tdc-1*) [83] in 2 neurons: RIM inter/motoneurons (to supress head oscillations) and RIC interneurons, but also is expressed in 2 types of non-neuronal cells: UV1 cells (expressed late L4) and gonadal sheath cells (highest TDC-1 levels are seen in 3 pairs of sheath cells [83] which move oocytes through the gonad) [118]. Mechanisms for TA re-uptake or degradation are unknown.

TA has 5 receptors (Table 2), with SER-2 stopping head movements (oscillations) needed for foraging behaviour when reversing, and inhibits pharyngeal pumping [98]. LGC-55 can also inhibit head movements via RMD, SMD and neck muscles, alongside locomotion via AVB neurons [106]. SER-2 on RIC and RIM neurons can promote XBP-1 transcription which activates the intestinal ER-mediated unfolded protein response (UPR^{ER}), causing decreased leaving of bacterial lawn and reduced exploration on food [100], whereas TYRA-3 promotes food leaving via ASK neurons [104]. TYRA-3 can

also trigger ASI neurons to release neuropeptides NLP-1, NLP-14 and NLP-9, which bind to neuropeptide receptors on AIA (NPR-11), ADL (NPR-10) and ASER (NPR-18), respectively, to inhibit these neurons, which cascades into inhibiting ASH neurons to stop aversive behaviour [105]. In summary, OA can promote roaming via promoting food leaving, whilst stopping aversive behaviour, head movements and pharyngeal pumping, but also stop lawn leaving and reduce exploration on food similar to a starvation response.

Octopamine (OA) is released upon starvation to inhibit quiescence and promote roaming

Octopamine (OA) is released upon starvation to promote roaming and suppresses quiescence, in opposition of TA that inhibits roaming and promotes dwelling [90]. OA can also supress innate immunity to likely allow increased food choice when roaming. OA, like TA, is similar to noradrenaline and adrenaline [117] and is synthesised from TA using tyramine β-hydroxylase (TBH-1) [83], with *tbh-1* expressed in RIC interneurons and gonadal sheath cells [83]. Octopaminergic neurons could also use/release TA, as TA needs to be synthesised and/or transported into these neurons to make OA. Mechanisms for OA re-uptake or degradation, like TA, are unknown.

OA has 5 receptors (Table 2), with OCTR-1 expressed in ASI and ASH to suppress the innate immune response. This occurs through downregulating non-canonical UPR genes (*pqn*/*abu*) [108] in the presence of non-pathogenic bacteria to not cause aberrant responses to potential food. Yet, RIC (OA-producing) neurons are inhibited in the presence of pathogenic bacteria to cause an increased immune response [119], indicating OCTR-1 does not have a role in pathogen avoidance [108], but likely functions to increase food preference that may be inhibited with a high immune response. In absence of food, OA binds to SER-3 and SER-6 on cholinergic SIA neurons [109] to promote roaming [90], whereas DA receptors DOP-2 (SIA) and DOP-3 (SIA and RIC) inhibit this [94]. OA can also promote or inhibit roaming via incorporation into ascaroside icas#9, which binds to GPCRs SRX-43 on ASI neurons and SRX-44 on ASJ neurons to promote roaming, whereas binding to SRX-44 on ADL inhibits roaming [72]. OA also promotes dwelling via SER-6 on AWB as previously discussed (Fig. 4) via other

neurons and 5-HT signalling to cause ASI to release FLP-7 causing fat breakdown and promoting dwelling [63]. OA also supresses quiescence and promotes roaming, acting in opposition of TA which inhibits roaming to promote dwelling [90].

In summary, OA function is linked through its receptors. SRX-43 and -44 can promote or inhibit roaming upon binding of OA-containing icas#9; SER-3 and SER-6 are bound by OA in food absence to promote roaming to find new food, and OCTR-1 is also bound to supress the immune system, which hypothetically would allow the worm to find and eat a larger variety of food types, even if it is not nutritionally beneficial.

Neuropeptides, like biogenic amines, can affect food-related behaviour

Humans have a variety of proteins apart from neurotransmitters involved in food-related behaviours, including ghrelin from the stomach, amylin, uroguanylin, glucagon, cholecystokinin from the intestine, alongside brain-specific proteins peptide YY, somatostatin, AGRP, NPY and POMC [10].

Neuropeptides are different to neurotransmitters in that they are smaller, many genes encode them, and they can be released from both neuronal and non-neuronal cells. There are 3 main types of neuropeptides: 40 insulin-like peptides (ILPs) i.e. *ins-1* to *ins-39* and *daf-28* [120], 71 FMRFamide-like peptides (FLPs) [121] and >100 neuropeptide-like peptides (NLPs) [122–124]. Like biogenic amines, neuropeptides require UNC-31 for tethering DCVs to the plasma membrane for release [71, 81], but before this, neuropeptides needed to be processed into their active forms by a variety of enzymes including EGL-3 (propeptide convertase 2) and EGL-21 (carboxypeptidase E) [125], with degradation carried out by neprilysins [121, 126, 127].

Functionally, at least 20 ILPs [120] and FLP-18 [121] have been associated with fat accumulation, FLP-1, FLP-18 [121] and 5 NLPs [128] are associated with locomotion, with NLPs involved in exciting (NLP-1A; NLP-2A; NLP-3C; NLP-10A) and inhibiting (NLP-8A) pharyngeal pumping [129], with NLP-24 binding to GPCR NPR-17 (both expressed on ASI neurons, a possible autocrine regulation mechanism) to stimulate pharyngeal pumping [130]. PDFR-1 promotes roaming [62], whilst NLP-12 and DOP-1 on DVA

interneurons post-synaptic to dopaminergic neurons respond to DA signalling to promote foraging in starvation [131], with FLP-11 and INS-1 involved in quiescence [132] . Overall, this shows despite >200 neuropeptides, many have not been characterised, which offers many genes to be investigated for roles in eating behaviours.

With the many advantages of this model organism, there are also caveats. *C. elegans* are an androdioecious species, having hermaphrodites and males, so studying sex-specific differences in the worm cannot be directly translated to human male/female sex-specific differences. Humans also have many other neuropeptides, neurotransmitters and dedicated brain structures e.g. the hypothalamus that are known to play roles in eating behaviour that are not present in the worm. Whilst this complex signalling between organs that effect behaviour might be missed in *C. elegans*, the fundamental processes of eating and sleeping behaviour are still conserved.

Project aims

There are still several unanswered questions related to how SKN-1B effects behaviour. How does SKN-1B signal from ASI neurons to effect exploratory behaviour? Why does loss of *skn-1b* only effect exploratory behaviour in hermaphrodites? What genes does SKN-1B effect? By understanding how these behaviours are controlled in worms will give us better insight into how these behaviours might be controlled in higher organisms, i.e. humans, to understanding overeating and undereating. This is especially promising, as SKN-1B is a mammalian homologue of NRF which is yet to investigated for a role in eating behaviour, offering a potential drug target for eating pathologies.

To answer these questions, the project focused on three key aims:

Aim 1: Determine how SKN-1B acts to signal from the ASIs to the rest of the worm

How SKN-1B signals from the ASI neurons is still unknown. Neurotransmitter and neuropeptide mutants were used to explore whether epistatic behavioural interactions occur with *skn-1b* mutants, determining if these neuromodulators are needed for SKN-1Bs role in exploration.

Aim 2: Determine why there are sex differences between hermaphrodite and male *skn-1b* mutants

It is unknown why hermaphrodite *skn-1b* mutants have reduced exploration, but male *skn-1b* mutants do not. To understand this, further characterisation of male exploration behaviour, mitochondria and *skn-1b* expression patterns were performed.

Aim 3: Identify SKN-1B target genes that contribute to its behavioural effects

The Tullet lab have generated RNA-Seq data comparing fed N2 vs *skn-1b(tm4241)* mutants, revealing 69 differentially expressed genes. RNAi was performed on these genes with N2 and *skn-1b* mutants in combination with an exploratory assay to reveal direct or indirect SKN-1B target genes implicated in exploratory behaviour. This was complemented by bioinformatic analysis of the 69 genes to determine whether these targets were direct.

Materials and Methods

Worm husbandry

Worm husbandry was performed following standard protocol [16], with either a platinum or eyebrow pick used for transferring worms between agar plates. See Table 3 for all reagents used. Worms were maintained at 20°C and fed OP50-1 (streptomycin-resistant) *E. coli* unless stated otherwise (and will be abbreviated to OP50-1 henceforth). OP50-1 was grown overnight (O.N.) for ~16 h in 250 mL conical flasks in 50 mL LB + 100 µL streptomycin sulfate (17.2 mM in dH_2O) and 50 µL nystatin (10.8 mM in DMSO).

NGM (Nematode Growth Medium) plates were made following standard protocol [16]. For a typical 1 L NGM solution: 3 g NaCl, 17 g agar, 2.5 g Bacto™ Peptone and 1 L of dH_2O were mixed, autoclaved, then cooled to 55°C. 25 mL KH_2PO_4 (1 M, pH 6) was added, and 1 mL each of the following: MgSO4 (1 M), $CaCl \cdot 2H_2O$ (1 M), cholesterol (12.93 mM in EtOH), nystatin and 2 mL streptomycin. 6 cm or 3.5 cm agar plates were filled with 10 mL or 5 mL NGM, respectively and dried O.N. before seeding with bacteria.

M9 was made (1 L) using 7g $Na_2HPO_4 \cdot 2H_20$, 3 g KH_2PO_4, 5 g NaCl, 0.25 g $MgSO4 \cdot 7H_20$ and 1 L dH_2O, mixed, then autoclaved.

Table 3. Reagent list.

Name	Supplier	Serial number
Agar	Melford	9002-18-0
Ampicillin	Melford	A40040-25.0
Aztreonam	Sigma	A6848-50MG
Bacto™ Peptone	Becton, Dickinson and Co	211677
BODIPY™ 493/503	ThermoScientific	D3922
Calcium chloride dihydrate ($CaCl \cdot 2H_2O$)	Melford	10035-04-8
Cholesterol	Sigma	C8667-5G
CyGEL™	BioStatus	CY10500
Isopropyl β- d-1-thiogalactopyranoside (ITPG)	Melford	I56000-25.0
Magnesium sulfate anhydrous ($MgSO_4$)	Melford	M24300-1000.0
Magnesium sulfate heptahydrate ($MgSO_4 \cdot 7H_2O$)	Sigma Aldrich (BioXtra)	M5921
Miller's Luria Broth (LB)	FisherScientific	BP9723-500
Nystatin	Melford	N82020-5.0
Potassium phosphate monobasic (KH_2PO_4)	Melford	P41200-1000.0
Sodium chloride (NaCl)	Fisher Chemical	S/3160/60
Sodium phosphate dibasic dihydrate ($Na_2HPO_4 \cdot 2H_2O$)	Sigma Aldrich (Fluka/BioXtra)	71645
Streptomycin sulfate	Melford	S62000-100.0
Tetracycline hydrochloride	Duchefa Biochemie	T0150.0025
Tetramisole hydrochloride	Sigma	L9756-10G

Strains and mutants

Strains used were: N2 CGCM, GA1058 *skn-1b(tm4241) IV*, CB928 *unc-31(e928) IV*, JMT91 *skn-1b(tm4241) IV; unc-31(e928) IV*, MT1241 *egl-21(n611) IV*, JMT92 *skn-1b(tm4241) IV*; *egl-21(n611) IV*, EG9631 *unc-13(s69) I*, JMT93 *unc-13(s69) I*; *skn-1b(tm4241)*, CX14295 *pdfr-1(ok3425) III*, MT14984 *tph-1(n4622) II*, JMT94 *tph-1(n4622) II*; *skn-1b(tm4241) IV*, MT1560 *cat-2(n4547) II*, JMT95 *cat-2(n4547) II*; *skn-1b(tm4241) IV*, MT13113 *tdc-1(n3419) II,* JMT96 *tdc-1(n3419) II; skn-1b(tm4241) IV*, MT9455 *tbh-1(n3247) X*, JMT97 *skn-1b(tm4241) IV*; *tbh-1(n3247) X*, SJ4103 *zcIs14 [myo-3::GFP(mit)]*, JMT90 *skn-1b(tm4241) IV*; *zcIs14 [myo-3::GFP(mit)]*,OH15262 *otIs669 V*, GA1017 *wuEx217[Pskn-1b/d::GFP]*, COP1836 *knu733[skn-1b::wrmScarlet] IV* and *otIs669 V/+*; *wuEx217[Pskn-1b/d::GFP]/+*.

All genetic cross genotypes were confirmed using PCR except JMT91 and JMT93 (screened for the unc phenotype) and JMT92 (screened for the bagging phenotype at 25°C). All crosses were confirmed for the *skn-1b(tm4241)* mutation using PCR (for primer sequences see Supplementary Table 1). No Chapter 2 mutants (*unc-31; egl-21; unc-13; pdfr-1; tdc-1; tbh-1; cat-2*; *tph-1* and associated *skn-1b* double mutants) were backcrossed due to time constraints, so all data from Chapter 2 has the possibility of being incorrect and influenced by previous background mutations.

RNAi

Whole organism RNA interference (RNAi) was performed by feeding worms with HT115 (DE3) RNAse III-deficient *E. coli* expressing RNAi in vector L4440 (abbreviated to HT115 (DE3) henceforth) [38]. RNAi were sourced from the library created by Dr Julie Ahringer's group [133] and distributed by Source BioScience. See Supplementary Table 2 for all RNAi constructs used.

RNAi NGM plates are standard NGM plates as described above, but ampicillin (134.6 mM in dH_2O) and IPTG (1 M in Milli-Q®) was added instead of streptomycin and nystatin at 1 mL each in a 1 L NGM solution.

Luria Broth (LB) ampicillin and tetracycline plates for RNAi were made (1 L) using LB broth (25 g), agar (17 g) and dH_2O (1 L), mixed, autoclaved then cooled to 55°C. 1 mL ampicillin and 1 L tetracycline (20.8 mM in DMSO) was added. 6 cm agar plates were filled to 10 mL with LB ampicillin and tetracycline mixture and dried O.N. before use.

HT115 (DE3) *E. coli* (ampicillin and tetracycline-resistant) were grown on ampicillin and tetracycline LB agar plates for 16 h at 37°C in a stationary incubator. After growth, 2-3 colonies were placed into a 250 mL conical flask containing 50 mL LB + ampicillin (50 µL) at 37°C in a shaking incubator for 16 h. Afterwards, bacterial cultures were concentrated by pouring into a 50 mL conical tube, then centrifuged at 2952 *g* for 10 mins to form a pellet. Supernatant was removed, and the pellet was resuspended in 10 mL fresh LB and seeded with 250 µL onto 6 cm and 3.5 cm RNAi agar plates. For the quicker RNAi screen, pellets were concentrated to 5 mL for all conditions, except to 10 mL for empty vector (EV) control.

Behavioural exploration assay

3 well-fed adult hermaphrodite worms were placed on 6 cm NGM agar plates seeded with OP50-1 for standard explorations. Well-fed worms were used as starvation can epigenetically influence progeny behaviour up to 3 generations [134].

Plates were placed for 3 days at 20°C then F1 L4 progeny were individually placed onto fully seeded (edge-to-edge) 3.5 cm plates (picking time: <2 h). Plates were placed at 25°C for ~16 h then immediately imaged (imaging time: <1 h) using WormLab (MBF Biosciences). Worms were noted to be alive if seen when taking images; plates where worms were clearly dead were not imaged. Images were superimposed onto a 121 square grid and the worm tracks were counted. The presence of a track(s) within a square was classed as 1 filled square, with a total of 109 squares as maximum (12 squares are not counted as it does not include the agar plate) (Fig. 6). Each track total was converted to a percentage, and the combined average across all biological repeats was used in all graphs shown.

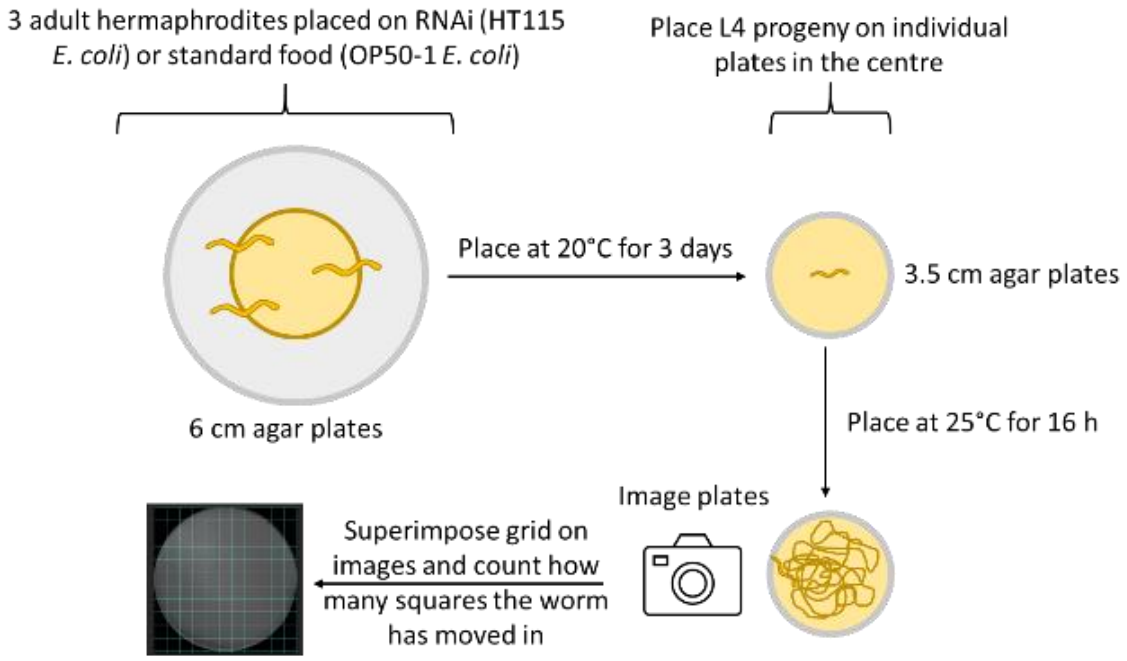

Figure 6. Schematic for an exploration assay. 3 adult worms were placed on 6 cm agar plates for 3 days at 20°C. L4 progeny were picked from these plates, then individually placed onto 3.5 cm plates for 16 h then imaged and analysed. For male explorations, 6 cm plates were used and placed at 25°C for 4 h then imaged (not shown).

For RNAi explorations, the standard protocol was performed except RNAi NGM plates were used and seeded with the respective HT115 (DE3) construct for the gene(s) of interest. HT115 (DE3) EV was used as a negative control for all experiments. N2 and *skn-1b(tm4241)* hermaphrodites were used for all experiments, both fed with the same HT115 (DE3) on separate plates.

For male explorations, the standard protocol was performed except 6 cm NGM agar plates were used for explorations (seeded edge-to-edge with 600 µL OP50-1) and placed at 25°C for 4 h then imaged. N2 and *skn-1b(tm4241)* males were used for all experiments, with males generated using heat shock (L4 hermaphrodites placed at 30°C for 5-6 h, then screened for male progeny).

Exploration plate preparation

After seeding with bacteria, edge-to-edge seeded agar plates were dried for 30-60 min with lids off at R.T., then dried with lids on for at least ~24 h before use. Plates were used after ~24 h to a week later with a ~20 min period of drying before use for exploration. Plates that had fungal contamination or dried out through visible agar separation from the sides of the plate were not used.

Thrashing

L4 stage worms were taken from plates using an eyebrow pick and placed in a 96-well plate filled with 1 mL of M9. Worms were given 30 sec to acclimatise to the M9 and allow any excess bacteria to be removed, then thrashes were counted manually for 30 sec. If worms had large amounts of bacteria attached to the cuticle, or showed obvious signs of damage, were not counted.

Microscopy

To prepare worms for microscopy, briefly, 2 microscope slides with thin tape were placed vertically onto a surface, then another slide was placed vertically between both slides without tape. 30 µL of 2% agarose was pipetted onto the non-taped slide, then another slide was then placed on top horizontally to create an agarose pad. 4 µL tetramisole hydrochloride (25 mM in M9) was added to the agarose pad, and worms were transferred to the pad using an eyebrow pick, covered with a rectangular cover slip then imaged on the Lecia DMR fluorescence microscope using HC PLAN S 10x /22 eye pieces, with the appropriate Lecia lens (HC PL Fluotar 10 x/0.30 and 20 x/0.50 lens, HCX PL Fluotar 40 x/0.75, and HCX PL APO 63x/1.40-0.60 oil), and imaged with a Leica DFC9000 GT using Lecia Application Suite X software. Filters used were i3 Ex 470/40 DAPI LP (yellow/green), GFP 495

525/50 (green) and N21 538/46 (red) controlled by *p*E-300^{ultra}. For inverted microscopy, an Olympus IX73 was used with a PlanApo 100x OTIRFM-SP 1.45 NA lens and processed using MetaMorph® (Molecular Devices) software. Slide preparation was the same as with fluorescence microscopy. For mitochondrial analysis, mitochondria between the mid body and tail were imaged using a HCX PL APO 63x/1.40-0.60 OIL lens for a maximum of 20 minutes, and if needed, a rectangular cover slip was used to roll worms into the correct orientation to image the mitochondria.

Bioinformatics

CeNGEN (https://cengen.shinyapps.io/CengenApp/), the *C. elegans* Neuronal Gene Expression Network single cell RNA-Seq (scRNA-Seq) project [124] was used to identify gene expression in every neuron in an L4 hermaphrodite. Data is given thresholds 1-4, with 1 being the least stringent with an 85% true positive rate (TPR) and 20% false discovery rate (FDR). 2 is 81% TPR and 14% FDR. 3 is 70% TPR and 10% FDR. 4 is the most stringent with a 58% TPR and 8% false discovery rate FDR. TPR gives the most accurate likelihood a gene expressed in the defined neuron, where FDR is the rate at which a gene might have been excluded from the data set when it is expressed in the neuron of interest. Threshold 2 was used for all analysis as recommended unless otherwise stated. ASI specific parameters for threshold 2 were: TPR: 80%, FDR: 22% and false positive rate: 11%, threshold 3 reduced the TPR to 56% justifying the use of threshold 2. 'All cells unfiltered' was an option used shows gene expression in both neuronal and non-neuronal tissues but has increased false discovery rates. Heat shock proteins were not identified as the cell extraction process can increase expression. Expression values are in transcripts per million (TPM) with no gene length normalisation that would normally occur with bulk RNA-Seq, with TPM rounded up to the first significant decimal figure e.g. 27.5278 is rounded to 27.5 TPM.

modENCODE (model organism ENCyclopedia Of DNA Elements) [135] was used to identify genes that had SKN-1 binding sites from L1-4 stage using the Snyder *skn-1::GFP* ChIP-Seq data set. modMine v33 28JUL2014 [136] was used for batch analysis of genes of interest (note modMine only analyses

from L1 to L3 binding, so L4 binding could not be determined). Binding score values are represented using *q*-values which is the *p*-value adjusted for FDR.

Nemanode [137] was used to create the hypothesised neural map which used EM images originally from Sulston and other groups to map chemical synapses and gap junctions. Only adult worms were used with only neuronal connections shown that have a minimum of 5 chemical synapses and 3 gap junctions.

WormCat [138] and SimpleMine [139] were used to screen the differentially expressed genes of the *skn-1b(tm4241)* mutant for GO terms, gene functionality and mutant phenotypes. STRING [140] analysis was performed to predict protein-protein interactions between these genes and SKN-1.

Statistics

Welch's t-test (two-tailed t test with unequal variance/heteroscedasticity) was used to calculate if there was a significance between samples of exploration. Chi-square test was used to calculate if there was significant difference between mitochondrial morphology. Statistical significance for all tests was $p = \leq 0.05$. Error bars represent standard error of mean ± SEM.

Chapter 1 results: SKN-1B requires neurotransmitters and neuropeptides to control exploratory behaviour

SKN-1B-related exploratory behaviour needs neuropeptide and/or biogenic amine release using UNC-31

Neurons such as ASIs use neurotransmitters and/or neuropeptides (including direct electrical signalling via gap junctions) to communicate to other neurons and tissues. For proneuropeptides to be processed into a mature form, EGL-21 is needed, with UNC-31 also needed to release neuropeptides and biogenic amines from the neuron (Fig. 5). How SKN-1B signals from ASI neurons to effect exploratory behaviour is unknown, so to explore whether neurotransmitters or neuropeptides are involved, *unc-31(e928)* and *egl-21(n611)* mutants alongside their respective double mutants with *skn-1b* were screened for an exploration phenotype (Fig. 7A and 7B).

skn-1b, *unc-31* and *egl-21* mutants all had reduced exploration compared to N2 worms (Fig. 7A and 7B), but the latter 2 mutants were not different in exploration to *skn-1b* mutants, although *unc-31* mutants sometimes had reduced exploration (data not shown). As *unc-31* mutants had an unc phenotype, it was unknown how much locomotion was being affected on a motor level, compared to having the ability to move, but choosing not to. To quantify this, a thrashing assay was performed which measures the physical ability to move due to forced swimming (Supplementary Fig. 1). *unc-31* mutants had reduced thrashing ability compared to N2 worms, *skn-1b* and *egl-21* mutants (p=<0.0001), with no difference between *skn-1b* (p = 0.199) and egl-21 (p= 0.323) compared with N2. This also confirmed the reduced exploration phenotype of *skn-1b* and *egl-21* mutants was not due to a physical inability to move.

With the double mutants, it was found *skn-1b; unc-31* mutants had significantly lower exploration than either N2 and *skn-1b* mutants, but not *unc-31* mutants i.e. the exploratory behaviour of *skn-1b* and *unc-31* mutations are non-additive (Fig. 7A), indicating neuropeptides and/or biogenic amines are likely needed for SKN-1B-related exploration. In contrast, the *egl-21; skn-1b* mutants had significantly lower exploration than N2, *skn-1b* and *egl-21* mutants, showing *skn-1b* and *egl-21*

mutations are additive for exploration (Fig. 7B). This indicates that neuropeptides are not needed for SKN-1B-related exploration, which was unexpected, as ASI neurons are likely peptidergic.

As well as biogenic amines, classical neurotransmitters are also needed in the worm for locomotion. To understand how classical neurotransmitters may interact with *skn-1b*, UNC-13, which allows classical neurotransmitter release from the synapse, like UNC-31 is needed for biogenic amines and neuropeptides, was screened using an *unc-13(s69)* mutant, and a double mutant of *skn-1b; unc-13.* Unfortunately, both the single and double mutant had low/no exploration (1-2 squares entered over 16 h, data not shown) due to its inability to move (did not thrash when placed in M9, data not shown), so due to its incompatibility with the exploration assay, it could not be used to interpret how classical neurotransmitters are needed in *skn-1b's* role in exploration.

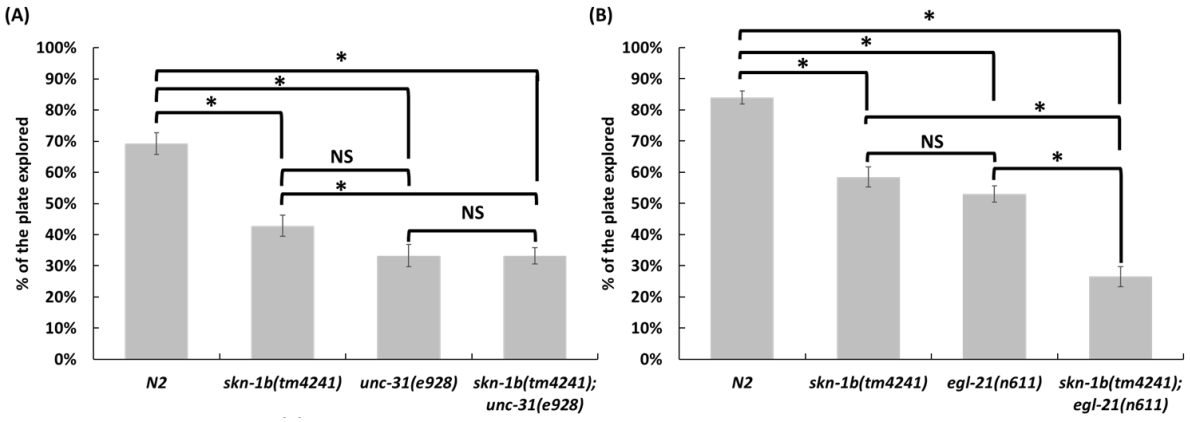

Figure 7. *skn-1b(tm4241); unc-31(e928)* mutant exploration is non-additive compared to *unc-31(e928)*, whereas *skn-1b(tm4241); egl-21(n611)* is additive compared to *skn-1b(tm4241)* and *egl-21(n611).* 16 h exploration of L4 hermaphrodites at 25°C. **(A)** All data points are significantly different (p=<0.031) from each other, except *skn-1b* mutants compared to *unc-31* mutants: p=0.0586, and *unc-31* mutants compared to *skn-1b*; *unc-31* mutants: p=0.989. Data is the average of 3 biological repeats with 10 worms each, except the third repeat for *skn-1b(tm4241)* which had 9 worms. **(B)** All data points are significantly different (p=<0.001) from each other, except *skn-1b* compared to *egl-21* mutants: p=0.188. Data is the average of 3 biological repeats with 10 worms per repeat, except the third repeat for *skn-1b* mutants which had 15 worms. **(A and B)** Asterisk (*) represents a significant difference using Welch's t-test (p = ≤0.05); NS represents no significant difference. Error bars represent ± SEM. Exact p-values can be found in Supplementary Table 2.

tdc-1; skn-1b mutants are non-additive in exploration with *skn-1b* mutants

Having established biogenic amines are required for SKN-1B related exploration, the contribution of how individually the 4 biogenic amines interact with SKN-1B to control exploration was investigated.

For this, individual biogenic amine synthesis mutants and double mutants with *skn-1b(tm4241)* were generated with each mutant's exploration tested (Fig. 8) e.g. *tdc-1(n3419)* for tyramine (TA) synthesis; *tbh-1(n3247)* for octopamine (OA) synthesis; *cat-2(n4547)* for dopamine (DA) synthesis and *tph-1(n4622)* for serotonin (5-HT) synthesis.

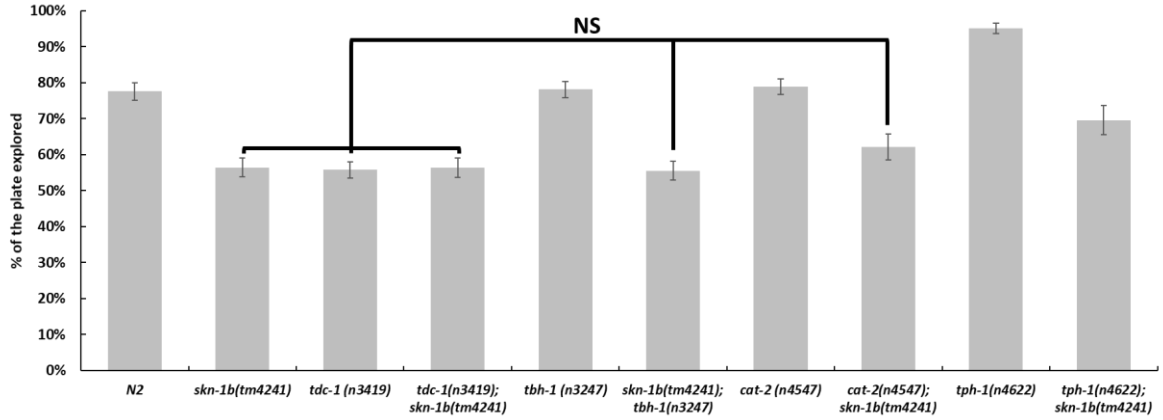

Figure 8. Of the 4 biogenic amines, tyramine is likely involved in exploration with *skn-1b*. 16 h exploration of L4 hermaphrodites at 25°C. All data points are significantly different (p=<0.046) from each other except *skn-1b, tdc-1*, *tdc-1; skn-1b*, *skn-1b; tbh-1* and *cat-2; skn-1b* mutants. *N2*, *tbh-1*, and *cat-2* mutants were not significantly different from each other. *tph-1; skn-1b* mutant exploration was not significantly different from N2, *tbh-1* and *cat-2; skn-1b* mutants. *tph-1* mutants had significantly increased exploration compared to all other genotypes. Data is the average of 3 biological repeats with 15 worms per repeat, except for *skn-1b*, *tdc-1*; *skn-1b*, *cat-2; skn-1b* and *tph-1; skn-1b* mutants which had 1 repeat with 14 worms, and *skn-1b; tbh-1* which had 1 repeat with 13 worms. NS represents no significant difference. Error bars represent ± SEM. Exact p-values can be found in Supplementary Table 2.

When testing exploration of the individual biogenic amine synthesis mutants, OA (*tbh-1*) and DA (*cat-2*) mutant exploration was no different to N2 worms, indicating the loss of these neurotransmitters caused no obvious difference in exploration. Yet upon introduction of the *skn-1b* mutation, both double mutants had exploration reduced to *skn-1b* mutant levels. This would indicate a role for these genes in SKN-1B-related exploration, but as no exploration change was seen with these mutants before the introduction of *skn-1b*, it indicates these genes are likely not involved in SKN-1B-related exploration. This is similar to 5-HT (*tph-1*) mutants, although *tph-1* mutants have increased exploration compared to N2 worms, but with the *skn-1b* mutation introduced, *tph-1; skn-1b* exploration was decreased, but not to *skn-1b* levels, indicating both mutations likely act in opposition of each other, as exploration is not the same as *tph-1* or *skn-1b* mutants individually.

However, with the TA (*tdc-1*) mutant, exploration was the same as the *skn-1b* mutant, as was the *tdc-1; skn-1b* double mutant. As both mutants caused no additive effect (Fig. 8), this indicated TA is likely needed for SKN-1B-related exploration.

Using the *C. elegans* connectome to understand SKN-1B neural circuitry

To understand how TA could be involved in SKN-1B function, three bioinformatic tools were used. CeNGEN, a scRNA-Seq gene expression atlas of the L4 hermaphrodite nervous system was used to predict neuropeptide and receptor expression (you input genes, and it outputs the neuron/s where the gene is expressed). modENCODE, a database that includes transcription factor binding site location data of the entire *C. elegans* genome was used via modMine. modMine allows inputting of your genes of interest, and screens each gene for transcription factor binding sites i.e. SKN-1 using modENCODE data. Nemanode, an online connectome tool was used to establish all synaptic partners and gap junctions in ASI neurons, and how its partners may allow signalling to either RIM or RIC (Fig. 8), as well as literature to establish a hypothetical neural circuit.

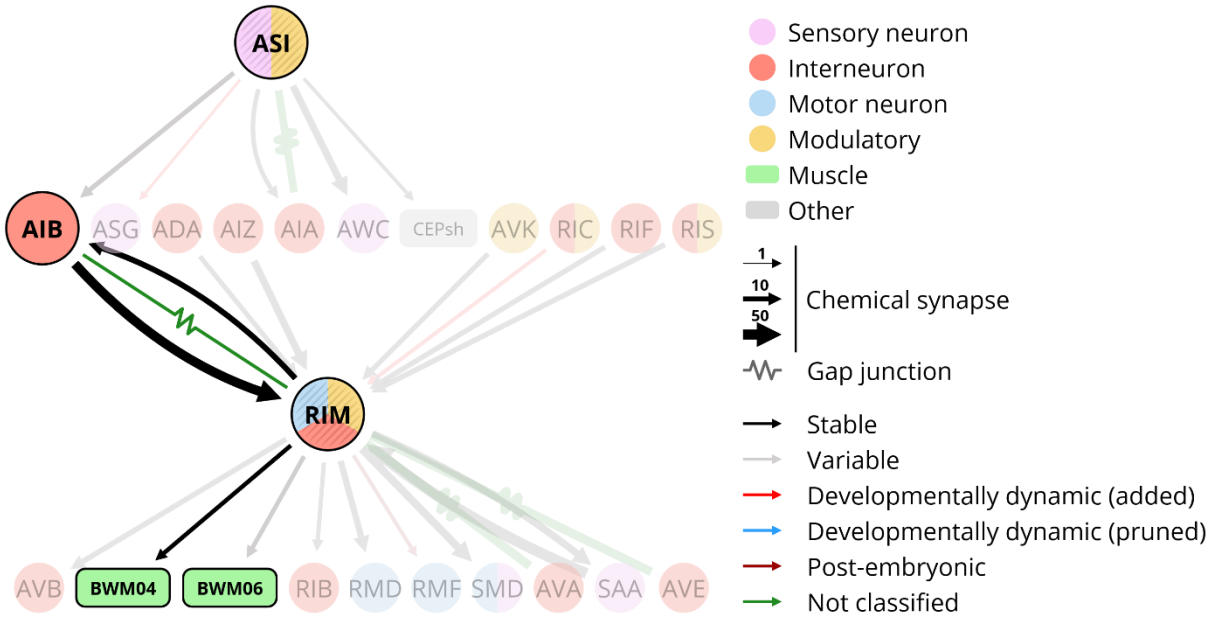

Figure 9. Interplay between ASI signals, interneurons and body wall muscle. Graphical representation where ASI signals to glutamatergic AIB interneurons, which signals to glutamatergic/tyraminergic RIM interneurons, which signal to body wall muscle. Data from Nemanode. 5 minimum chemical synapses and 3 minimum gap junctions. ASG only synapsed by ASIL (data not shown).

First, it needed to be established how ASI neurons would signal to RIM and RIC neurons that express TA. It was expected ASI neurons would indirectly signal to RIC or RIM interneurons, as ASI neurons are not close enough for direct synaptic connection [141], which was found to be true. ASI neurons are not predicted to have any pre-synaptic connections, but likely have 5 post-synaptic connections to CEPsh glia, AIA, ASG, AWC and, interestingly, AIB neurons (Fig. 9). AIB neurons are synaptic partners of RIM interneurons, and RIM can then signal to RIC, but also directly to body wall muscle, indicating possible control over these muscles e.g. for locomotion.

Now that the synaptic route was established for ASI to RIM neurons, the type of signalling to allow this was then investigated. ASI neurons could directly signal to AIB, which could then signal to RIM, or ASI could signal to RIM neurons through neuropeptides, as neuropeptide can target distant tissues [63, 65], so expression data from CeNGEN and literature was used to see what neuropeptides ASI express, which neuropeptide genes were predicted to be transcribed by SKN-1 using modMine, and of which neuropeptide receptors on AIB, RIC and RIM neurons would allow this communication.

ASI neurons were found to express all 3 neuropeptides groups: 15 ILPs, 7 FLPs and 19 NLPs, including PDF-1 and PDF-2 (Table 4), but no specific neuropeptides were expressed only in ASI neurons. To narrow down what neuropeptides SKN-1B might interact with, modMine was used to predict SKN-1 binding on all neuropeptides predicted and/or known in the ASI neuron. 5 neuropeptides (INS-30; NLP-14; NLP-21; NLP-55 and PDF-1) predicted to bind SKN-1 (Table 4), 3 of which have known receptors: INS-30 binds DAF-2; NLP-14 binds NPR-10 [105] and CKR-2 [142] whilst PDF-1 binds PDFR-1 to promote roaming [62].

Table 4. Neuropeptide expression (ILPs, FLPs and NLPs) in ASI neurons. Data from CeNGEN. All neuropeptides expressed in ASI neurons are shown. *ins-1* to *ins-39* and daf-28 were shown for the 40 ILPs, 15 were in ASI neurons. All 31 FLPs were analysed (*flp*-29 to -31 do not exist) with 6 expressed in ASI neurons. 77 NLPs were analysed, but -37 and -39 were missing from CeNGEN, 19 were in ASI neurons. Note *ins-8* and *ins-31* were not found in CeNGEN, so expression levels cannot be confirmed. Expression is in order of highest to lowest for each neuropeptide class. 5 genes were predicted binding of *skn-1::GFP* from modENCODE ChIP-Seq binding data via modMine, with those classified as being bound having significant *q*-values ≤0.05. Note, a CeNGEN caveat: *ins-7*, which interacts with *skn-1* does not have expression at any threshold (including unfiltered) in ASI neurons.

Neuropeptides	Gene	ASI expression level	Receptor	SKN-1 binding	Refs
Insulin-like peptides (ins)	*ins-26*	59850.96			
	ins-6	29091.49			[143]
	ins-3	28441.2			
	daf-28	15241.74			[144]
	ins-9	10514.11			[145]
	ins-30	10420.16		Y	
	ins-22	2671.652			
	ins-4	2175.561			[146]
	ins-5	1087.78			
	ins-24	871.4196			
	ins-18	468.982			
	ins-1	346.2353			[147]
	ins-21	156.5348			
	ins-32	106.126			
	ins-14	44.72563			
	ins-7	N/A			[148]
FMRFamide-related peptides (FLPs)	*flp-5*	4109.046			
	flp-9	1551.857			
	flp-7	284.217	NPR-22 [63]		[63, 65]
	flp-19	277.9623			
	flp-2				[149]
	flp-10				[149]
	flp-21				[149]
Non-insulin non-FLP (NLPs)	*nlp-57*	2270.663			
	nlp-14	727.9945	NPR-10 [105], CKR-2 [142]	Y	[128]
	nlp-21	723.3652		Y	
	nlp-1	682.8325	NPR-11 [105]		[128]
	nlp-3	367.5119			
	nlp-47	326.9626			
	nlp-80	204.9313			
	nlp-8	132.5721			
	nlp-7	121.5028			[128]
	nlp-55	70.9677		Y	
	nlp-27	2.244961			[128]
	nlp-25	1.651368			
	nlp-9	N/A	NPR-18 [105]		[128]
	nlp-18	N/A			[128]
	nlp-24		NPR-17 [130]		[128]
	nlp-6				[128]
	nlp-5				[128]
	pdf-2	93.76138	PDFR-1		
	pdf-1		PDFR-1	Y	[150]

Now that the most likely neuropeptides to be used by ASI in conjunction with SKN-1B were known, using CeNGEN, AIB, RIC and RIM were checked for DAF-2, NPR-10, CKR-2 and PDFR-1 expression. NPR-10 was not expressed in any neurons, CRK-2 was expressed in only AIB and RIM, whilst PDFR-1 and DAF-2 was expressed in all 3 neurons. Overall, ASI could possibly release INS-30 and PDF-1 to bind all 3 neurons via DAF-2 or PDFR-1, respectively, whilst ASI could release NLP-14 and bind to CRK-2 on AIB and RIM.

ASI neurons could also respond to feedback from RIM neurons via a TA receptor that might be dependent on SKN-1B expression, so all neurotransmitter synthesis genes, receptors, transporters, and degradation enzymes were analysed for SKN-1 binding using modMine and found at L3 stage that 4 of the 5 known TA receptors have SKN-1 binding sites (Table 5). This further supported the link between SKN-1B, ASI and TA.

Table 5. Predicted SKN-1 binding sites on the promoters of neurotransmitter receptors, the OA biosynthesis gene and a monoamine degradation enzyme. 36 genes that encompassed neurotransmitter synthesis genes, receptors, transporters, and degradation enzymes were analysed at L3 stage using modMine with the Synder *skn-1::GFP* ChIP-Seq data set. L3 stage was only included as it was more relevant to behaviours of L4 and adults. L4 data was not used as it was not compatible with modMine analysis. Significant *q*-values ≤0.05 are shown.

Gene	*q*-value	Function
tyra-2	0.009402	TA receptor
tbh-1	0.009766	OA biosynthesis
tyra-3	0.009819	TA receptor
ser-2	0.010789	TA receptor
amx-1	0.014464	Monoamine degradation
lgc-55	0.014465	TA receptor
lgc-53	0.018108	DA receptor
ser-7	0.02096	5-HT receptor

Chapter 1 discussion

Eating and sleeping behaviour is controlled through a variety of mechanisms, one of which is the nervous system. To understand the role of *skn-1b* for this behaviour, knowing which neurotransmitters and/or neuropeptides is used to allow *skn-1b* to signal from the ASI neurons was needed. To begin to address this question, 3 mutants that stopped release of classical neurotransmitters ACh, GABA and glutamate (*unc-13(s69)*), biogenic amines and neuropeptides (*unc-31(e928)*) and neuropeptide processing (*egl-21(n611)*) were screened for an exploration phenotype. This allowed a broad 'net' to be cast to understand if exploration involving *skn-1b* needs either classical or biogenic amine neurotransmitters, neuropeptides, a mixture of these molecules or none.

SKN-1B signals using biogenic amines and/or neuropeptides

To narrow down if SKN-1B related exploration needed neurotransmitters or neuropeptides, *unc-31* and *egl-21* mutants were used and found *unc-31; skn-1b* mutants were non-additive (Fig. 7A), indicating that SKN-1B acts either through biogenic amines or neuropeptides. Thrashing assays showed a reduced movement with *unc-31* compared to *skn-1b* mutants (Supplementary Fig. 1), likely effecting exploration ability. This added a variable to the interpretation of the data, as ASI neurons use UNC-31 to release neuropeptides [63], and reduced neurotransmitter and neuropeptide release in ASI neurons via tetanus toxin light chain expression to cleave synaptobrevin reduces exploration [72], indicating that SKN-1B needs neuropeptides and/or biogenic amines for normal exploration behaviour. Yet *egl-21; skn-1b* double mutants (Fig. 7B) had significantly lowered exploration compared to both *skn-1b* and *egl-21* mutants alone i.e. an additive effect, indicating neuropeptides are not needed for SKN-1B-related exploration. This was unexpected and could be due to several reasons:

1) No backcrossing of the *egl-21(n611)* strain occurred, so there may be additional mutations causing this additive effect.

2) The double mutant may have reduced capacity for locomotion. This is unlikely, as an unc phenotype was not seen when using these mutants, and both individual mutants had normal thrashing (Supplementary Fig. 1). For future validation, thrashing assays of all double mutants could be performed to learn if locomotion was affected.
3) If backcrossing and thrashing assays do not change the double mutants phenotype, then it would indicate SKN-1B signals without neuropeptides. This is highly unlikely as ASI neurons are likely peptidergic [63, 72] and need EGL-21 to process neuropeptides to their active form. It is likely quiescence is abolished in these double mutants, as *egl-21(n476)* mutants do not quiesce (at least, after fasting-then-refeeding at 3 or 6 h) [4], which occurs with *daf-11; skn-1b* and *daf-7; skn-1b* double mutants [39]. Lack of quiescence, but no roaming, would only allow dwelling to occur, and presumably, *skn-1b* mutants would have originally dwelled less if they quiesced more, so the reduced dwelling of *skn-1b* mutants may have been "carried over" into the double mutant. Simply, it could indicate ASI's can use other non-peptidergic and non-canonical neurotransmitters to signal via SKN-1B to effect exploration which is reduced in this mutant e.g. electrical signalling.
4) This may link with the hyperfused mitochondria of *skn-1b* mutants [39], as dysfunctional mitochondria (either not being transported into axons via RIC-7, or disrupting mitochondrial ROS breakdown via SOD-2) triggers hypoxia which causes reduced neuropeptide (NLP-21) secretion [151]. If the *skn-1b* mutation affects mitochondria and reduces neuropeptide secretion, which would cause reduced exploration, introduction of the *egl-21* mutation to completely abolish neuropeptide processing may cause mitochondria to even further be affected, which would decrease exploration further in this double mutant. Are the mitochondria effected first, which then causes neuropeptide decrease to reduce exploration, or vice versa?

Due to this confusing result, individual neuropeptide mutants could have been screened for involvement in SKN-1B-specific exploratory behaviour. But as there are >140 neuropeptide genes [120, 121, 124], screening all >140 neuropeptides was not feasible in the time given. Performing an RNAi

screen for neuropeptide and neuropeptide receptors with a neuron-sensitive RNAi strain (*eri-1; lin-15b* [130]) [152], and ASI-specific RNAi [105] could be performed to narrow down potential genes involved in SKN-1B exploration. Neuropeptide and neuropeptide receptor mutants could also be used. One neuropeptide receptor mutant was investigated in this thesis, PDFR-1, the PDF receptor. PDFR-1 was chosen as it had the most reduced roaming of 57 other mutants screened in a previous study [62], and is needed to promote roaming behaviour, possibly the same role as SKN-1B. Exploration of *pdfr-1(ok3425)* mutants was very low (~12%, Supplementary Figure 2), and distinguishing between an additive or non-additive effect with a *skn-1b;pdfr-1* double mutant would be unfeasible without tracking technology to differentiate between the 3 behavioural states (caveats for the exploration assay will be discussed in Chapter 3). For future study, PDFR-1 ligand mutant *pdf-1(tm1996)* could be used, as its reduced exploration phenotype is less severe than PDFR-1 [62]. PDF-1 is also predicted to be transcribed by SKN-1 (Table 4) which may link with the possible neural circuit between ASI releasing PDF-1 to act on the PDFR-1 receptor on AIB and RIM, as well as other neurons.

Neuropeptides known to be expressed in ASI neurons (Table 4) and/or already known to have a role in eating behaviours could investigated first e.g. *ins-1* RNAi increases quiescence [132], as does the *nlp-24(tm2105)* mutant (usually expressed in ASI neurons), with reduced roaming and increased dwelling and quiescence [130], similar to the *skn-1b* mutant. Whereas *flp-11* RNAi decreases quiescence [132], showing an interaction but a functional distinction between neuropeptide classes. NLP-14 is released from ASI neurons through TA binding to TYRA-3 on neurons that activate ASI neurons, among other neuropeptides to inhibit aversive behaviour [105], so could also be investigated. ASI can also inhibit ADL using NLP-14, which binds to NPR-10 on ADL neurons, indicating ASI and ADL are linked [105], which should be further investigated as ADL neurons express SKN-1B in starvation [39].

For neuropeptides and receptors that are uncharacterised but may have functionality in SKN-1B signalling, a current project by Oliver Hobert's group is currently undergoing to create an atlas/map

of neuropeptide expression in *C. elegans* alongside a project to match all neuropeptides to their respective GPCR (https://worm.peptide-gpcr.org/project/). This, alongside the neurotransmitter atlas and scRNA-Seq data from CeNGEN would allow better identification of neuropeptides and their following receptors needed for SKN-1B signalling.

Overall, from this first set of data, it showed that SKN-1B-specific exploratory behaviour requires biogenic amines, but neuropeptides needed to be investigated in future study. Fortunately, individual biogenic amine mutants were more feasible to analyse, so were investigated for a role in SKN-1B-related exploration.

Tyramine (TA) is likely needed for SKN-1B-specific exploratory behaviour

The four biogenic amines 5-HT, DA, TA and OA are all involved in food-related behaviours [62, 90, 94, 98], therefore exploration behaviour for all four biogenic amine synthesis mutants was investigated. Tyramine is likely needed for SKN-1B exploration, as only loss of TA and OA (*tdc-1*) in both single and *skn-1b* double mutant backgrounds was non-additive in exploration. Loss of either OA (*tbh-1*) or DA (cat-2) had no effect on exploration, but *tbh-1; skn-1b* and *cat-2; skn-1b* mutants had exploration reduced to *skn-1b* mutant levels, indicating *tbh-1* and *cat-2* signalling is downstream of SKN-1B (Fig. 8 and Supplementary Table 2). Interestingly, loss of 5-HT *(tph-1)* increases roaming, yet introduction of the *skn-1b* mutation reduces exploration to N2 levels. Unlike the three other biogenic amine mutants, *tph-1* is the only one that is not reduced to *skn-1b* levels, indicating these pathways are likely in opposition of each other e.g. 5-HT promotes dwelling, whilst SKN-1B possibly promotes roaming.

Tyramine has been shown to have roles similar to SKN-1B e.g. in fasted *tdc-1(n3419)* mutants, roaming is reduced with dwelling and fasting quiescence increased, similar to fed N2 worms [90] and *skn-1b* mutants [39], strengthening the idea that TA and SKN-1B are linked in promoting quiescence after starvation-then-refeeding. However, fasted OA (*tbh-1(n3247))* mutants have the same phenotype as fasted *tdc-1(n3419)* mutants [90], suggesting OA may be needed more in starvation

than TA for SKN-1B signalling, but as OA is increased in starvation to trigger fasting quiescence [90], whereas SKN-1B supresses this [39] indicates this is unlikely. Also, as exploration of *tdc-1*, but not *tbh-1* mutants is the same as *skn-1b* mutants in fed conditions (Fig. 8), it overall suggests SKN-1B interacts with TA rather than OA.

To confirm these results, all biogenic amine mutants need to be backcrossed to the N2 background strain to confirm no background mutations have influenced exploration and other mutant alleles should be used, with all 3 behavioural states (roaming, dwelling and quiescence) quantified to allow better insight into the exact behavioural states SKN-1B influences with specific biogenic amines. Also, biogenic amines have many roles, so it cannot be ruled out that exploration was affected by loss of other functions e.g. DA effects egg laying [153] that may affect exploration outside of SKN-1B-specific exploration. It is also unknown if the precursor products for 5-HT (5-HTP) and DA (L-DOPA) synthesis can affect exploratory behaviour.

For future study to confirm OA does not affect exploration in fed conditions, exogenous OA supplemented to *tdc-1* and *skn-1b* mutants could be used. If exploration is unchanged upon supplementation, it would indicate TA is needed. Alternatively, neuron-specific inverted Cre-Lox recombination [62] could be used to insert *tdc-1* back only into RIC neurons and gonadal sheath cells in a *tdc-1* mutant background. This would allow normal TA and OA synthesis to occur but lose TA synthesis in RIM to confirm only TA loss in RIM affects exploration. Exogenous TA could then be used on *tdc-1* and *skn-1b* mutants to see in exploration is rescued. Further identification of which TA receptors are needed for SKN-1B signalling could then be investigated. If a TA receptor is identified to have the same exploration phenotype as *skn-1b* mutants, this mutant could be supplemented with TA to see if the phenotype is rescued to better understand TA and its receptors in the neural circuit for SKN-1B signalling.

SKN-1B in ASI neurons likely signals to RIM interneurons to effect food-related behaviour

With TA established to be needed for SKN-1B-related exploration, a proposed model of how this signalling was hypothesised. SKN-1B-expressing ASI neurons may syanpse to glutamatergic AIB interneurons which then signal via chemical synapse and/or gap junction to glutamatergic/tyraminergic RIM moto/interneurons, which can directly signal to body wall muscles to possibly regulate locomotion (Fig. 9). RIM is both a pre and post-synaptic partner of AIB, indicating both may signal each other in order regulate this behaviour.

AIB neurons expresse glutamate receptor GLR-5, and upon activation, triggers release of unknown neuropeptide/s to activate RIM neurons which inhibit feeding and promote roaming [154], strengthening this proposed neural circuit further. AIB can also inhibit RIM to trigger reversals via GLR-1 [154], showing despite the same neurotransmitters used, opposing effects can occur dependent on receptor.

This proposed neural circuit integrates into previous work on feeding behaviours. ASI, AIY and RIF promote roaming, but upon eating, 5-HT is released from NSM and HSN neurons, binding to MOD-1 on ASI, AIY and RIF neurons to inhibit these neurons and promote dwelling (feeding) [62]. Whilst dwelling, a transition to quiescence would be triggered if fully satiated. In fed conditions, ASI releases DAF-7, binds to DAF-1, inhibiting RIM and RIC neurons and promote quiescence. Yet in starvation, DAF-7 is repressed to relieve RIM and RIC neurons to promote roaming [23], with RIM likely directly innervate body wall muscle as suggested by this neural circuit model to physically trigger roaming (Fig. 9 and 10). This may answer how DAF-7 promoting quiescence is repressed by SKN-1B in fasted-and-refed conditions [39] as it is likely needed to promote roaming by signalling to RIM neurons.

This also indicates a caveat with pure connectome/neural circuit modelling, as it shows ASI does not synapse directly to RIM (Fig. 9), but likely requires direct extrasynaptic signalling with DAF-7 from ASI to DAF-1 on RIM. Extrasynaptic signalling occurs with neurotransmitters [93] and neuropeptides

(including ASI neurons [63, 65]), suggesting both direct synapsing and/or gap junctions and extrasynpatic signalling with other neurons to possibly control SKN-1B signalling occurs.

Neuropeptide PDF signalling is likely integrated with this circuit, as PDF-1 (which is predicted with CeNGEN to be released from multiple neurons, including ASI neurons) binds to PDFR-1 on RIM, RIA, AIY (and other neurons) to promote roaming [62]. PDF-2 is released from and binds to PDFR-1 on RIM neurons (autocrine) to decrease threat tolerance by signalling with TA to TYRA-2 on ASH neurons to cause aversion behaviour. However, in starvation, RIM is inhibited, which inhibits ASH aversion behaviour, but increases threat tolerance (and increases the longer the starvation). As the worm would die without food, being able to tolerate/not respond to danger cues that would normally be present in well fed conditions is understandable [155]. TA can also bind to TYRA-3 on ASI neurons which through various signalling (including inhibition of 5-HT signalling), inactivates ASH neurons to stop aversive behaviour [105]. TYRA-3 promotes food leaving in ASK neurons [104] whereas in starvation (once food is found) TA receptor SER-2 inhibits food leaving via XBP-1 (expressed in RIM and RIC) [100]. This is more akin with *skn-1b* mutants who do not leave the bacterial lawn [39]. As ASI neurons express TA GPCRs TYRA-2 [101] and TYRA-3A [105], and with SKN-1 modENCODE data at L3 stage revealing SKN-1 potentially binds *tyra-2* and *tyra-3* (Table 5), indicates SKN-1B and RIM may be linked through these receptors. ASI neurons also have 5-HT (SER-1) and OA (SER-6) receptors [86], indicating a multitude of signalling is involved to be investigated.

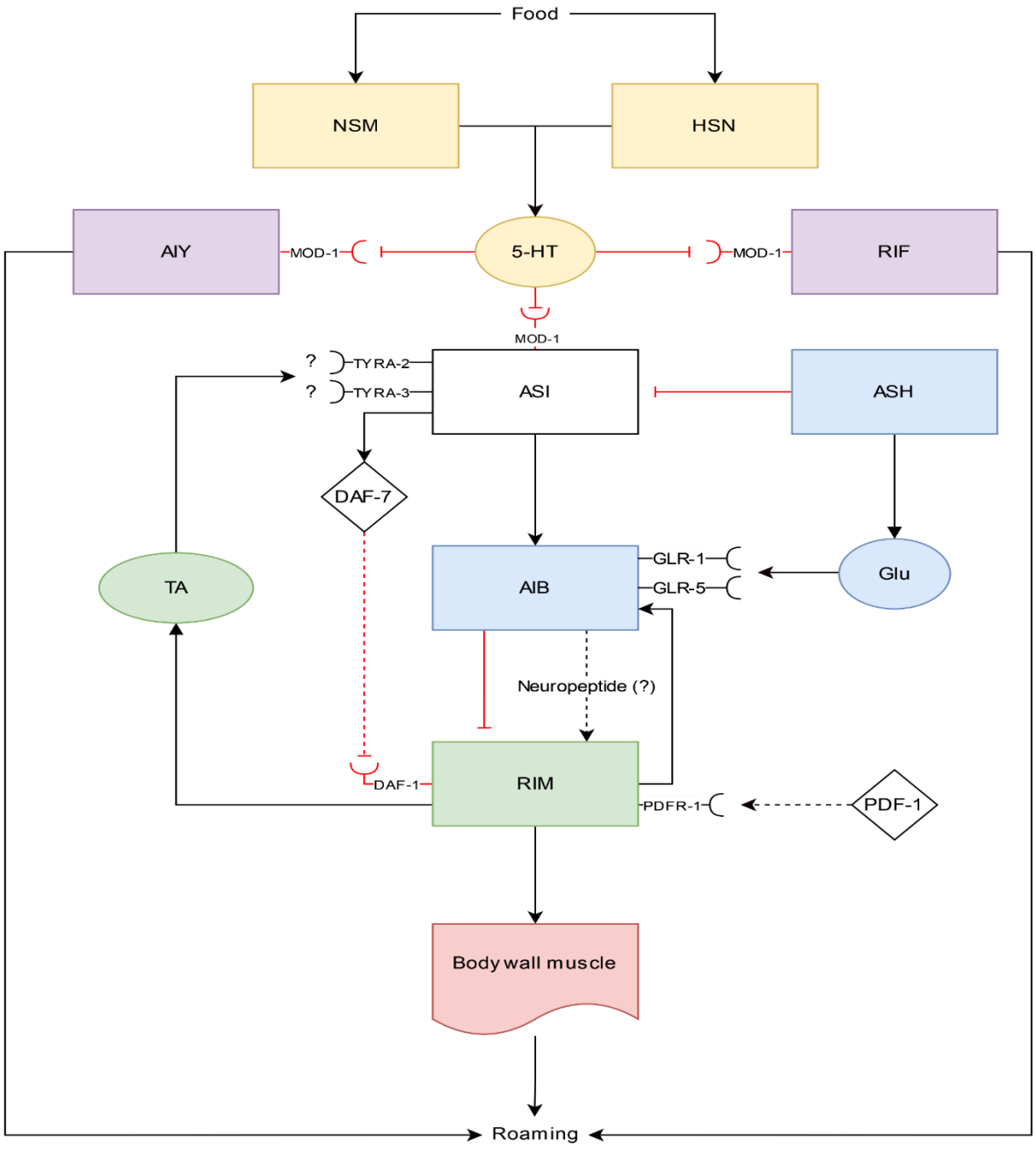

Figure 10. Proposed neural circuit integrating SKN-1B into the exploration pathway. In the presence of food, NSM and HSN neurons release 5-HT to inhibit AIY, RIF and ASI neurons, stopping roaming and promoting dwelling. ASI neurons can possibly signal directly via AIB. ASI neurons can release DAF-7 in fed conditions to inhibit RIM neurons, but upon starvation and refeeding, it is likely SKN-1B represses DAF-7 (not shown), allowing RIM to be active, signal to other neurons (not shown) and innervate body wall muscle to promote roaming. AIB can be activated by glutamate (Glu) from ASH, and depending on the receptor Glu binds, AIB can activate or inhibit RIM neurons (GLR-5 or GLR-1, respectively). PDF signalling is likely involved as it promotes roaming through binding to RIM and other neurons. Other neuropeptides e.g. INS-30, NLP-14 are possibly released from ASI onto RIM for these behaviours (not shown). RIM likely regulates many neurons using TA, including ASI, but how this may affect SKN-1B is yet unknown. Yellow: serotonergic neurons. Purple: cholinergic neurons. Blue: glutamatergic neurons. Green: Tyraminergic neurons (note RIM also releases glutamate, not shown). No colour: no known neurotransmitter/peptidergic. Squares are neurons, circles are neurotransmitters and diamonds are neuropeptides. Red lines with a dash: inhibitory. Made using diagrams.net/draw.io.

In addition of TA signalling, other neurotransmitters and neuropeptides likely have a role in SKN-1B signalling to yet be investigated and integrated into this neural circuit. CeNGEN data predicted ASI neurons could release INS-30 which could bind to DAF-2 on AIB, RIC or RIM neurons, and ASI neurons could release NLP-14 and bind to CRK-2 on AIB and RIM neurons. Another example is ASH neurons are sensitised by food or 5-HT to release neuropeptide NLP-3 which binds to NPR-17 on ASH (autocrine) to stimulate aversive behaviour. This is regulated with OA, that activates $G\alpha_o$ in ASH neurons which inhibit $G\alpha_s$ and $G\alpha_q$, both of which are needed to activate ASH, with $G\alpha_s$ specifically needed to release NLP-3 [156]. Whereas in starvation, NLP-24 expression is increased 5X and promotes pharyngeal pumping (feeding) through binding to NPR-17 on ASI neurons. How and if SKN-1B is involved is this starvation response is yet unknown. NPR-17 is also expressed in the intestine, but seemingly has no role in promoting pharyngeal pumping (note NLP-24 is increased in the intestine in starvation, so these might interact for another function – readying the intestine for influx of food?) [130].

Overall, this indicates TA signalling, but likely a host of different neurons, neurotransmitters and neuropeptides are possibly involved in normal SKN-1B-related exploration.

Future study

Repeat experiments under fasting-and-refed conditions with specific-SKN-1B rescue in ASI or ADL

All experiments were performed in well fed conditions, but as SKN-1B's function changes in starvation [39], as do the biogenic amines, experiments should be repeated in fasted and refed conditions to better understand how SKN-1B signalling changes with biogenic amines in fed and starved states. The *skn-1b::gfp* reporter crossed with the biogenic amine synthesis mutants could show if biogenic amine loss effects SKN-1B expression. If certain biogenic amines are more relevant for SKN-1B in starvation, SKN-1B-specific rescue in ASI or ADL (ADL expresses SKN-1B in starvation [39]) in *skn-1b* mutants would reveal if ASI, ADL or both are needed for SKN-1B's starvation response.

RT-qPCR of biogenic amine synthesis genes in *skn-1b* mutants may also show if there is a change in starvation compared to fed.

5-HT and DA is possibly downregulated in *skn-1b* mutants, increasing fat content

Loss of 5-HT (*tph-1(mg280)*) increases fat storage, but reduces DAF-7 expression in the ASI neurons [85]. ASI can control fat storage in the intestine via GPCR STR-2 (Watts lab, unpublished) and as *skn-1b* mutants have increased DAF-7 [39], this indicates fat storage is either normal in these worms, or is decreased. But other data suggests *skn-1b* mutants have increased fat stores due to being slightly larger, having downregulated *cat-4* (needed for 5-HT and DA synthesis [111], Supplementary Table 3) and being in a starved state (linking with 5-HT being downregulated in starvation [157]), indicating these mutants cannot access energy stores, one of which might be the inability to trigger fat breakdown. This possibly links with DOP-3 binding and supressing SER-3 and SER-6 OA G_q-coupled GPCRs to negatively regulate body size without affecting food intake or development [95]. As DA signalling might be reduced in *skn-1b* mutants due to *cat-4* downregulation, DOP-3 would no longer negatively regulate body size, and with possible increased OA signalling (discussed in Chapter 3) which would increase body size, shows how all biogenic amines are involved in SKN-1B signalling, either positively or negatively. How this links with the reduced exploration phenotype of *skn-1b* is unclear as 5-HT and DA promotes dwelling, which still occurs in *skn-1b* mutants, with *tph-1* and *cat-2* mutants having increased exploration over *skn-1b* and N2 (Fig. 8). This is likely receptor-dependent which is yet to be investigated.

To confirm fat levels in the *skn-1b* mutant, and double mutants if necessary, fat staining using BODIPY 493/503 could be used, with co-localisation with another lipid stain (LipidTOX deep red or Nile red [158]) at a different wavelength to confirm only fat is being stained by BODIPY. Lipid reporters or lipidomics could also be used. If there is increased fat content, receptor mutants for 5-HT and DA could be further investigated in the role of fat storage in the SKN-1B pathway. Alternatively, as will be discussed in Chapter 3, the increased size of *skn-1b* mutants might be to do with increased cuticle size and not fat storage.

Does loss of TA contribute to increased mitochondrial fission in the *skn-1b* mutants?

As TA is likely involved in exploration with SKN-1B, and exploration is rescued upon causing fission of the hyperfused *skn-1b* mutant mitochondria [39], would *tdc-1* mutants also have the same mitochondria as *skn-1b* mutants? Mitochondrial reporter SJ4103 *zcIs14 [myo-3::GFP(mit)]* is available to characterise mitochondrial fission and fusion states which would reveal the specifics of how TA contributes towards SKN-1B signalling, and if TA is needed for mitochondrial fission like SKN-1B.

Opposingly, the *tph-1* mutant and *tph-1; skn-1b* could be investigated, as the exploration reduction of *skn-1b* is rescued in the *tph-1* mutant background (Fig. 8). Would the mitochondrial phenotype of *tph-1; skn-1b* be rescued, or have hyperfission? If so, it would indicate TA and 5-HT have opposing effects both in exploration but also in mitochondrial dynamics e.g. TA promotes fission/roaming, whilst 5-HT promotes fusion/dwelling. How this links with the reduced *cat-4* expression (Supplementary Table 3) in *skn-1b* mutants is unclear.

OA likely has roles in SKN-1B signalling

RIC releases OA upon starvation, binding to OCTR-1, which is needed in ASI and ASH neurons to suppress the immune system (downregulates *pqn/abu* genes) through the UPR response. This allows the worm to find and eat a larger variety of food types, even if not nutritionally beneficial [108], but RIC is inhibited upon exposure to pathogens to regulate this response [119]. *skn-1b* mutants are known to have no food preference compared to N2 [39], and with *pqn-73* downregulated in *skn-1b* mutants (Supplementary Table 3), this indicates the immune system in *skn-1b* mutants is possibly supressed, indicating increased OA signalling occurs in *skn-1b* worms (at least via OCTR-1). RT-qPCR could be used to see if OA synthesis is changed in *skn-1b* mutants, or a SKN-1B::GFP reporter could be crossed with the biogenic amine mutants to see if expression is increased or reduced upon loss of biogenic amines as previously suggested. This would strengthen the idea *skn-1b* mutants act as if in a starved state, but this goes against the exploratory phenotype expected: OCTR-1 would promote

roaming, whereas the *skn-1b* mutant has reduced exploration. Data indicates SKN-1B would be upstream of OA signalling in terms of exploration, even if OCTR-1 is bound. This indicates multiple receptors and complex signalling are needed to regulate the drive for roaming in starvation, but also triggering the most optimal time for dwelling and quiescence to occur. Further characterisation of OCTR-1, OA and SKN-1B is needed e.g. in starvation.

Summary

In this chapter, three major conclusions were found. 1) SKN-1B needs UNC-31 for release of biogenic amines and/or neuropeptides for its release. 2) TA is likely needed for normal SKN-1B signalling. 3) SKN-1B expressing ASI neurons and tyraminergic RIM interneurons are connected via AIB interneurons for a possible circuit of communication, with ASI possibly signalling to AIB and/or RIM via DAF-7 release, with RIM innervating body wall muscle as a possible route to control SKN-1B-related exploratory behaviour.

Chapter 2 results: Sex differences between hermaphrodite and male *skn-1b(tm4241)* mutants

L4 *skn-1b* mutant males have significantly reduced exploration than L4 N2 males, but no exploration difference occurs with adult N2 and *skn-1b* males

Males, like hermaphrodites, have the three exploration behaviours (roaming, dwelling and quiescence), but unlike hermaphrodites, males also have a sex-specific behaviour: mate searching. Mate searching can overtake food-related behaviours for the male to find a hermaphrodite to mate with [21, 31]. As shown previously by the Tullet lab [39], *skn-1b* mutant hermaphrodites have decreased roaming and increased dwelling. Interestingly, in the original study of *skn-1b*, male *skn-1b* mutants exploration was also tested, and found that Day 1 adult (D1) male N2 worms and *skn-1b* mutants had no significant difference in exploration [39]. This indicated that the effect of *skn-1b* on appetite behaviours like exploration might be sex-specific.

The exploration assay used with hermaphrodites was on 3.5 cm NGM plates for 16 h, but it was found both N2 and *skn-1b* mutant males would explore the plate completely in this time, not allowing analysis of an exploration difference if it occured. Therefore, a 4 h assay on 6 cm plates was used, different from the 2 h assay used in the previous study [39], as 4 h was found to be enough time to produce enough worm tracks to analyse, but not cause the entire plate to be explored. 4 h explorations also had the advantage of allowing analysis of L4 males exploratory behaviour, which cannot perform sex-specific behaviours i.e. act similar to L4 hermaphrodites. Sex-specific behaviours can only occur once the male tail has fully developed, with the last male tail neurons differentiating at the end at the end of the L4 stage [159–161].

To investigate if the lack of an exploration phenotype in D1 *skn-1b* males is due to tail development that allows male-specific behaviours i.e. mate searching overtaking food-related behaviour, *skn-1b* males at L4 stage were used in an exploration assay for 4 h to see if they had the same exploration as D1 males (Fig. 11B). It was found that whilst both D1 N2 males and D1 *skn-1b* males explored more than N2 worms and *skn-1b* hermaphrodites in 4 h (Fig. 11A), it was found *skn-1b* L4 males had

reduced exploration compared to L4 N2 males (Fig. 11B), similar to the 16 h assays where *skn-1b* hermaphrodite exploration is reduced compared to N2 worms. This indicated the *skn-1b* mutant reduced exploration/dwelling phenotype was not sex-specific, but possibly repressed when males entered adulthood and their sex-specific behaviours take over food-related behaviours.

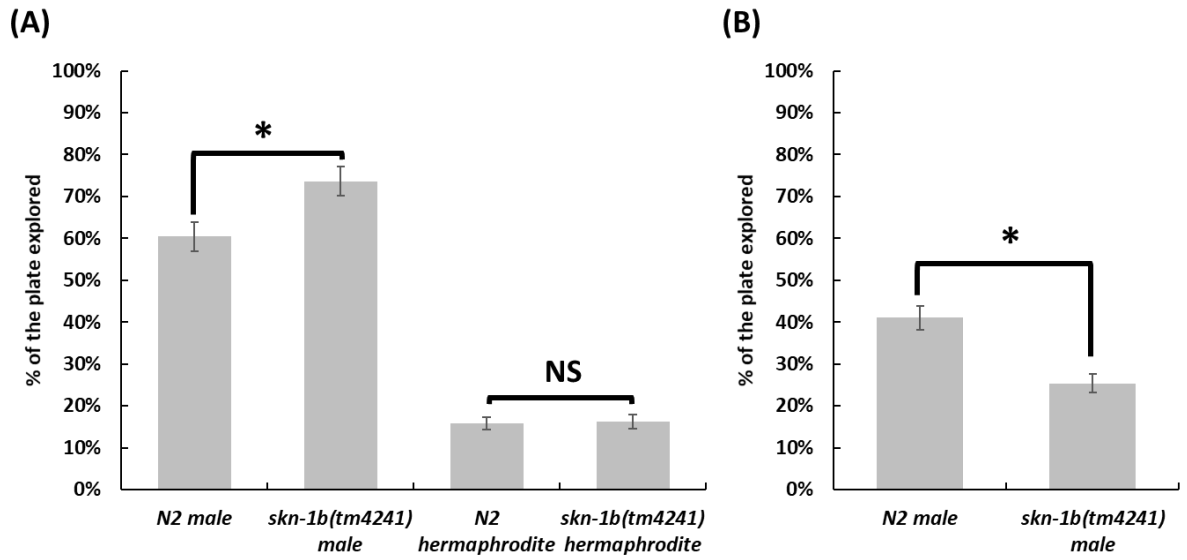

Figure 11. D1 *skn-1b* mutant males explore the same or more than D1 N2 males, but L4 *skn-1b* mutant males have significantly lower exploration than L4 N2 males. 4 h exploration at 25°C on OP50-1 seeded 6 cm NGM plates before imaging. **(A)** All significantly different from each other (p= <0.009), except between N2 hermaphrodites and *skn-1b* mutant hermaphrodites (p=0.84). Data is the average of 5 biological repeats in (A) for N2 males (total 47 worms) and *skn-1b* mutant males (total 43 worms), but 3 biological repeats for N2 and *skn-1b* mutant hermaphrodites (10 worms for each repeat, except one repeat with 8 for *skn-1b* mutant worms). **(B)** L4 N2 and *skn-1b* male mutants are significantly different (p=0.00005) in exploration. Data is average of 3 biological repeats, between 9-11 worms used for each repeat. Asterisk (*) represents a significant difference using Welch's t-test (p = ≤0.05). NS represents no significant difference using Welch's t-test. Error bars represent ± SEM.

Mature *skn-1b* mutant males do not exhibit altered mitochondrial networks

The *skn-1b* mutant hermaphrodite body wall mitochondria are highly fused (disorganised), which is found in nutrient-poor conditions [52], and was linked to the reduced exploration phenotype. This phenotype was rescued using RNAi on *fzo-1* and *eat-3* which inhibit mitochondrial fusion [39], indicating SKN-1B was involved in mitochondrial fission. As *skn-1b* was not needed in male adulthood for SKN-1B-related exploration, was SKN-1B also not needed for mitochondrial fission in males? It was suspected the normal exploration of D1 *skn-1b* mutant males (Fig. 11A) would indicate mitochondrial morphology would also be normal. Using fluorescence microscopy with a

mitochondrial body wall muscle reporter in D1 N2 worms and D1 *skn-1b* mutant males, it was found both D1 N2 and *skn-1b* mutant males had no difference in mitochondrial morphology (*p= 0.913,* Fig. 12), resembling N2 hermaphrodite worms previously reported [39], further indicating SKN-1B and food-related exploration is linked to mitochondrial dynamics, but not to male exploration.

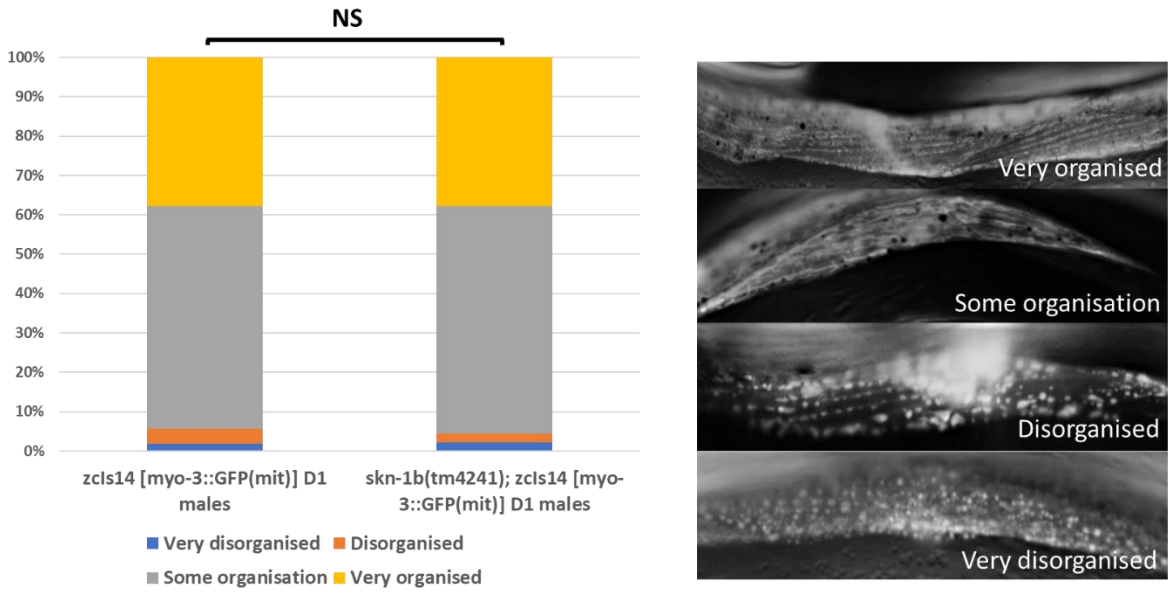

Figure 12. Mitochondrial morphology is not significantly different between D1 N2 and *skn-1b* males. D1 N2 and *skn-1b* males were not significantly different from each other (chi-square test, *p*=0.913). NS indicates no significant difference. 3 biological repeats were performed, with 16 worms for first trial, 19 and 18 second trial, 18 and 11 third trial, for a total 53 worms for *skn-1b::gfp* mitochondrial body wall muscle reporter (*zcIs14 [myo-3::GFP(mit)]*) over 3 trials, and 45 worms for *zcIs14 [myo-3::GFP(mit)]*; *skn-1b(tm4241)*. All images taken using a Lecia fluorescence microscope with a 63 x oil lens.

SKN-1B::GFP is exclusively expressed in or near the VA11 neuron near the male tail in D1 adults

As no change in exploration or mitochondria occurred in D1 *skn-1b* mutant males, the investigation turned to SKN-1B expression. It was presumed males may not have SKN-1B expression due to the lack of exploratory and mitochondrial defects, unlike in hermaphrodites where SKN-1B is expressed exclusively in the ASI neurons in well fed conditions [39]. To confirm if SKN-1B is expressed in D1 males, a *skn-1b::gfp* reporter was used.

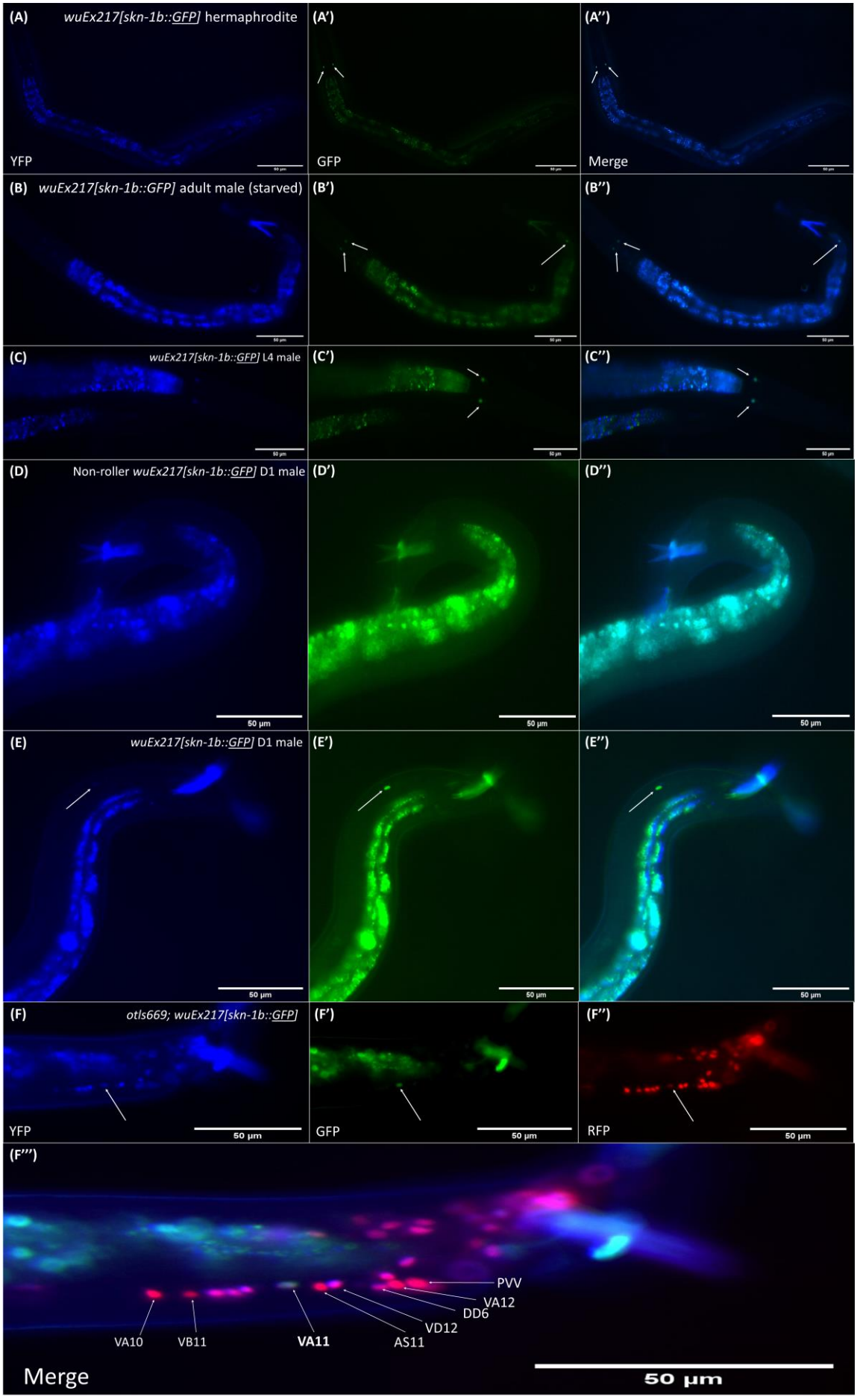
(A) wuEx217[skn-1b::GFP] hermaphrodite
(A') GFP
(A'') Merge
YFP
(B) wuEx217[skn-1b::GFP] adult male (starved)
(B')
(B'')
(C) wuEx217[skn-1b::GFP] L4 male
(C')
(C'')
(D) Non-roller wuEx217[skn-1b::GFP] D1 male
(D')
(D'')
(E) wuEx217[skn-1b::GFP] D1 male
(E')
(E'')
(F) otIs669; wuEx217[skn-1b::GFP]
(F')
(F'')
YFP
GFP
RFP
50 µm
(F''')
PVV
VA12
DD6
VD12
AS11
VA11
VB11
VA10
Merge
50 µm

Figure 13. SKN-1B::GFP is expressed in the ASI of L4 and D1 males, and in or near the VA11 exclusively in D1 males. (A-A'') SKN-1B::GFP expression in hermaphrodites only occurs in the ASI neurons. **(B-B'' and E-E'')** SKN-1B::GFP expression in adult males occurs in both ASI neurons and near the tail. **(C-C'')** SKN-1B::GFP expression in L4 males only occurs in ASI neurons. **(D-D'')** Negative control D1 male, with no SKN-1B::GFP expression. **(F-F''')** SKN-1B::GFP is expressed in or near the VA11 neuron in D1 males. **(A-F''')** YFP channel is pseudo-coloured blue for clarity, with GFP and RFP pseudo-coloured their respective colour. Merge represents YFP, GFP (and RFP for Fig. 3F) images overlaid. *wuEx217[skn-1b::GFP]* reporter was used with Lecia fluorescence microscope using a 20 x lens (A-C'') and 40X lens (D-F'''). Heterozygous *otIs669 V/+*; *wuEx217[Pskn-1b/d::GFP]/+* was used for neuron identification.

In fed conditions, L4 and D1 males expressed SKN-1B::GFP in ASI neurons like hermaphrodites (Fig. 13A-C). Unexpectedly, it was also expressed in one additional cell, near the tail (Fig. 13B and 13D) only in D1 males, and not seen near the tail of L4 males or hermaphrodites (Fig. 13A and 13C). Non-roller *wuEx217[skn-1b::GFP]* D1 males which had lost the transgene was used as a control for the general background of the strain to accommodate for non-specific fluorescence, also had no SKN-1B::GFP near the tail (Fig. 13E). Overall, this indicated SKN-1B tail expression was specific to adult males which was further confirmed using endogenous reporter *knu733[skn-1b::wrmScarlet]* (Supplementary Figure 3).

To identify which neuron near the tail SKN-1B was expressed in, a *skn-1b::gfp* reporter (*wuEx217[Pskn-1b/d::GFP]*) was crossed with the NeuroPAL strain *otIs669* [161, 162]. NeuroPAL visualises all neurons in the red fluorescence channel, to allow visualisation with the GFP reporter and perform co-localisation to identify your neuron of interest [162]. The identity of the neuron was approximated to be VA11, sex-shared ventral A (VA) motoneuron (Fig. 13F). Overall, this indicated SKN-1B has a sex-specific-role in the adult male, but the male-specific loss of *skn-1b* in both ASI and VA11 does not affect general exploration or mitochondrial morphology.

Chapter 2 discussion

Reduced exploration and hyperfused mitochondria are key hallmarks in hermaphrodite *skn-1b* mutants. Among other phenotypes of this mutant, it has been proposed the mutant is in a constant starved state, with SKN-1B involved in food-related behaviour [39]. The opposite is true in D1 *skn-1b* males, with no exploration reduction (Fig. 11) or disturbed mitochondria (Fig. 12), indicating *skn-1b* is not needed for these roles in the male and is likely not in a starved state upon its loss. However, *skn-1b* is expressed in the male, as evidenced by fluorescent SKN-1B reporter activity in the ASI neurons at L4 and D1 adult stages (Fig. 13B, 13C and 13E), but also has expression in or near the VA11 neuron only in D1 males (Fig. 13F and 14). This data indicates that SKN-1B expression is not translationally repressed in the male, and likely has both shared (ASI) and sex-specific functions (VA11). Interestingly, VA11 is a neuron present in both hermaphrodites and males, indicating a sex-specific mechanism is repressing SKN-1B expression in hermaphrodites, but also temporally in males, as VA11 is made post-embryonically at late L1 stage [32, 73], indicating sex-specific temporal repression occurs until adulthood. What could these mechanisms be and why are they used?

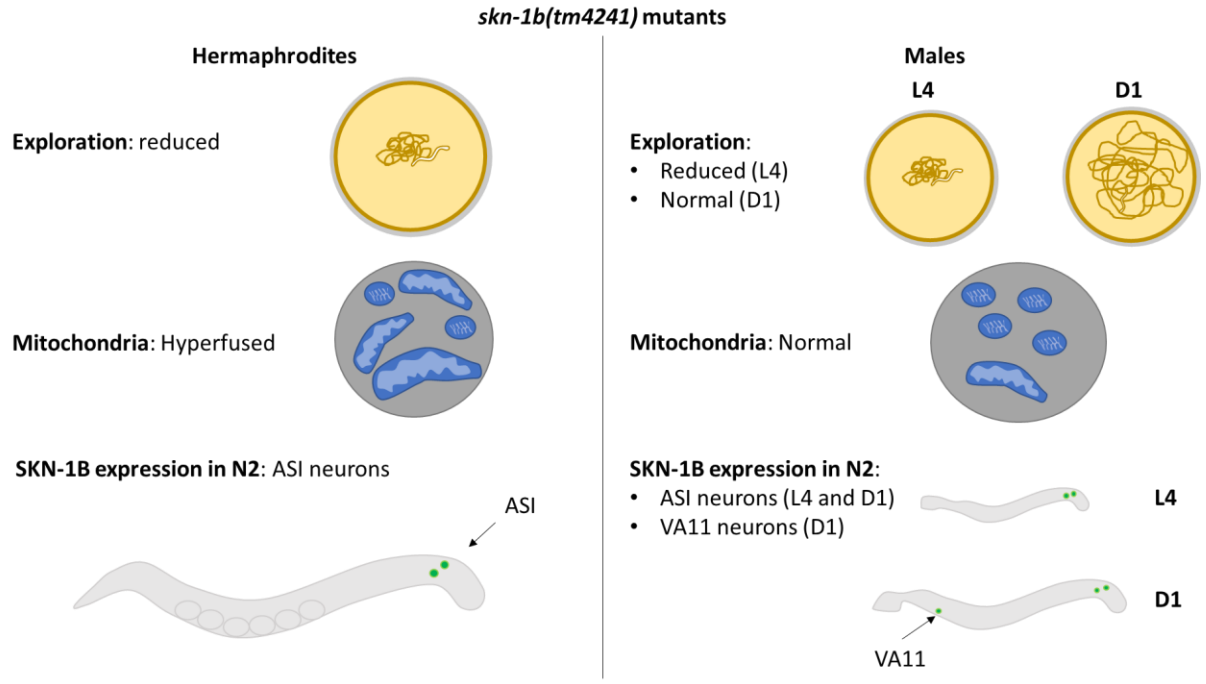

Figure 14. *skn-1b* mutant hermaphrodites and males have different phenotypes in exploration and mitochondrial morphology, with D1 N2 males expressing SKN-1B in VA11 neurons. D1 *skn-1b* mutant males have normal exploration and mitochondrial morphology. L4 *skn-1b* mutant males have reduced exploration like hermaphrodites (L4 male mitochondria have not been characterised). SKN-1B is expressed in ASI neurons in N2 hermaphrodites and N2 L4 and D1 males, with D1 males having sex-specific expression of SKN-1B in VA11 neurons.

Just-in-time differentiation may control temporal SKN-1B expression in D1 males

Male-specific neurons receive their final identity at the mid-to-late L4 stage, the same time specific male tail structures are made e.g. fans, rays and spicules. This is called "Just-in-time" differentiation, which occurs in both sexes, where synaptic identity is only finalised when the appropriate structure is made. An example would be a neuron generated in L1 that innervates the male spicula muscle, which would not need to be fully differentiated or synthesise neurotransmitters until the mid-to-late L4 stage when the spicula would be made. This includes generating new synaptic connections over development e.g. PVX is generated at L1, but synaptically connects to PCA, CP and ray neurons that are generated at L3 and L4 stages [161].

This mechanism could likely explain the reduced exploration of L4 *skn-1b* males compared to the normal exploration *skn-1b* D1 males (Fig. 11B). This shows the loss of *skn-1b* still causes an exploratory reduction in the male, but only before male-specific anatomy are generated [160] into

induce male-specific behaviours. This strengthens the idea that when male-specific anatomy is formed, and male behaviours take over i.e. mate searching, food-related exploration involving SKN-1B signalling is supressed.

Therefore, the "Just-in-time" mechanism may also occur with VA11 to temporally control SKN-1B expression only when its needed e.g. D1 males, but repress (although not translationally) SKN-1Bs function with exploration in ASI neurons.

Is SKN-1B needed for DAF-7s role in males?

ODR-10, a chemoreceptor that detects food-related odour diacetyl and promotes feeding, is expressed in L3 and L4 males, as well as hermaphrodites, which promotes feeding, but on becoming adult males, *odr-10* expression is reduced to stop feeding and promote exploration. In fed conditions, DAF-7 is released from ASJ neurons, interacting with the IIS pathway via DAF-2 to inhibit *odr-10* to promote exploration. But, in starvation, this pathway is inhibited, and *odr-10* expression is increased to promote feeding [163]. As SKN-1B is needed to repress DAF-7 in starvation conditions to promote roaming, it links to this pathway. Although as *skn-1b* is not known to expressed in ASJ neurons, ASI would have to signal to the ASJ to do so. DAF-7 is also known to promote quiescence in hermaphrodites rather than roaming, indicating other regulatory mechanisms are occurring in a sex-specific manner. The fact *skn-1b* is also expressed near the tail may offer a link to functionality with sex-specific behaviours (of which the tail is crucial) which need to be repressed on starvation. This would also clarify why D1 male exploration is normal (Fig. 11A), as all experiments were performed in well fed conditions, so no starvation phenotype would be seen.

In the context of satiety-related behaviours, understanding how males do not acquire the starvation phenotype of hermaphrodites may be more beneficial long term in understanding how animals, including humans, can have sex-specific responses to food-related cues. For future study, exploration assays under starvation would be carried out to see if *skn-1b* is needed in the D1 male to

repress DAF-7 (and if exploration is affected i.e. reduced) and promote feeding (or at least, promote roaming to find food rather than to find a mate).

Would D1 *skn-1b* male mutants have normal mitochondria in starvation?

It was shown that unlike the hyperfused body wall mitochondria of hermaphrodites, D1 *skn-1b* mutant males had normal body wall muscle mitochondria, possibly because SKN-1Bs role in mitochondrial fission is just for food-related behaviours, which is not needed if the adult male is mate searching. L4 *skn-1b* mutant males have reduced exploration (Fig. 11B) like *skn-1b* mutant hermaphrodites, and does not perform male-specific behaviours, so it is possible that L4 *skn-1b* mutant male mitochondria would also be hyperfused like hermaphrodites. This could be investigated in future study to further show *skn-1b* does have a role in males, just that it is repressed in adulthood where mate searching behaviour takes over. Following this, as N2 hermaphrodites have been shown to have increased mitochondrial fusion upon starvation, with *skn-1b* hermaphrodites also having further mitochondrial fusion [39], would D1 *skn-1b* mutant males that had normal mitochondria (Fig. 18) also have increased fusion upon starvation compared to D1 N2 males? If so, it would indicate SKN-1B is needed in the adult male, but only upon starvation, where mate searching is reduced and food-related behaviour takes over [21, 31].

From a technical standpoint, the caveats of muscle mitochondria analysis are that only one mitochondrion is imaged. For more detailed analysis, imaging Z stacks using confocal microscopy of the entire worm would allow the viewing of the entire body wall muscle mitochondria, removing the bias of only looking at one mitochondrion in the worm. To know if mitochondria are affected in other tissues, tissue-specific mitochondrial reporters e.g. neuronal, could also be used.

Does the ASI and VA11 neuron interact to control sex-shared and sex-specific behaviour?

Nemanode (once male data has been made available), WormWiring and WormAtlas could be used in the future to understand which neurons are synaptic partners of VA11, and if any of these neurons link to ASI neurons. This is possibly the case, as Nemanode (although with hermaphrodite data),

shows a connection of ASI to VA11 through two other neurons (ASI->AIB->AVA->VA11->Body wall muscles, data not shown). How accurate this might be is questionable, as only a small number of synapses and gap junctions are present and predicted using hermaphrodite data. Simply, neuropeptides may also contribute to signalling. Unfortunately, scRNA-Seq data is not available for male *C. elegans*, nor general functions of many neurons involved in the male are known. Another answer is that SKN-1B in VA11 has complete separate functions from SKN-1B in the ASI, and forcing an interaction together would be unempirical.

Does SKN-1B interact with male-specific tyraminergic neurons?

It is proposed that TA is involved in SKN-1B signalling (Chapter 1), and *tdc-1* is expressed RIC and RIM neurons in males [70]. If there are male-specific neurons that also use TA, it may indicate additional roles for SKN-1B signalling with TA in the male. Of the 93 sex-specific neurons in males, none use OA, but sensory neurons HOA (also glutamatergic like RIM) and rays R8A and R8B use TA [70]. The function of these neurons and if they link to SKN-1B signalling could be investigated, especially if there is a starvation response found in male *skn-1b* mutants. Would this involve these neurons as well as the sex-shared RIM neuron?

Does *skn-1b* have a role in male behaviour?

Is *skn-1b* needed for male behaviours? Genes for male behaviours (mate-finding; drive (via PDFR-1 [31]); response; turning; vulva location and spicule insertion) are known [164], so genes could be screened with D1 *skn-1b* mutant males through RT-qPCR to see if expression is effected in the worm, with RNAi or double mutants with *skn-1b* mutants to see if removal would show a behavioural change. For example, turning behaviour requires *cat-4* [111], and *cat-4* is downregulated in hermaphrodite *skn-1b* mutants (Supplementary Table 3). To know if *cat-4* is downregulated in *skn-1b* mutant males, mutants could first be screened using a turning assay [111]. RT-qPCR could then be used to confirm is this is due to a *cat-4* expression difference. For confirmation, RNA-Seq with *skn-1b* mutant males would need to be performed. Having both hermaphrodite and male *skn-1b* mutant

RNA-Seq data would allow identification of sex-shared and sex-specific roles for *skn-1b*. RNA-Seq of L4s and D1 *skn-1b* mutant male could be performed to understand how gene regulation has changed from an immature male (L4) to an adult male (D1).

Confirmation of SKN-1B in or near the VA11 neuron is needed

Whilst it was approximated that SKN-1B is expressed in the adult male tale sex-shared VA11 neuron (Fig. 13F), it could possibly have been AS11 (shared), VD12 (shared) or CP9 (male-specific), the neuron anterior to VA11. To confirm the exact neuron where SKN-1B is expressed, first homozygous *skn-1b::gfp; otIs669* would need to be made to allow brighter, therefore, easier identification of these neurons as only heterozygotes were managed to be created. Once homozygous *skn-1b::gfp; otIs669* are made, confocal microscopy should be performed, as multiple lasers can excite each neuron to fluoresce a specific colour, allowing precise identification of each neuron, which could not be achieved on the fluorescence microscope used. If it is confirmed to be a sex-shared neuron, hermaphrodites of the same reporter should be used to identify the same neuron, to confirm SKN-1B::GFP is not expressed in hermaphrodites. SKN-1B antibody staining would also confirm this.

If VA11 is confirmed to expresses SKN-1B, the functionality of VA11 may give insight into SKN-1Bs possible role. VA11 are cholinergic [70] neurons, part of 12 VA motoneurons which excite ventral muscles to promote backward locomotion, whereas VB and DB motoneurons promote forward locomotion [165]. Given SKN-1B's role in exploratory behaviour, being expressed in a neuron that promotes locomotion would not be unusual. Yet, *skn-1b* mutant males have no obvious exploration defect. Ablation or optogenetic inhibition of this neuron may offer insight into its role in males.

The presence of SKN-1B near the male tail was not quantified, so further repeats at large sample sizes needs to be performed. Unfortunately, large sample sizes may be difficult to acquire. The *skn-1b::gfp* reporter used has a roller phenotype, which was difficult to maintain male populations. This would would likely not be alleviated by introducing a *him-5* mutation to increase incidence of males

[19], as maintaining a *him-5* mutation in this roller background would be difficult, even more so if wanting to introduce *otIs669* in helping correctly identifying the neuron.

Finally, under starvation, *skn-1b::gfp* variably appears in other areas near the male tail, as well as other head neurons (data not shown). As SKN-1B is known to be expressed in ADL neurons under starvation in hermaphrodites [39], but the role of SKN-1B and ADL is unknown, characterisation of SKN-1B expression in starvation of hermaphrodites and males would be useful in further understanding SKN-1B-related exploration in both fed and starved states between sexes.

Summary

Before male adulthood, L4 males need SKN-1B for normal exploration, but adult males seem to not need SKN-1B's usual role in exploration, as evidenced by normal exploration and mitochondrial morphology. Yet, SKN-1B is expressed in ASI neurons in adulthood, but also only in male adults in the sex-shared neuron VA11. The function of SKN-1B in the VA11 neuron is currently unknown, but as VA11 is a VA motoneuron involved in controlling locomotion, it most likely is involved in some form of male locomotion or has a different function to be investigated.

Chapter 3 results: Investigation of differentially expressed genes in hermaphrodite *skn-1b(tm4241)* mutants

SKN-1B has roles in food-related exploration behaviour, but what genes (apart from tyramine synthesis gene *tdc-1*) contributed to this behaviour was unknown. To identify these genes in question, RNA-Seq was previously performed in the lab with *skn-1b(tm4241)* mutants compared to N2 worms. Comparing the genes between *skn-1b* mutants and N2 worms would narrow down the genes that are directly or indirectly involved in *skn-1b* function. From the RNA-Seq data, a small number (69) of genes were found differentially expressed in *skn-1b* mutants compared to N2 worms (p=<0.05), with 17 genes upregulated (0.6 to 1.8, log2 fold change) and 52 genes downregulated (-0.7 to -4.5, log2 fold change) (Supplementary Table 3).

To understand the location and functionality of these genes, bioinformatic analysis was coupled with an RNAi screen of 46 of these genes for exploration behaviours to reveal if any were implicated in SKN-1B-related exploration behaviour.

42 differentially expressed genes in *skn-1b* mutants are in neurons with 16 predicted to be directly transcribed by SKN-1

The nervous system is needed for exploration behaviour to occur, and as *skn-1b* is expressed in ASI neurons, were any of the differentially expressed genes of the *skn-1b* mutant also expressed in ASI neurons or the nervous system overall to contribute to food-related behaviour? If any were in ASI neurons, could they also be *skn-1b* transcriptional targets? To identify in which neurons the genes were expressed and if they were transcribed by SKN-1, CeNGEN and modMine were again used as in Chapter 1.

The 69 genes differentially expressed genes were inputted into CeNGEN, but only 55 could be identified, with 42 of 55 genes expressed in neurons. Of these 42 genes, only 5 were expressed in ASI neurons: *tbb-4*; *T10D4.6; B0491.6*; *T20F5.4* and *C01G6.9*, but none were exclusive to ASI neurons. To understand if any of these 5 genes could be bound by SKN-1, all 63 coding genes

differentially expressed in *skn-1b* mutants (6 were pseudogenes which were not analysed) were analysed for SKN-1 binding using modMine. Of the 63 genes, 16 genes were bound by SKN-1, with 11 genes expressed in neurons, but only *B049.16* was bound by *skn-1* (Table 6) and expressed in ASI neurons. This would indicate it is a possible *skn-1b* direct target, but as *B049.16* was also expressed in 117 out of 128 neurons, it indicated *B049.16* is possibly a general *skn-1* target, and likely does not have a role in specific *skn-1b* functionality.

Table 6. 16 genes differentially expressed in *skn-1b(tm4241)* mutants are bound by *skn-1::GFP* from modENCODE ChIP-Seq binding data. 63 genes from the *skn-1b(tm4241)* mutant RNA-Seq data set were screened using modMine with the Synder *skn-1::GFP* ChIP data set. Pseudogenes (6) were not analysed. 44 genes bound *skn-1*, with 16 genes having significant *q*-values ≤0.05 which are shown. Stages L1 to L3 were analysed, but *skn-1* only bound genes at L1-L3 stages. No single gene was bound by *skn-1* at all 3 stages. If a gene was bound by *skn-1* at multiple sites in a larval stage, the highest *q* value was used rather than multiple values. Multiple binding sites is denoted with (+*n*), with *n* representing additional binding sites e.g. *B049.16* at L2 stage had 3 additional binding sites for *skn-1*, shown as (+3)). No *q*-value indicates no *skn-1* was bound at that larval stage. *not expressed in neurons using CeNGEN. **Only found in 'All cells unfiltered' data.

Gene	Larval stage		
	L1	L2	L3
B0491.6	6.95E-21 (+1)	4.66E-20 (+3)	
B0511.11		9.31E-04	
bath-25*			3.97E-02
C29A12.6*		2.07E-05 (+2)	
cdh-8		3.13E-03	
dve-1	3.84E-04	6.27E-03	
F13E9.11		3.45E-03	
F22H10.2		6.49E-04 (+2)	
F55G11.2*	2.31E-05	1.46E-13 (+2)	
F55G11.8*		3.12E-10 (+2)	
F57B1.6		1.70E-05 (+1)	
hil-7	4.98E-14 (+1)		
asp-14 (K10C2.3)*		7.12E-30 (+4)	
lgx-1			3.53E-02
sup-12	1.13E-03		
Y97E10AR.1	6.67E-08		

15 differentially expressed genes not in neurons were found expressed in glia, muscle, or the intestine

As none of the genes differentially expressed in *skn-1b* mutants were solely expressed in ASI neurons, and with 37 genes expressed in different neurons, it indicated at least 27 genes were likely expressed in non-neuronal tissues. As there are many non-neuronal tissues, only 3 cell types were screened. Glial cells were screened as they are the supporting cells of neurons, so may have a role in supporting exploration behaviour, alongside screening genes expressed in muscle and intestine as *skn-1b* mutants have hyperfused body wall muscle mitochondria and reduced food-related exploration [39]. CeNGEN was again used as it offers an 'all cells unfiltered' setting, which increases the detection of genes but has a much higher false positive rate, whilst also showing gene expression in both neuronal and non-neuronal tissues. This latter option increased the detection of the genes from 55 to 68 out of 69 genes (*F45D11.5* not identified by CeNGEN), with genes expressed in the 42 neurons were also co-expressed in glia (31), muscle (37) and intestine (22), with only *F57B1.6, Y102A5C.5*, and *Y34F4*.3 specifically neuronal (Supplementary Table 4).

26 non-neuronal genes were found in glia (9), muscle (7) and the intestine (6), 8 of which were tissue-specific, and 9 which were expressed in other tissues but not analysed (Supplementary Table 4). Of the 3 glial-specific genes, *R05G9R.1* was also expressed in the AMso glia that surround the amphid neurons (including ASI neurons) [53], but also had expression in non-specific glia. This indicated *skn-1b* effects both neuronal and non-neuronal tissues, but none were specific to ASI neurons via AMso interactions, but some may have roles in muscle or the intestine. Only *hch-1* was not expressed in the 169 distinct cell types that were detected by CeNGEN, likely as *hch-1* is normally expressed in embryogenesis [166], and CeNGEN data is of L4 stage hermaphrodites. As *hch-1* was found to be differentially expressed in Day 1 adult *skn-1b* mutants, it would indicate it has a role outside of embryogenesis yet uncharacterised.

F-box proteins and cuticlin proteins are enriched in *skn-1b* mutants

Now that the anatomical expression of differentially expressed genes was known, the identification of gene functionality was now needed to inform how these genes may contribute to SKN-1B-related exploration. To infer gene functionality, a *C. elegans*-specific gene ontology (GO) tool, WormCat [138], was used to analyse all differentially expressed genes of the *skn-1b* mutant, and found F-box (*fbxa-192*, *fbxb-40*, *-41*, *-45* and *fbxc-39*, *-40*, *-42*) and cuticlin (*cut-3*, *-4* and *-6*) genes were significantly enriched in *skn-1b* mutants (Fig. 15). Note *fbxa-191* and *fbxa-193* were not classed with the GO term 'F-box', but instead 'pseudogene' by WormCat. Interestingly, apart from *fbxa-192*, all the enriched genes are downregulated in the *skn-1b* mutant, with *fbxc-40* being the most downregulated of all the genes (Supplementary Table 3), indicating SKN-1B may normally positively regulate a select number of F-box and cuticulin genes.

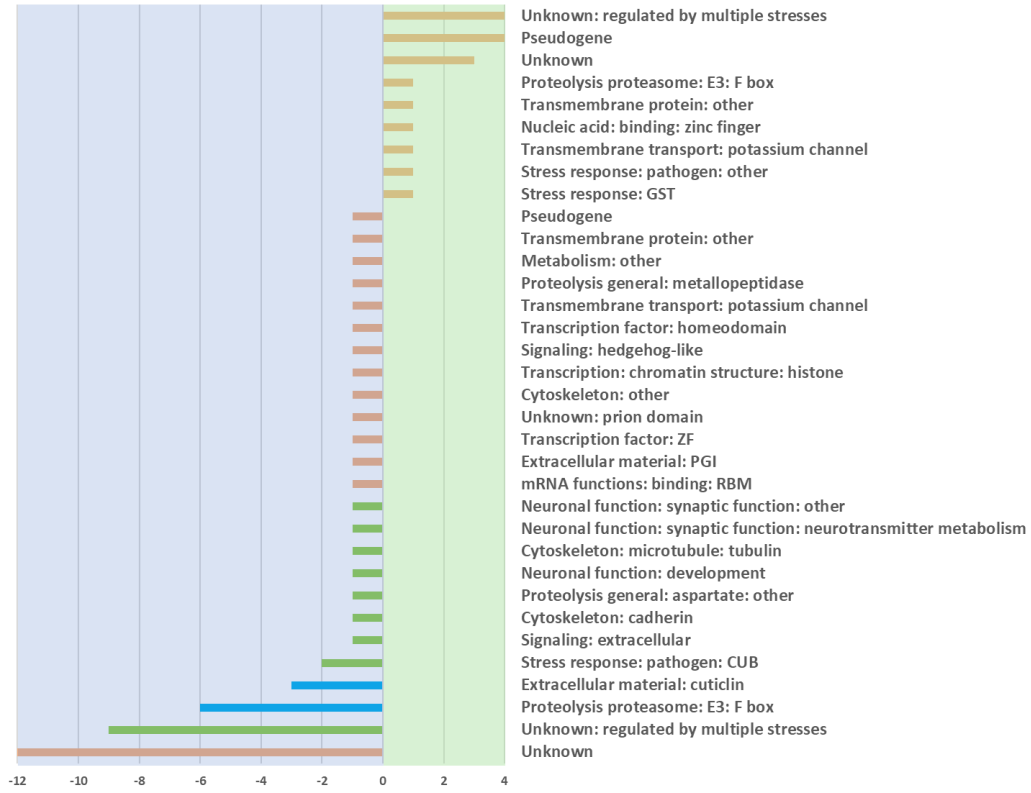

Figure 15. A significant amount of F-box and cuticlin genes are differentially expressed in *skn-1b* mutants. WormCat was used to analyse all 69 genes differentially expressed in *skn-1b* mutants. X-axis is the number of genes with that GO term, with downregulated and upregulated genes on the left (0 to -12, highlighted blue) and right (0-4, highlighted green), respectively. Peach/orange bars represent non-significant genes. Green bars represent significant genes (p=≤0.05) but not corrected for FDR. Blue bars represent significant genes with Bonferroni correction (p=<0.005). Note *W06A11.4* is recognised as a protein, although it is known as a pseudogene, hence the graph has 5 pseudogenes instead of 6.

8 differentially expressed genes in *skn-1b* mutants are involved with roaming, dwelling, metabolism and/or mitochondria

Further analysis combining WormCat with SimpleMine, a data mining tool specific for WormBase data, was used to screen terms of interest relating to *skn-1b* mutant phenotypes e.g. behaviour, neuronal, metabolism, muscle, mitochondria and locomotion. Phenotypes caused through RNAi and/or mutations were also screened, to understand if any differentially expressed genes have already been implicated in the above terms of interest. This would help understand how downregulation or upregulation of these genes may contribute the overall phenotype of *skn-1b* mutants. From the analysis, genes were found to be involved in transcription, neuronal activity, including neurotransmitter metabolic activity (*cat-4*) (Table 7). 24 genes also had known

RNAi/mutation phenotypes, 8 of which had phenotypes in roaming, dwelling, metabolism (including fat storage) and mitochondria (Table 7). These 8 genes were downregulated in *skn-1b* mutants except *gst-10*, yet *syg-1* and *cat-4* are downregulated in *skn-1b* mutants, but increased roaming upon RNAi of these genes has been previously known (Table 7), opposite of the reduced exploration phenotype of *skn-1b* mutants. It was also noted at least 4 genes were implicated in immunity, with F22H10.2 shown to interact with transcription factor ATFS-1 needed to activate the immune response via UPR^{mt} activated in stress e.g. pathogen response [167]. SKN-1 (likely SKN-1C) is needed for pathogen resistance [168], but the relationship between immunity and food-related exploratory behaviour has not yet investigated with SKN-1B.

Table 7. Functionality and phenotypes of *skn-1b(tm4241)* mutant differentially expressed genes. Gene function from WormCat, WormBase and SimpleMine. RNAi and/or mutation phenotype information from SimpleMine. Gene expression is in order of upregulated to downregulated (log2fold) from *skn-1b(tm4241)* mutant RNA-Seq data compared to N2. Terms screened: behavior/behaviour; fat/lipid; metabolism/metabolic; mitochondria/mitochondrial; energy/ATP; locomotion/chemotaxis, muscle, and neuronal/glia/neurotransmitter/biogenic/amines. Those with N/A may have had functions or phenotypes attributed but were not relevant to the terms analysed. *fbxb-41* RNAi was found to stop antimicrobial peptide expression after infection but was not the focus of the analysis.

Gene	Gene expression	Function	RNAi and/or mutation phenotype
gst-10	0.8	Glutathione S-transferase	fat content increased
dve-1	-0.7	Transcription factor, involved in UPR^{mt} [169]	foraging variant (less on food), larval lethality
syg-1	-0.8	Neuronal	roaming increased
cat-4	-0.8	Neurotransmitter metabolic activity	dwelling reduced, foraging hyperactive, serotonin and dopamine deficient
hbl-1	-1.1	Transcription factor	locomotion variant (unc), larval lethality
eva-1	-1.1	Has carbohydrate binding activity	mitochondria alignment variant (expressed in striated muscle dense bodies)
C01G6.9	-1.3	?	fat content reduced
hil-7	-1.4	Histone-H1 like protein	larval lethality
dyf-7; plx-2; hch-1; tsp-17	N/A	Neuronal	N/A
ncs-4; cdh-8	N/A	Calcium binding activity	N/A
F22H10.2; F55G11.8; F55G11.2	N/A	Innate immunity, the latter 2 with predicted CUB domains	N/A

Next, it was explored how these SKN-1B targets could interact at a functional level to control behaviour e.g. *cat-4* has a role in neurotransmitter synthesis, so does it interact with SKN-1 for exploration behaviour? STRING analysis, which predicts protein-protein interactions, was performed with SKN-1, SKN-1's known interacting proteins, and the 69 differentially expressed genes of *skn-1b* mutants. This revealed from the 69 genes analysed, SKN-1 only interacts with GST-10, but as *gst-10* is not expressed in ASI neurons (CeNGEN), it likely does not have direct protein-protein interactions with SKN-1B. Instead, GST-10 may indirectly interact with SKN-1 through SKN-1 partners DAF-16, GST-4, WDR-23 and GCS-1 which are all expressed in ASI neurons, or simply GST-10 interacts with another SKN-1 isoform in another tissue. PHA-4 which interacts with SKN-1 was shown to interact with DVE-1, HBL-1 and LGX-1, but as *pha-4* is not expressed in ASI neurons, like GST-10, it is likely not a direct interaction involving SKN-1B (data not shown).

As the known SKN-1 interacting proteins have not been shown to directly interact with SKN-1B, these protein-protein interactions may not occur. So, STRING analysis was performed with SKN-1 and the *skn-1b* mutants differentially expressed genes (Fig. 16). From the 67 proteins analysed, a 22-protein string had only 4 proteins with functions in neuron generation, migration and dendrite extension, whilst 3 proteins had no annotated function and the 15 other proteins had no obvious similar function. A 7-protein string were with the F-box proteins, BTB-11 and F45D11.5, indicating these latter two proteins are involved in F-box functionality, although FBXA-192 and FBXC-42 was not included. For any obvious phenotypes relating to *skn-1b* mutants i.e. exploratory behaviour, it was interesting that SYG-1 and CAT-4 did not have any predicted protein interactions, even though RNAi causes both to have increased roaming, indicating they may function separately to promote the same exploratory behaviour (Table 7).

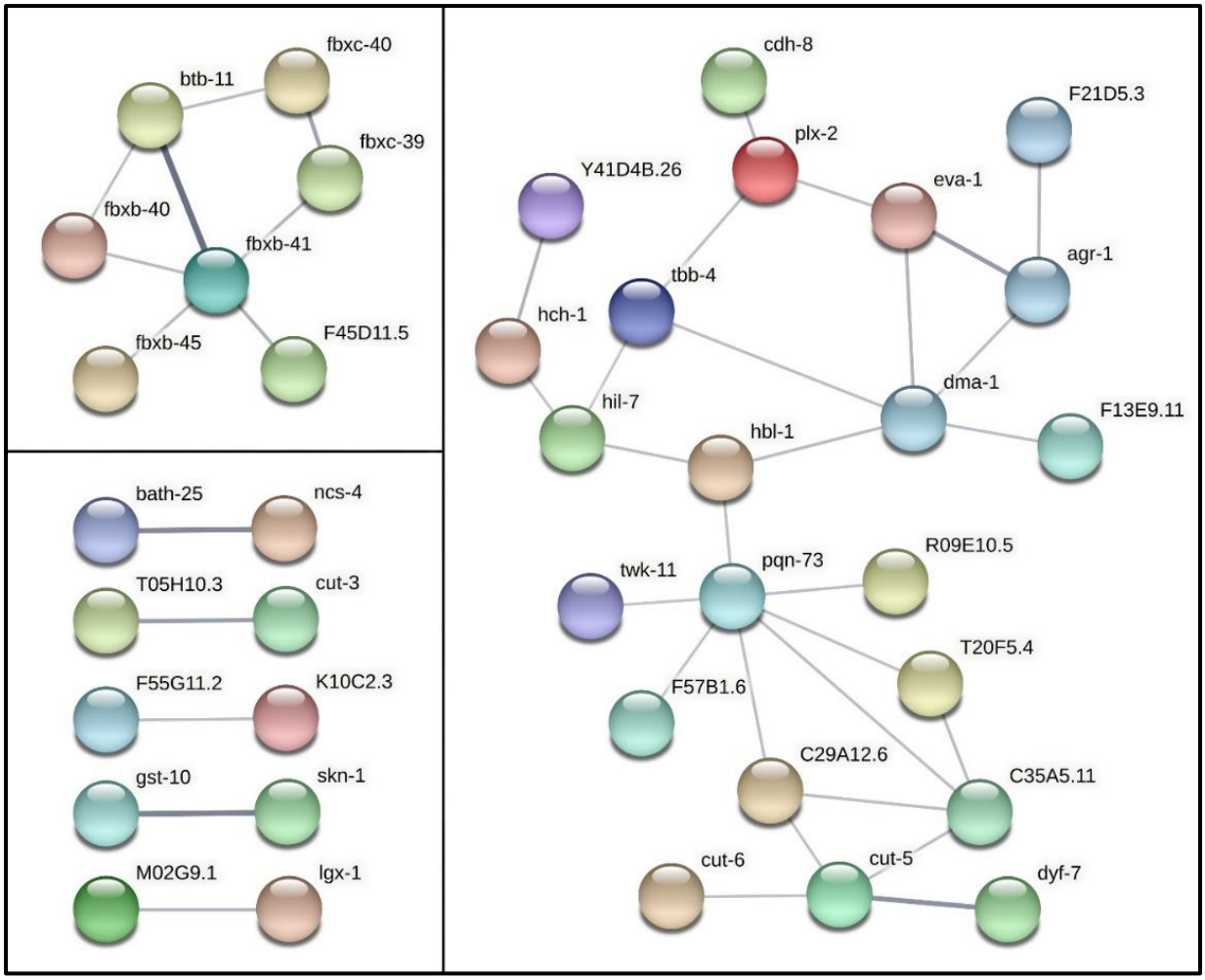

Figure 16. 7 protein-protein interactions of SKN-1 with each of the differentially expressed genes of the *skn-1b* mutant. 29 proteins did not have any interactions therefore was not shown. FBXA-191, FBXA-193 and Y102A5C.5 were not able to be analysed using STRING as these are non-protein coding pseudogenes (yet pseudogenes Y102A5C.6, W06A11.4, F45D11.1 were able to be analysed, but had no interactions).

Finally, as 23 genes had no known function, but could potentially have roles in exploratory behaviour, these genes were compared with fly, fish, mouse, rat and human genomes using Alliance Genome's SimpleMine to learn if they had orthologs in other organisms with known functions that could infer their functionality in *C. elegans*. No orthologues in were found. This indicated either many of these genes are yet to be investigated in other organisms, or that they are specific to *C. elegans*.

K02E7.15, a large circular RNA contains all F-box B and C genes differentially expressed in the *skn-1b* mutant

As there was a large 22 STRING network found with similar gene/protein families differentially regulated in *skn-1b* mutants, it indicated that these genes may be genetically regulated together. Operons are known to regulate a group of genes, therefore the 69 differentially expressed genes were analysed for operons using WormMine. Two operons were found, with *pqn-73* part of operon CEOP2360, and *fbxa-191, 192* and *193* part of operon CEOP5460 (*fbxa-129* is also part of CEOP5460, but not in the RNA-Seq data set (WormBase)). As no other genes in the RNA-Seq list had known operons, chromosome distance for all these genes was instead analysed, with 4 instances of multiple genes next to each other on the chromosome found (Table 8). One set was of 10 downregulated genes, that covered all F-box B and C genes, *math-34*, *btb-11*, *F45D11.1* and *F45D11.5*. Note that F-box A genes are on a different chromosome and are upregulated, whereas the F-box B and C genes are downregulated. Interestingly, this set of 10 genes was encoded by K02E7.15, a massive (67988 nt) circular RNA (not a gene), alongside 17 other genes/pseudogenes/RNAs, but specific functionality of this circRNA is not known. The region of K02E71.5 did not have any SKN-1 binding sites of SKN-1 promoter interaction identified by modENCODE (data not shown), indicating indirect SKN-1 regulation outside of SKN-1 may occur, or not involve SKN-1 at all.

Table 8. List of *skn-1b* mutant differentially expressed genes that are either predicted to be in an operon, or close to each other on the chromosome. Genetic 'closeness' is defined as the genes being within one significant decimal place of each other e.g. 15.5, with different colours representing each possible gene cluster. Only *fbxa-191*, *-92* and *-93* are known to be in operons. *pqn-73* is also in an operon but was not shown as no other genes in the data set are close in genetic map position. WormMine was used to search for operons. SKN-1 binding was inferred using modENCODE data as previously described.

Gene	WormBase ID	Genetic Map Position	Known Operon	Bind SKN-1
fbxb-45	WBGene00019705	II -15.57	N.A.	N
math-34	WBGene00019699	II -15.57	N.A.	N
fbxb-40	WBGene00019704	II -15.57	N.A.	N
fbxb-41	WBGene00019703	II -15.57	N.A.	N
btb-11	WBGene00019700	II -15.57	N.A.	N
F45D11.1	WBGene00018448	II -15.573440	N.A.	N
F45D11.5	WBGene00018452	II -15.573870	N.A.	N
fbxc-40	WBGene00016295	II -15.58	N.A.	N
fbxc-39	WBGene00018456	II -15.58	N.A.	N
fbxc-42	WBGene00018455	II -15.58	N.A.	N
F42A9.6	WBGene00018335	IV 3.908456	N.A.	N
F21D5.3	WBGene00009008	IV 3.957834	N.A.	N
F55G11.8	WBGene00010128	IV 6.759376	N.A.	Y
F55G11.2	WBGene00010123	IV 6.783019	N.A.	Y
Y102A5C.36	WBGene00044213	V 11.357200	N.A.	N
Y102A5C.5	WBGene00014954	V 11.357780	N.A.	N
Y102A5C.6	WBGene00014955	V 11.358160	N.A.	N
fbxa-192	WBGene00010212	V 12.94	CEOP5460	N
fbxa-191	WBGene00010209	V 12.94	CEOP5460	N
fbxa-193	WBGene00010295	V 12.95	CEOP5460	N

No biologically relevant exploration change occurred upon knockdown of 47 differentially expressed genes in *skn-1b* mutant hermaphrodites

From the bioinformatic analysis performed, many of the differentially expressed genes of *skn-1b* mutants were expressed in the nervous system, some with specific neuronal functioning, but with many having no known function at all. Only *syg-1* and *cat-4* were known to have increased roaming upon RNAi (Table 7), the opposite phenotype of *skn-1b* mutants. To understand how and if any of the 69 genes contributed towards the reduced exploration phenotype of *skn-1b* mutants, an RNAi screen of 46 of these genes (Supplementary Table 3) were performed on N2 and *skn-1b* mutant worms, which were then tested for changes in exploratory behaviour. To perform this screen, worms were raised for one generation on individual RNAi, then L4 progeny were taken and placed on 3.5

cm NGM plates for 16 h at 25°C. In this 16 h, worms move and create tracks on the food-covered NGM plate, and after 16 h the tracks were manually counted and analysed for reduced exploration (Fig. 6). 22 of the 69 genes were not tested either because the *HT115* (DE3) bacterial strain carrying the RNAi construct did not grow, RNAi was not commercially available for the specific genes, or that the RNAi caused a developmental defect and did not allow behavioural analysis (e.g. *dve-1*).

N2 worms normally explore ~70% of an NGM plate, with *skn-1b* mutants at ~40-50% (Fig. 17A and 17B) [39]. For the reduction of *skn-1b* mutant exploration to occur, it was presumed one or some of the 69 differentially expressed genes of the mutant would be involved, and upon performing RNAi on these genes, either decrease N2 worms exploration to *skn-1b* levels, or rescue *skn-1b* mutants exploration to normal levels. With this in mind, genes most up or downregulated were screened first, as it was presumed these would have the most impact on exploratory behaviour. Of these 9 genes, RNAi of *ncs*-4, (Fig. 17B), *asp-14*, *TD104.6* and *B0511.11* (Fig. 17C) significantly lowered the exploration of N2 worms. In particular, RNAi of *B0511.11* lowered exploration of N2 worms to *skn-1b* mutant levels, but RNAi of *B0511.11* on *skn-1b* mutants caused no exploration change (Fig. 17C). This indicated these genes, especially *B0511.11* may contribute to exploration behaviour, but as the exploration of RNAi empty vector (EV) controls for N2 worms and *skn-1b* mutants had increased from 71% to 88% and 42% to 69%, respectively, from Fig. 17A and 17B compared to Fig. 17C, results should be cautiously interpreted and are possibly false (especially as RNAi controls for *skn-1b* mutants in Fig. 17C were exploring nearly the same as N2 worms in Fig. 17A and 17B).

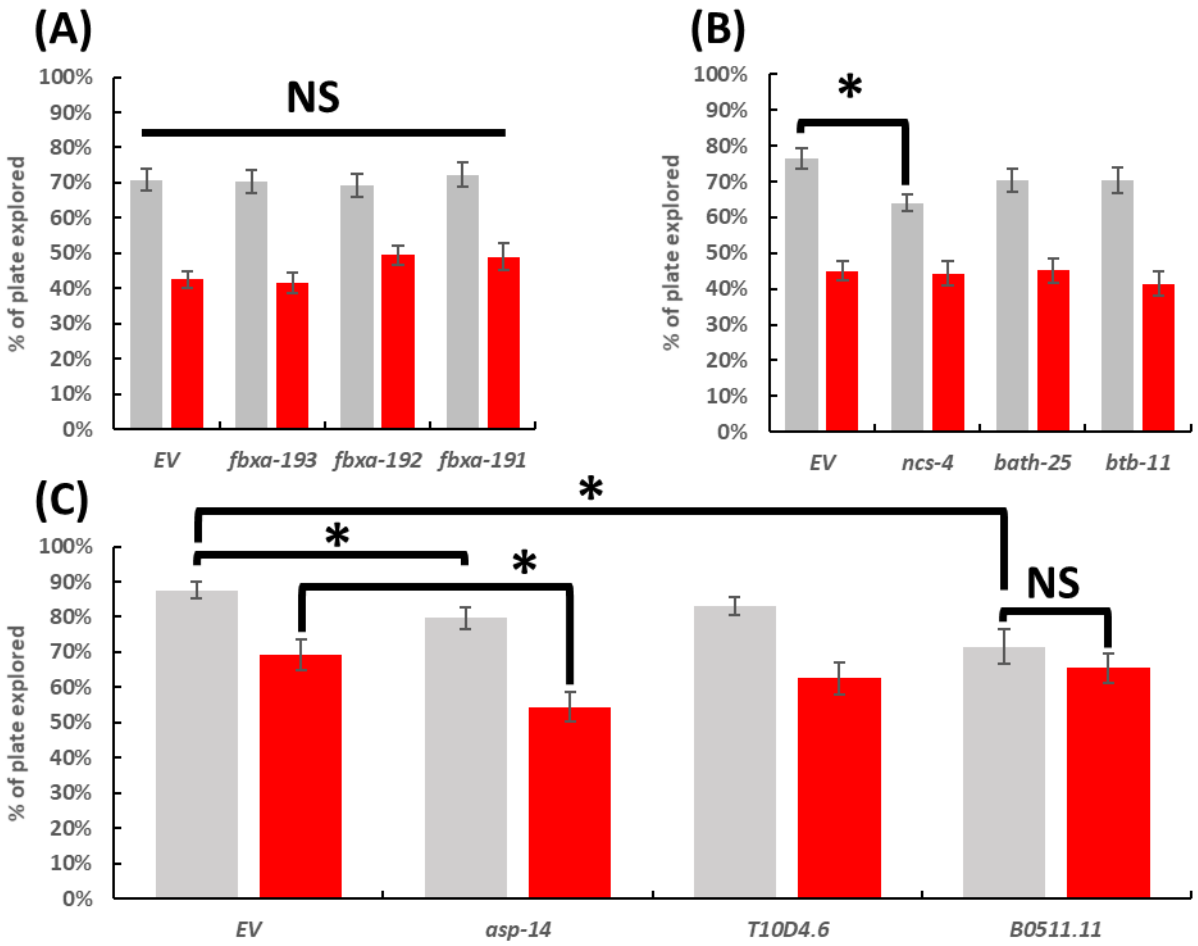

Figure 17. Most up and downregulated genes from *skn-1b(tm4241)* RNA-Seq show no significant difference in exploration compared to controls. 16 h exploration assay of L4 hermaphrodites. Grey bars represent N2; red bars represent *skn-1b* mutants. (**A and B**) N2 compared to *skn-1b(tm4241)* are all statistically significantly different from each other. *skn-1b* mutant EV compared to other *skn-1b* mutant RNAi showed no significant difference. N2 EV compared to N2 RNAi showed a significant decrease in exploration with N2 *ncs-4* RNAi. **(C)** Only *B0511.11* was not significantly different between N2 RNAi and *skn-1b* mutant RNAi. *skn-1b* mutant *asp-14* RNAi was significantly different than *skn-1b* mutant EV. *asp-14* and *B0511.11* N2 RNAi were significantly different than N2 EV. Data is the average of 3 biological repeats for **(A and B)**, and 2 biological repeats for **(C)**. Between 10-12 worms was used for each biological repeat. Asterisk (*) represents a significant difference using Welch's t-test (p = ≤0.05). NS represents no significant difference using Welch's t-test. Error bars represent ± SEM.

In Fig. 17B and 17C, although some explorations were significantly different, exploration difference was small (~7%), unlike the larger difference between N2 and *skn-1b* mutants (>20%). Therefore, a shorter, quicker screen for larger exploration differences was performed on the 37 remaining genes (Fig. 18). Interestingly, individual RNAi on these 37 genes did not reduce N2 exploration to *skn-1b* mutant levels, indicating no (individual) differentially expressed genes contribute towards *skn-1b* mutants reduced exploration phenotype. Yet, RNAi of *syg-1*, *CO1G6.9* and *M02G9.1* increased *skn-*

1b mutants exploration to N2 levels, with RNAi of the same genes on N2 worms not changing exploration, indicating *skn-1b* mutant exploration was rescued. Further, increased exploration above controls was common e.g. RNAi of 20 genes on N2 worms, and RNAi of 14 genes on *skn-1b* mutants increased exploration compared their respective controls, with RNAi of *F54C8.6* causing higher exploration than both N2 worms and *skn-1b* mutant controls (95% and 91% exploration, respectively). This indicated *F54C8.6*, and possibly a large amount of these genes was involved in promoting dwelling, with reduction in expression causing hyperactive roaming/increased exploration.

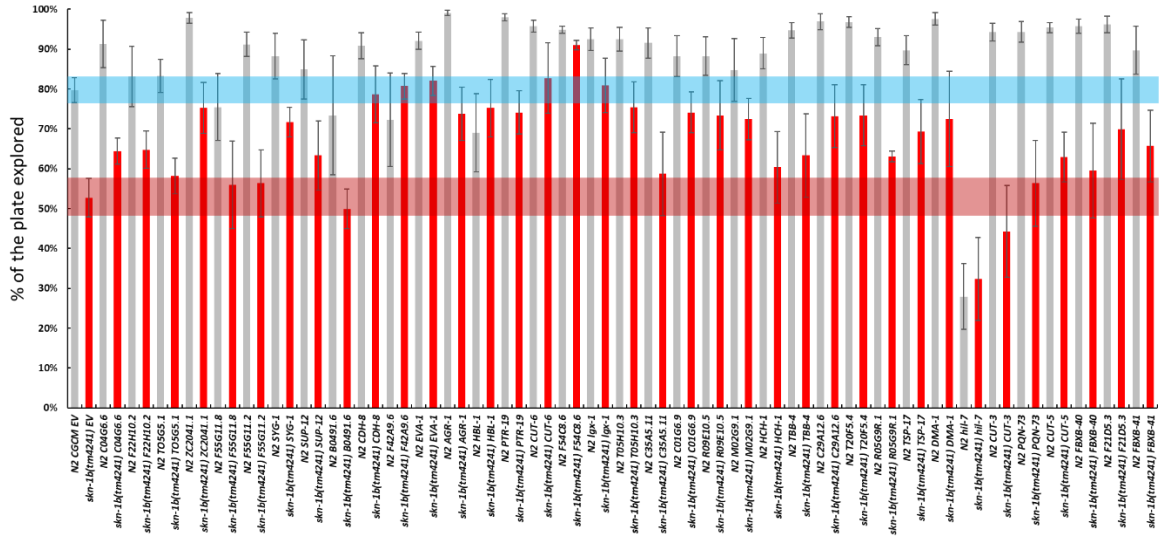

Figure 18. Only *hil-7* RNAi significantly decreases exploration of both N2 and *skn-1b* mutants. 16 h exploration assay. RNAi was performed on 37 genes in L4 hermaphrodite N2 and *skn-1b* mutants. Genes are in order of expression in *skn-1b* mutants, with upregulated to downregulated (left-to-right). EV is the RNAi empty vector control. EV bars are 4 combined trials (20 worms overall), with all other bars having 5 worms each (except *C04G6.6* RNAi on N2 and *skn-1b* mutants, and *T20F5.4* RNAi on N2 which all had 4 samples). Blue and red bars represent ± SEM bar coverage for N2 EV and *skn-1b* mutant EV, respectively. Error bars represent ± SEM. For raw data and exact *p*-values, see Supplementary Table 5.

As all the 37 genes screened did not phenocopy *skn-1b* mutants, it was a surprise that RNAi of *hil-7* reduced exploration of both N2 (28%) and *skn-1b* mutants (32%), with N2 worms significantly different from both controls. To confirm this result, an experiment with a larger sample size was performed and confirmed the reduction in exploration (Fig. 19). Whilst RNAi of *hil-7* may have contributed to the decreased exploration of *skn-1b* mutants, the exploration was variable, ranging

from 2% to 67%. To test the ability of body wall muscle to conclude if exploration was due to food-related exploration rather than the inability to move, worms were placed in a drop of its physiological buffer M9 and its ability to swim (thrash) was measured. The thrashing ability of 3 *hil-7* RNAi progeny revealed that worms with higher exploration thrashed more than those with lower exploration (9 thrashes = ~10 squares covered; 57 and 67 thrashes for ~50% plate coverage, results not shown), indicating a locomotion defect was a major factor in causing exploration variability, although only 3 progeny were screened, with only one EV control (113 thrashes), so statistical significance could not be determined. This coincides with the slightly uncoordinated (unc) phenotypes seen in some *hil-7* progeny (alongside translucent/pale cuticles), and previously known larval lethality occurring with *hil-7* (Table 4), indicating RNAi of *hil-7* impacted development rather than food-related behaviour.

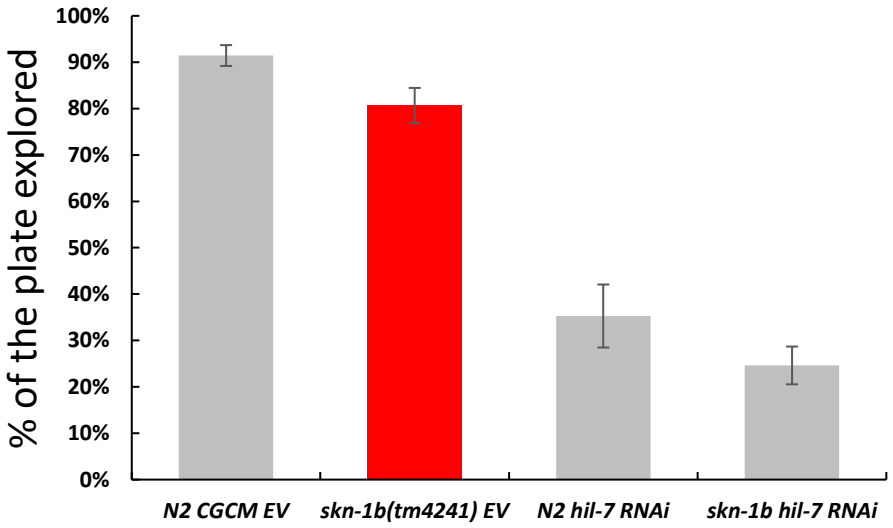

Figure 19. *hil-7* decreases exploration of both N2 and *skn-1b* mutant to the same levels. 16 h exploration assay. RNAi was performed on *hil-7* in L4 hermaphrodite N2 and *skn-1b(tm4241)* mutants. EV is empty vector control. One biological repeat with 12 worms for each point was used. Due to only one biological repeat, statistical significance using Welch's t-test was not calculated.

As well as *hil-7*, developmental defects also occurred with RNAi of *hbl-1* and *dve-1*. RNAi of *hbl-1* caused protruding vulvas and a slight egg laying defective (egl) phenotype, but exploration of N2 and *skn-1b* mutants were not significantly different from each other, though it was noted that RNAi of *hbl*-1 caused N2 worms to have a dwelling phenotype. RNAi of *dve-1* caused very low progeny in

both N2 and *skn-1b* mutants, so only a low sample size was obtained (3 N2 and 5 *skn-1b* mutants) which could not be measured for exploration. Overall, these results found no obvious epistatic relationship between *skn-1b* and *skn-1b*'s differentially expressed genes, but it did reveal many of these genes may promote dwelling, with RNAi of 3 genes rescuing *skn-1b* mutant exploration to N2 (normal) levels.

Chapter 3 discussion

RNAi of differentially expressed genes in *skn-1b(tm4241)* hermaphrodites did not reduce food-related exploration

The overall goal of this chapter was to better understand *skn-1b'*s place in the food-related exploratory pathway by finding which genes differentially expressed in *skn-1b* mutants may contribute to the reduced exploration phenotype.

46 of 69 genes differentially expressed were screened using RNAi (Fig. 17, 18 and 19). If there were a role for these genes in *skn-1b*-related exploration, it was expected that RNAi of N2 worms would decrease exploration to *skn-1b* mutant levels, but *skn-1b* mutant exploration would stay the same (presuming *skn-1b* is needed for these genes to have a role in exploration). Food-related exploration reduction was not seen in any genes screened to the level of *skn-1b* mutants. The only reduction in exploration was with RNAi of *hil-7*, which decreased both N2 worms and *skn-1b* mutants to ~30% exploration, below controls (Fig. 19). This was interpreted as a developmental phenotype rather than an exploratory phenotype due to low progeny size, unc phenotypes, variable exploration (2% to 67%), low/variable thrashing and larval lethality (Table 4).

Another possibility was that RNAi of a gene might rescue exploration of *skn-1b* mutants to N2 levels, but not increase N2 levels. This occurred with RNAi of *syg-1*, *CO1G6.9* and *M02G9.1*, but as there was general large increase and variability of exploration in both N2 and *skn-1b* mutant controls (general problems and caveats with these experiments are discussed later), it cannot be interpreted as a rescue of exploration, especially as *syg-1* RNAi is known to increase roaming (Table 4).

Bioinformatics was used to understand possible location and functionality of *skn-1b* mutants differentially expressed genes, but this did not seem to show any correlation with exploration e.g. *F54C8.6*, the gene with the highest exploration of both N2 and *skn-1b* mutants (Fig. 18 and Supplementary Table 4) was found in 78 of 128 neurons, but not ASI neurons (CeNGEN). This may indicate SKN-1B indirectly regulates many of these genes in a cell non-autonomous capacity rather

than directly, as *B049.16* (Fig. 18 and Supplementary Table 4) was predicted to be expressed in ASI neurons (CeNGEN) and be directly transcribed by SKN-1 (Table 4), but had no significant exploration difference.

Overall, no obvious link between exploration, ASI-specific expression and *skn-1* binding was found, nor the RNAi screen revealed gene/s involved in SKN-1B-related exploration behaviour (Fig. 20).

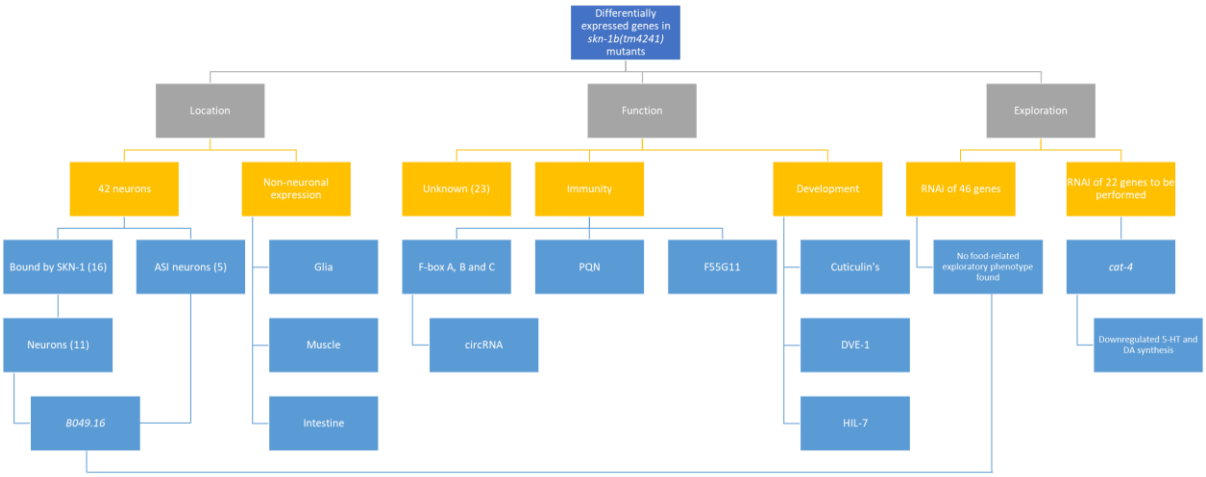

Figure 20. *skn-1b* mutant differentially expressed gene location, function, and effect on exploration via RNAi. In 'Location', genes expressed are predicted from CeNGEN data in at least 42 neurons, with the brackets indicating the number of genes belonging to each category e.g. 'ASI neurons (5)' is predicted to express 5 differentially expressed genes found in *skn-1b* mutants.

Caveats of RNAi and exploration assay

As only RNAi on 46 of 69 genes was performed, genes that contribute to exploratory behaviour could have been missed, e.g. *cat-4* is one of genes downregulated in *skn-1b* mutants, but RNAi of *cat-4* was not performed. As *cat-4* is needed for serotonin and dopamine synthesis [111], it was the only gene known to be directly involved in food-related exploration behaviour, with RNAi of *cat-4* known to reduce dwelling and increased roaming [170] (Table 4), similar to the roaming increase in 5-HT and DA synthesis mutants (Fig. 15). *cat-4* is downregulated in *skn-1b* mutants, but the downregulation does not cause increased roaming in *skn-1b* mutants, as reduced exploration is the main exploratory phenotype of this mutant. -0.8 log2fold *cat-4* downregulation may not be enough to cause the phenotype seen with RNAi or mutation, but *cat-4* RNAi on N2 worms and *skn-1b*

mutants would need to be performed for confirmation. Simply, with 69 genes differentially expressed in *skn-1b* mutants, it is likely more than one gene causes the exploration phenotype, so knockdown of multiple genes might be required to reduce exploration e.g. the clustered family of F-box genes.

From a technical perspective, exploration behaviour requires neurons, and as RNAi is not effective in neurons [152], gene knockdown may not have been effective to reduce exploration behaviour. Also, each RNAi may degrade the amount of mRNA differently, and the required amount of degradation to cause an exploration phenotype may also vary e.g. *fbxa-192* RNAi might decrease mRNA by 10% but a 50% reduction might be needed to cause reduced exploration. As confirmation of gene knockdown was not performed using RT-qPCR, it was unknown if RNAi was 1) targeting the correct mRNA, and 2) if it was being targeted correctly, how much was reduced. To solve the problem of low RNAi uptake, growing worms for two generations on RNAi before exploration can increase RNAi uptake into neurons (but can lead to false-positive results) [30] or a RNAi-sensitive strain can be used e.g. *rrf-3* [152]. For more defined targeting with RNAi, pan-neuronal specific RNAi or ASI-specific RNAi [105] could be performed, with the latter may help in identifying a direct SKN-1B target. Following from RNAi experiments, mutants of *skn-1b* mutants differentially expressed genes would confirm if an exploratory phenotype occurs and if any show a phenotype, then generating a double mutant with *skn-1b(tm4241)* would be the next logical step in understanding *skn-1b*'*s* role in the exploration pathway.

Increased exploration occurred after moving laboratories

Other technical problems were that all worms were having increased exploration, with *skn-1b* mutants sometimes exploring to levels of N2 worms. This phenomenon occurred after moving laboratories (with Fig. 17A and 17B data acquired beforehand), but it was never identified to what caused the increase, despite testing multiple parameters that may affect exploration (tested exploration with different NGM components, water pH, incubators, agar plate and LB brands). This

problem was not resolved but offset with a larger sample size of worms in Chapter 1 and 2, but for the quicker RNAi screen, this led to problems interpreting results.

The quicker RNAi screen (Fig. 18) only used a maximum of 5 worms each with only one biological trial. This low number of worms was originally justified as it was a quick screen to find any obvious phenotypes to then follow up with a larger set of worms and biological repeats. But due to the general increased worm exploration problem, if one or two of these worms was having higher than normal exploration, then knowing if this was true data or due to the overall exploration increase cannot be determined. For example, RNAi of 20 and 14 genes in N2 and *skn-1b* mutants, respectively, had increased exploration over controls, indicating either many of these genes were involved in exploration, with knockdown causing increased/hyperactive roaming and overriding the dwelling phenotype of *skn-1b* mutants, but it was more probable that RNAi may have caused a subtle effect but was likely masked by the exploration variability.

For the RNAi screen (Fig. 18), only RNAi empty vector (EV) controls had 4 biological repeats as controls were used for each screen which was split into 4 trials as 37 genes could not be screened in one assay, so the control data was combined in the graph. Whilst combining the EV data increased accuracy, it did not reflect the set of genes screened for on that day, but if only 5 samples were included for controls, it would have then caused further problems of interpreting the data set with larger margins of error.

Better RNAi controls are needed for future exploration assays

For future study, better controls for RNAi could be used e.g. food source and positive controls. All worm stocks are raised on OP50-1, but transferring worms from OP50-1 onto RNAi plates, which are HT115 *E. coli*, likely causes a different response to exploration as it is known worms grown on HT115 compared to OP50 develop faster, consume more oxygen, produce more ATP, store less fat, feed slower/pump less, leave food more, have slower locomotion, higher reversals, and can quiesce [171]. To be more consistent, using OP50 as the RNAi bacteria may produce different effects from HT115

[171], which would also reflect the food source that N2 and *skn-1b* mutants were raised on (OP50-1) when creating the RNA-Seq data. Also, as many genes knocked down using RNAi showed no large exploration difference from EV, there could be a possibility that the RNAi was not always successful (IPTG not inducing RNAi). RNAi of *dve-1* caused embryonic lethality, so could be used as positive control by screening for low/no progeny to confirm NGM plates had successful IPTG induction.

General exploration assay caveats: humidity, vibration, and circadian rhythm

There are caveats for the exploration assay in general (regardless of RNAi). The exploration assay is not sensitive. Any tracks around the side of the plate cannot be seen as light casts a shadow around the edges, so tracks might be missed, and worms would be falsely reported as having lower exploration. Lower exploration may occur if a thicker layer of bacteria forms around the plate edge, attracting worms to the bigger food source and away from the middle of the plate. Environmental differences may also effect exploration behaviour e.g. humidity differences effects behaviour of starved worms which prefer drier areas [172], vibration stops pharyngeal pumping (unpublished data by Monica Sholz's lab) and *C. elegans* have a circadian rhythm [173], so not controlling day-night cycling of light may also affect behaviour. To make that data more robust, extra controls for humidity, vibrations and circadian rhythm could be used as these were not controlled for in any experiments**.**

Automatic tracking software is needed for identifying roaming, dwelling and quiescence behaviour

The exploration assay used for all experiments in this thesis measured movement coverage, which can measure the percentage of a plate explored after 16 h, but cannot distinguish between the individual behavioural states roaming, dwelling and quiescence throughout those 16 h. This becomes a problem when a worm has clear tracks that resemble those of a dwelling worm, but the dwelling has occurred in a large area that, once converted into a %, would indicate the worm has normal exploration for which is does not. For future experiments, software could be used to automatically track worms to distinguish all three behavioural states temporally, alongside movement speed and other parameters [153]. This could be used alongside WorMotel, to allow high-

throughput behavioural assays to be performed [90]. For the current data produced, a program that can detect roaming and dwelling patterns from images would more accurately interpret the exploration data.

ASI-specific RNA-Seq and in starved conditions may elucidate further roles of SKN-1B-related exploration

A possibility to why RNAi did not reduce exploration of N2 worms to *skn-1b* levels was due to inaccurate RNA-Seq data, so RNAi may have been performed on the wrong genes. However, when *skn-1b* mutant RNA-Seq data was compared with previously published *skn-1* RNAi microarray data, which had 233 upregulated and 63 downregulated genes, 6 genes were shared between the two data sets (*cat-4, asp-14, F55G11.2, F55G11.8, gst-10* and *F22H10.2*) [148], indicating RNA-Seq was likely performed correctly. Interestingly, all 6 genes are upregulated in *skn-1* RNAi, but only *gst-10* and *F22H10.2* are upregulated in *skn-1b* mutants (Supplementary Table 2), indicating overlapping functionality between isoforms, but also regulatory differences.

Another reason for no obvious reduction of N2 exploration to *skn-1b* mutants was that the RNA-Seq performed was not sensitive enough due to being whole body RNA-Seq rather than ASI-specific RNA-Seq. Whole worm RNA-Seq was performed as *skn-1b* mutants have hyperfused body wall muscle mitochondria which would not be accounted for in ASI-specific RNA-Seq. Having both whole body and ASI-specific data might help understand how *skn-1b* may directly affect gene expression in the ASIs, and by knowing which genes are differentially expressed in the ASIs help elucidate the pathway from the ASI to the rest of the body. If budget allowed, scRNA-Seq could be performed on *skn-1b* mutants to identify gene expression changes within each cell of the organism. Also, as SKN-1B is active under starvation, having an RNA-Seq data set with N2 worms and *skn-1b* mutants in starved and re-fed worms may elucidate why N2 worms have reduced exploration under starvation, whilst starved and non-starved *skn-1b* mutants have no exploration change [39].

Does SKN-1B have functions outside of exploratory behaviour? Developmental defects, collagen and cuticlin genes in the *skn-1b* mutant

Following on from the lack of reduced exploration from the RNAi screen, it indicated (alongside the bioinformatic analysis) that *skn-1b* had additional roles outside of exploratory behaviour of which *skn-1b* mutants differentially expressed genes may contribute.

A number of genes in the *skn-1b* mutant are downregulated, with RNAi of *dve-1*, *hil-7* and *hbl-1* caused developmental defects i.e. larval lethality (which was already known to occur with RNAi, see Table 4). This indicated whilst these genes are downregulated in the *skn-1b* mutant, it is not to an extent to cause any obvious phenotypes as seen with RNAi knockdown. This may mean these genes may be affected partially by SKN-1B, but not to the extend to cause a phenotype, or that they have other roles outside of development, possibly exploration. To bypass embryonic development, knocking down these genes at L1 (or further) stages would elucidate if these genes have an additional role in exploration.

C. elegans need a cuticle to be protected from the outside environment, but also to allow normal locomotion. SKN-1B may be involved in cuticle development, as the cuticle is predominantly composed of collagens and cuticlins [174] and genes between p= 0.05 to 0.1 from the *skn-1b* mutant RNA-Seq data set revealed 33 extra genes, including 4 collagen (*col*) genes downregulated and 1 upregulated (data not shown). Whilst these are out of statistical significance, it links with the downregulated *cut* genes in *skn-1b* mutants. *cut* genes are needed for the development of the cuticle in L1, dauer and adult stages in *C. elegans*, with CUT-3 and CUT-5 needed for L1 cuticle development. *cut-3*, *-5* and *-6* are all downregulated in *skn-1b* mutants, and reduced *cut-3* or *cut-5* expression causes worms to be larger in diameter due to increased lateral cuticle width [175]. This may link with *skn-1b* mutants being slightly larger than N2 worms [39]. However, locomotion is normal in *skn-1b* mutants, with no unc phenotype seen [39], overall indicating SKN-1B may have a role in cuticle development that it is not essential for movement.

As many of these genes seem to have links with organ development and maintenance, it would indicate loss of *skn-1b* might cause developmental defects, but no obvious phenotype (unc, egl, dumpy, developmental delay etc.) was seen in *skn-1b* mutants when carrying out experiments or when analysed previously [39]. Detailed analysis of the cuticle, pharynx and nervous system may give insight into if there are subtle changes.

To understand if these genes influence *skn-1b* expression (not necessarily to effect exploration), an RNAi screen with *skn1b::gfp* worms followed by measuring GFP fluorescence would show if *skn-1b* expression is changed upon RNAi of these genes, followed by *skn-1b* RT-qPCR to confirm if there was a change.

***gst-10* is upregulated in starvation to remove ROS, indicating increased ROS in *skn-1b* mutants**

Radical oxygen species (ROS) may be increased in *skn-1b* mutants as *gst-10* is upregulated in *skn-1b* mutants, and *gst* genes are upregulated upon increased ROS to remove it e.g. *gst-10* is increased in starvation [176], linking to the starvation phenotypes seen in *skn-1b* worms. Interestingly, *gst-10* upregulation is associated with reduced IIS [59], linking SKN-1B with IIS, although no insulin-like peptides were seen in the *skn-1b* mutant RNA-Seq data, indicating a direct role in IIS is unlikely.

SKN-1B likely has roles in the innate immune response (CUB, *F-box* and *pqn* genes)

An interesting finding throughout the bioinformatic analysis seemed to be the implication that *skn-1b* had roles in innate immunity. *F55G11.8* and *F55G11.2* are innate immune response CUB-domain containing genes [177] and are downregulated in *skn-1b* mutants (Supplementary Table 2). CUB-domain genes primarily respond to extracellular pathogens e.g. *F55G11.2* and F55G11.8 are upregulated upon *P. aeruginosa* infection [178, 179], as CUB-domain genes are downregulated upon intracellular bacterial *N. parisii* infection [180]. *F55G11.8* and *F55G11.2* are genetically close chromosomally (Table 5) but are not in an operon, but they are predicted to be transcribed by SKN-1 (Table 5), with *F55G11.2* bound and likely transcribed by SKN-1 as loss of *skn-1* (though likely *skn-1a*) represses *F55G11.2* expression [179].

Downregulation of *F55G11.8* and *F55G11.2* may indicate *skn-1b* mutants cannot respond to bacterial infection, at least, once infected, as *skn-1b* mutants can still avoid *P. aeruginosa* [39]. OA GPCR OCTR-1 is needed in ASI and ASH neurons to suppress the immune system (downregulates *pqn*/*abu* genes [108]). As *pqn-73* is downregulated in *skn-1b* mutants, and *pqn* genes are needed to survive against pathogenic infection [181] this would further indicate the immune system is suppressed in *skn-1b* mutants. Overall, this indicates SKN-1B may have a role in promoting the extracellular bacterial innate immune response.

Another indication of *skn-1b* having a role in immunity is that F-box proteins may have immune function, as STRING analysis found PQN-73, the family of genes needed to survive against pathogenic infection, interacted with FBXA-192 (q=0.01, data not shown). F-box A (*fbxa*) genes are the most upregulated in *skn-1b* mutants, with F-box B and C the most downregulated, as 6 of the 12 most downregulated genes are either F-box B or C genes, with *fbxc-42* the most downregulated (-4.5 log2fold, Supplementary Table 2). These are the most represented gene family in the RNA-Seq data set. Is this to do with immune function?

F-box domains are the 4th most common domain in *C. elegans* [182], with ~520 F-box genes predicted [183] compared to 11 in budding yeast, 22 in *Drosophila* and ≥38 in humans [182]. These are related to MATH and BTB genes [183], which were also differentially expressed in *skn-1b* mutants. F-box proteins allow protein-protein interactions, with the most well-known (called Skp1−Cul1−F-box protein (SCF)) making up an E3 ligase to allow ubiquitination and degradation of proteins. F-box proteins with E3 activity are involved in the innate immune response [184], in particular to intracellular pathogens (proteins made by intracellular pathogens can be degraded by ubiquitination) [180]. The reason for the large number of F-box genes compared to other species is hypothesised as an evolutionary response to pathogens, with more gene variations needed to survive the ever increasing/changing pathogens in the environment. As *C. elegans* do not have professional immune cells, the increase of F-box genes may be occur to compensate this [185]. Whilst likely true, F-box proteins also have roles

outside of innate immunity e.g. spermatogenesis [182], promote GABA release [186] and more relevantly, *xrep-4* is needed for SKN-1-dependent expression of detoxification genes [187].

Interestingly, in aryl hydrocarbon receptor 1 (*ahr-1*) mutants (*ia03* and *ju145*), *fbxa-191*, *-192* and -*193* are the most downregulated genes (apart from one gene) from a set of 139 genes (14 upregulated, 125 downregulated) [188]. This contrasts the *skn-1b* mutant RNA-Seq data where these 3 genes are upregulated, with *fbxa-192* being the highest upregulated of the 69 genes. If loss of *ahr-1* causes downregulation, but loss of *skn-1b* causes upregulation, it might indicate these genes may have opposing functions. However, they may have joined functionality, as *hil-7* was downregulated in the *arh-1(ia03)* RNA-Seq set [188], as in the *skn-1b* mutant RNA-Seq set (Supplementary Table 2).

In mammals, AHR-1 transcribes xenobiotic-metabolising enzymes, which link to Nrf2-transcribed antioxidant enzymes for ROS stress, with Nrf2 being a target gene of AhR [189]. In *C. elegans*, *ahr-1* expression in URX neurons promotes social feeding (aggregation) behaviour on the bacterial lawn edge and hypoxia avoidance [190]. *ahr-1* mutants also have reduced body bends/movement (an unc phenotype) and changes in lipid composition, with up and downregulation of fatty acid synthesis genes [191]. AHR-1s putative binding site (GCGTG) is in the upstream sequence of *skn-1a* and the 5' UTR of *skn-1b* indicating it may regulate skn-*1* transcription (data not shown, WormBase). Overall, this indicates *ahr-1* may have overlapping/or similar roles to *skn-1*, and therefore the *fbxa* genes may also have roles relating to these functions, and possibly not immunity like other F-box genes.

But overall, the small amount of research into these F-box genes is surprising, considering the amount. This is likely due to RNAi being performed on many F-box and MATH-BTB genes with no phenotype seen [183, 192]. This matches the lack of phenotypes seen in the F-box and MATH-containing genes in the RNA-Seq data set of *skn-1b* mutants (Fig. 17 and 18). It is intriguing that SKN-1B may be involved in regulating the immune response, specifically to intracellular pathogens (*fbxa-191*, *-192* and -*193* are upregulated, as is *bath-25*). But as none of the F-box proteins in the RNA-Seq data set have had functional characterisation, this currently speculation, and could likely have other

functions. But as other immune function genes have been seen in this data set, it indicates there is a possible function in immunity for SKN-1B.

Operons and clustered genes in the *skn-1b* mutant

Many genes in the *skn-1b* mutant RNA-Seq data set were related in function, so it was speculated some genes might be in operons. This was the case for *fbxa-191*, *-192* and *-193* and *pqn-73* (Table 5). The finding of an operon in this set is likely not a unique phenomenon, as 15% of *C. elegans* genes are in operons [193]. The F-box B and C genes were not predicted to be in an operon, but instead (alongside *math-34*, *btb-11*, *F45D11.1* and *F45D11.5*) were all genetically close to each other (Table 5), and all found in part of circRNA *K02E7.15*. This indicates these genes instead are possibly regulated and/or transcribed through this circRNA.

The fact that F-box A genes are on a different chromosome and are upregulated, whereas the F-box B and C genes (and the other 4 in the set of 10) are downregulated, indicated the F-box B/C genes are likely transcribed together. Although as the circRNA had 17 other genes/pseudogenes/RNAs encoded within its region which were not differentially expressed in *skn-1b* mutants, indicated specific regulation of these 10 genes occurred when SKN-1B is expressed.

In *C. elegans*, there are ~1166 circRNAs, with functions linked to immunity (and the cause of autoimmunity in humans) [194], transcription regulation, protein binding, with some circRNA translated into proteins via cap-independent mechanisms [195]. But why are these 10 genes (among the other 17) in a circRNA, and what could this mean in terms of SKN-1 signalling? Does this give any clues to the function of this set of genes? A reason why these genes might be in an operon-like structure is to respond quickly to a change in environment e.g. starvation. Promoting transcription through an operon to up or downregulate many genes would be quicker than individual transcription [196]. This also gives a possible reason to why single RNAi of these genes did not show any exploration difference (Fig. 17 and 18) because if they are transcribed together/and or regulated by the *K02E7.15* circRNA, they likely have related functions, and may compensate for loss of one via

RNAi, hence no exploration difference (presuming they have a role in exploration). As no SKN-1 binding was found in or near the circRNA or for any closely related genes found (Table 5), it is unclear how these relate to SKN-1, and why these are encoded in a circRNA compared to a traditional operon is also unknown.

Pseudogenes in the *skn-1b* mutant is likely a normal occurrence, but may have a role with F-box A genes

6 pseudogenes were found in the 69 total genes in the *skn-1b* mutant RNA-Seq data set: *fbxa-191, fbxa-193, Y102A5C.6, W06A11.4, Y102A5C.5* and *F45D11.1,* which is likely a normal occurrence, as it is estimated ~20% of the *C. elegans* genome are pseudogenes [197]. Pseudogenes are usually non-coding genes which have a variety of functions, including gene regulation (upregulation or downregulation) of their 'parent' protein-coding gene [198]. This may be the role for the *fbxa* genes, with *fbxa-191* and *-193* regulating the highest upregulated protein-coding gene of the *skn-1b* mutant, *fbxa-192*. As the genes have differential expression in the *skn-1b* mutant, it indicates they likely have some function and are likely outside of the control of the operon they are in (Table 5), as the operon contains another *fbxa* gene which is not part of the differentially expressed genes in the mutant. What these genes functionally do is still unknown, with no exploration changes when RNAi was performed to give any insight (Fig. 17).

Bioinformatic limitations/caveats

There are many caveats of CeNGEN, including certain genes were not included in the data set e.g. *F45D11.5* and that data is based on L4 hermaphrodites, so cannot be assumed L4 gene expression matches adult stage in hermaphrodites. This is particular caveat when comparing the *skn-1b* mutant differentially expressed genes, as Day 1 adults were used to create the *skn-1b* mutant RNA-Seq data, so gene expression changes between L4 and Day 1 adult stages would have been unaccounted for.

Gene isoforms cannot be differentiated in the CeNGEN data set either, so *skn-1* expression encompasses all isoforms, including *skn-1b*. Specific *skn-1* expression in ASI neurons and

modENCODE data was used to narrow down the likelihood of a *skn-1b* target, but specific isoform experiments would need to be performed to confirm a *skn-1b* target.

modENCODE data also had caveats, as only SKN-1 overall binding is analysed, with no SKN-1B-specific data available. DNA-protein pulldown assays mixed with ChIP-Seq would give more specific results. No isoform-specific data was also a problem with STRING analysis, as the general SKN-1 protein is used, so SKN-1B-specific interactions may have been missed. SKN-1B protein-protein pull-down assays could be performed to understand SKN-1B interactions further. Following STRING analysis (and GO term analysis), problems included many proteins and genes were unannotated/unknown in function or specific expression pattern, so inferring function could not always be performed. Protein modelling and function prediction software may help understand the roles of these proteins involvement with SKN-1B.

To not rely solely on CeNGEN or other bioinformatic analysis, *skn-1b* mutant scRNA-Seq would be useful to understand cell specific gene expression changes of the whole organism, which may shed light on the mitochondrial muscle morphology changes as previously mentioned. Also, combining the RNA-Seq data set and performing *skn-1b* ChIP-Seq to identify what genes are specifically bound by SKN-1B could be used to learn if any differentially expressed genes in the *skn-1b* mutant correlates with those that have direct binding, but also to show if *skn-1b* has DNA binding activity.

Future study

For future study, understanding what transcribes *skn-1b* (including in well-fed vs starved conditions), or its translational regulation e.g. RNA-binding proteins or miRNAs binding to its UTRs, would further elucidate its place in the exploration pathway (and other possible functions) in the worm.

Summary

Overall, RNAi of 46 of 69 differentially expressed genes in *skn-1b* mutants caused no large change in food-related exploration, including those predicted to be expressed in neurons, glia, muscle and intestine. No genes were a likely SKN-1B direct target as none had ASI-specific expression in parallel

with potential SKN-1B binding. Genes not screened may affect exploration e.g. *cat-4*, which would need to be tested. Alternatively, SKN-1B may have roles outside of exploration e.g. immunity, that have yet to be explored (Fig. 20).

Thesis summary

This thesis has explored the role of *skn-1b* in 3 contexts. Firstly, the biogenic amine TA is likely needed for SKN-1B to signal from the ASI neurons to the rest of the worm to effect exploration. Secondly, how loss of *skn-1b* is sex-specific, with D1 males showing no exploratory defect, but still have SKN-1B::GFP expressed in ASI neurons and D1 male-only expression in the VA11 neuron near the tail for yet unknown functions. Thirdly, *skn-1b(tm4241)*s differentially expressed genes may not have a role in exploration, but roles in immunity.

Overall, this study has elucidated SKN-1Bs function further and with the discussed future experiments in each chapter, should be continued to be investigated. In mice, Nrf1 and Nrf2 have involvement in glycolysis and mitochondrial biogenesis [199, 200] with exogenous Nrf1 expression improving insulin sensitivity in obese mice [201], and as both isoforms are expressed in the brain [202] [203]). These studies indicate SKN-1/Nrf may have conserved food-related roles, but Nrf food-related behaviour has yet to be investigated. Fly and mouse studies could be performed e.g. RNA-Seq of *Drosophila* and mice that have SKN-1B/CnC/Nrf mutant homologs, and compare data sets for both conserved and divergent genes that these SKN-1/CnC/Nrf may regulate to bridge the gap from *C. elegans* to higher organisms and further understand the molecular control of food-related behaviours. If Nrf does affect food-related behaviour, it would offer the potential for further understanding mammalian eating behaviours and a potential drug target or marker for pathological eating behaviour.

Acknowledgements

Tullet and Ezcurra labs: Antonis Karamalegos, Dan Scanlon, Jennifer Tullet, Laura Freeman, Marina Ezcurra, Mireya Vazquez-Prada, Nathan Dennis, Nikolaos Tataridas-Pallas, Yasir Malik and Zoe King. Thank you all for the scientific and non-scientific chats over the year, from making art, playing pool (badly) to having a BBQ and singing, it's been a good one! Also, a special thanks to Jenny. I'm forever grateful for your feedback and general guidance over the year, reading the many drafts of this thesis (!), whilst always trying to keep my mind on the story (as much as it likes to do 10 things at once)!

Thanks to Julian Cook, Lisa Munday, and Robert Akerman: because technicians make it happen!

Thanks to all those in the Kent Fungal Group (KFG) and beyond!

Thanks to Dan Mulvihill, Ian Brown, and Karen Baker for microscopy assistance.

Thanks to WormBase and WormBook, and some strains were provided by the CGC, which is funded by NIH Office of Research Infrastructure Programs (P40 OD010440).

References

1. Hruby, A., and F.B. Hu. 2015. The Epidemiology of Obesity: A Big Picture. Pharmacoeconomics. 33: 673–689.
2. Gibson-Moore, H. 2009. Satiation, satiety and their effects on eating behaviour. Nutr. Bull. 34: 412–416.
3. Amin, T., and J.G. Mercer. 2016. Hunger and Satiety Mechanisms and Their Potential Exploitation in the Regulation of Food Intake. Curr. Obes. Rep. 5: 106–112.
4. You, Y. jai, J. Kim, D.M. Raizen, and L. Avery. 2008. Insulin, cGMP, and TGF-β Signals Regulate Food Intake and Quiescence in C. elegans: A Model for Satiety. Cell Metab. 7: 249–257.
5. Chen, Y., Y.C. Lin, T.W. Kuo, and Z.A. Knight. 2015. Sensory Detection of Food Rapidly Modulates Arcuate Feeding Circuits. Cell. 160: 829–841.
6. Augustine, V., S. Lee, and Y. Oka. 2020. Neural Control and Modulation of Thirst, Sodium Appetite, and Hunger. Cell. 180: 25–32.
7. Chen, Y., R.A. Essner, S. Kosar, O.H. Miller, Y.C. Lin, S. Mesgarzadeh, and Z.A. Knight. 2019. Sustained NPY signaling enables AgRP neurons to drive feeding. Elife. 8.
8. Schwartz, M.W., S.C. Woods, D. Porte, R.J. Seeley, and D.G. Baskin. 2000. Central nervous system control of food intake. Nature. 404: 661–671.
9. Garrison, J.L., and Z.A. Knight. 2017. Linking smell to metabolism and aging. Science (80-.). 358: 718–719.
10. You, Y.J., and L. Avery. 2012. Appetite control: Worm's-eye-view. Animal Cells Syst. (Seoul). 16: 351–356.
11. Hetherington, A.W., and S.W. Ranson. 1940. Hypothalamic lesions and adiposity in the rat. Anat. Rec. 78: 149–172.
12. Bolborea, M., and N. Dale. 2013. Hypothalamic tanycytes: Potential roles in the control of feeding and energy balance. Trends Neurosci. 36: 91–100.
13. Bolborea, M., E. Pollatzek, H. Benford, T. Sotelo-Hitschfeld, and N. Dale. 2020. Hypothalamic tanycytes generate acute hyperphagia through activation of the arcuate neuronal network. Proc. Natl. Acad. Sci. U. S. A. 117: 14473–14481.
14. Byerly, L., R.C. Cassada, and R.L. Russell. 1976. The life cycle of the nematode Caenorhabditis elegans. Dev. Biol. 51: 23–33.
15. Cassada, R.C., and R.L. Russell. 1975. The dauerlarva, a post-embryonic developmental variant of the nematode Caenorhabditis elegans. Dev. Biol. 46: 326–342.
16. Stiernagle, T. 2006. Maintenance of C. elegans. WormBook. : 1–11.
17. Gems, D., and D.L. Riddle. 2000. Defining wild-type life span in Caenorhabditis elegans. Journals Gerontol. - Ser. A Biol. Sci. Med. Sci. 55: 215–219.
18. Nigon, V. 1949. Les modalites de la reproduction et le determinisme du sexe chez quelques nematodes libres. .
19. Hodgkin, J., H.R. Horvitz, and S. Brenner. 1979. NONDISJUNCTION MUTANTS OF THE NEMATODE CAENORHABDITIS ELEGANS. Genetics. 91: 67–94.

20. Chasnov, J.R., and K.L. Chow. 2002. Why Are There Males in the Hermaphroditic Species Caenorhabditis elegans ? Genetics. 994: 983–994.

21. Flavell, S.W., D.M. Raizen, and Y.J. You. 2020. Behavioral states. Genetics. 216: 315–332.

22. Ben Arous, J., S. Laffont, and D. Chatenay. 2009. Molecular and sensory basis of a food related two-state behavior in C. elegans. PLoS One. 4: e7584–e7584.

23. Gallagher, T., J. Kim, M. Oldenbroek, R. Kerr, and Y.J. You. 2013. ASI regulates satiety quiescence in C. elegans. J. Neurosci. 33: 9716–9724.

24. Trojanowski, N.F., and D.M. Raizen. 2016. Call it Worm Sleep. Trends Neurosci. 39: 54–62.

25. Driver, R.J., A.L. Lamb, A.J. Wyner, and D.M. Raizen. 2013. DAF-16/FOXO regulates homeostasis of essential sleep-like behavior during larval transitions in C. elegans. Curr. Biol. 23: 501–506.

26. Wu, Y., F. Masurat, J. Preis, and H. Bringmann. 2018. Sleep Counteracts Aging Phenotypes to Survive Starvation-Induced Developmental Arrest in C. elegans. Curr. Biol. 28: 3610-3624.e8.

27. Raizen, D.M., J.E. Zimmerman, M.H. Maycock, U.D. Ta, Y.J. You, M. V. Sundaram, and A.I. Pack. 2008. Lethargus is a Caenorhabditis elegans sleep-like state. Nature. 451: 569–572.

28. McClanahan, P.D., J.M. Dubuque, D. Kontogiorgos-Heintz, B.F. Habermeyer, J.H. Xu, A.M. Ma, D.M. Raizen, and C. Fang-Yen. 2020. A quiescent state following mild sensory arousal in Caenorhabditis elegans is potentiated by stress. Sci. Rep. 10: 1–16.

29. Gonzales, D.L., J. Zhou, B. Fan, and J.T. Robinson. 2019. A microfluidic-induced C. elegans sleep state. Nat. Commun. 10: 1–13.

30. Meneely, P.M., C.L. Dahlberg, and J.K. Rose. 2019. Working with Worms: Caenorhabditis elegans as a Model Organism. Curr. Protoc. Essent. Lab. Tech. 19: 1–35.

31. Barrios, A., R. Ghosh, C. Fang, S.W. Emmons, and M.M. Barr. 2012. PDF-1 neuropeptide signaling modulates a neural circuit for mate-searching behavior in C. elegans. Nat. Neurosci. 15: 1675–1682.

32. White, J.G., E. Southgate, J.N. Thomson, and S. Brenner. 1986. The Structure of the Nervous System of the Nematode Caenorhabditis elegans. Philos. Trans. R. Soc. B Biol. Sci. : 1–340.

33. Oikonomou, G., and S. Shaham. 2011. The glia of caenorhabditis elegans. Glia. 59: 1253–1263.

34. Molina-García, L., C. Lloret-Fernández, S.J. Cook, B. Kim, R.C. Bonnington, M. Sammut, J.M. O'shea, S.P.R. Gilbert, D.J. Elliott, D.H. Hall, S.W. Emmons, A. Barrios, and R.J. Poole. 2020. Direct glia-to-neuron transdifferentiation gives rise to a pair of male-specific neurons that ensure nimble male mating. Elife. 9: 1–32.

35. Sulston, J.E., E. Schierenberg, J.G. White, and J.N. Thomson. 1983. The embryonic cell lineage of the nematode Caenorhabditis elegans. Dev. Biol. 100: 64–119.

36. Lai, C.H., C.Y. Chou, L.Y. Ch'ang, C.S. Liu, and W.C. Lin. 2000. Identification of novel human genes evolutionarily conserved in Caenorhabditis elegans by comparative proteomics. Genome Res. 10: 703–713.

37. Nance, J., and C. Frøkjær-Jensen. 2019. The caenorhabditis elegans transgenic toolbox. Genetics. 212: 959–990.

38. Conte, D., L.T. MacNei, A.J.M. Walhout, and C.C. Mello. 2015. RNA Interference in

Caenorhabditis elegans. Curr. Protoc. Mol. Biol. 2015: 26.3.1-26.3.30.

39. Tataridas-Pallas, N., M. Thompson, A. Howard, I. Brown, M. Ezcurra, Z. Wu, T. Keurten, I.G. Silva, T.K. Blackwell, and J. Tullet. 2020. Neuronal SKN-1B Modulates Nutritional Signalling Pathways and Mitochondrial Networks to Control Satiety. PLoS Genet. : 1–28.

40. Dresen, A., S. Finkbeiner, M. Dottermusch, J.S. Beume, Y. Li, G. Walz, and E. Neumann-Haefelin. 2015. Caenorhabditis elegans OSM-11 signaling regulates SKN-1/Nrf during embryonic development and adult longevity and stress response. Dev. Biol. 400: 118–131.

41. Blackwell, T.K., M.J. Steinbaugh, J.M. Hourihan, C.Y. Ewald, and M. Isik. 2015. SKN-1/Nrf, stress responses, and aging in Caenorhabditis elegans. Free Radic. Biol. Med. 88: 290–301.

42. Ogawa, T., Y. Kodera, D. Hirata, T.K. Blackwell, and M. Mizunuma. 2016. Natural thioallyl compounds increase oxidative stress resistance and lifespan in Caenorhabditis elegans by modulating SKN-1/Nrf. Sci. Rep. 6.

43. Bowerman, B., B.A. Eaton, and J.R. Priess. 1992. skn-1, a maternally expressed gene required to specify the fate of ventral blastomeres in the early C. elegans embryo. Cell. 68: 1061–1075.

44. Walker, A.K., R. See, C. Batchelder, T. Kophengnavong, J.T. Gronniger, Y. Shi, and T.K. Blackwell. 2000. A conserved transcription motif suggesting functional parallels between Caenorhabditis elegans SKN-1 and Cap'n'Collar-related basic leucine zipper proteins. J. Biol. Chem. 275: 22166–22171.

45. Lehrbach, N.J., P.C. Breen, and G. Ruvkun. 2019. Protein Sequence Editing of SKN-1A/Nrf1 by Peptide:N-Glycanase Controls Proteasome Gene Expression. Cell. 177: 737-750.e15.

46. Bishop, N.A., and L. Guarente. 2007. Two neurons mediate diet-restriction-induced longevity in C. elegans. Nature. 447: 545–549.

47. Tullet, J.M.A., M. Hertweck, J.H. An, J. Baker, J.Y. Hwang, S. Liu, R.P. Oliveira, R. Baumeister, and T.K. Blackwell. 2008. Direct Inhibition of the Longevity-Promoting Factor SKN-1 by Insulin-like Signaling in C. elegans. Cell. 132: 1025–1038.

48. Lehrbach, N.J., and G. Ruvkun. 2019. Endoplasmic reticulum-associated SKN-1A/Nrf1 mediates a cytoplasmic unfolded protein response and promotes longevity. Elife. 8: 1–25.

49. Lehrbach, N.J., and G. Ruvkun. 2016. Proteasome dysfunction triggers activation of SKN-1A/Nrf1 by the aspartic protease DDI-1. Elife. 5: 1–19.

50. Paek, J., J.Y. Lo, S.D. Narasimhan, T.N. Nguyen, K. Glover-Cutter, S. Robida-Stubbs, T. Suzuki, M. Yamamoto, T.K. Blackwell, and S.P. Curran. 2012. Mitochondrial SKN-1/Nrf mediates a conserved starvation response. Cell Metab. 16: 526–537.

51. Birnby, D.A., E.M. Link, J.J. Vowels, H. Tian, P.L. Colacurcio, and J.H. Thomas. 2000. A transmembrane guanylyl cyclase (DAF-11) and Hsp90 (DAF-21) regulate a common set of chemosensory behaviors in Caenorhabditis elegans. Genetics. 155: 85–104.

52. Spurlock, B., J.M.A. Tullet, J.L. Hartman, and K. Mitra. 2020. Interplay of mitochondrial fission-fusion with cell cycle regulation: Possible impacts on stem cell and organismal aging. Exp. Gerontol. 135: 110919.

53. Singhvi, A., and S. Shaham. 2019. Glia-Neuron Interactions in Caenorhabditis elegans. Annu. Rev. Neurosci. 42: 149–168.

54. Greene, J.S., M. Brown, M. Dobosiewicz, I.G. Ishida, E.Z. Macosko, X. Zhang, R.A. Butcher, D.J. Cline, P.T. McGrath, and C.I. Bargmann. 2016. Balancing selection shapes density-dependent

foraging behaviour. Nature. 539: 254–258.

55. Yeon, J., A. Takeishi, and P. Sengupta. 2021. Chronic vs acute manipulations reveal degeneracy in a thermosensory neuron network. microPublication Biol. 2021.

56. Peckol, E.L., E.R. Troemel, and C.I. Bargmann. 2001. Sensory experience and sensory activity regulate chemosensory receptor gene expression in Caenorhabditis elegans. Proc. Natl. Acad. Sci. U. S. A. 98: 11032–11038.

57. Kim, K., K. Sato, M. Shibuya, D.M. Zeiger, R.A. Butcher, J.R. Ragains, J. Clardy, K. Touhara, and P. Sengupta. 2009. Two chemoreceptors mediate developmental effects of dauer pheromone in C. elegans. Science (80-.). 326: 994–998.

58. White, J.Q., and E.M. Jorgensen. 2012. Sensation in a Single Neuron Pair Represses Male Behavior in Hermaphrodites. Neuron. 75: 593–600.

59. Park, D., K.L. Jones, H. Lee, T.P. Snutch, S. Taubert, and D.L. Riddle. 2012. Repression of a potassium channel by nuclear hormone receptor and TGF-β signaling modulates insulin signaling in Caenorhabditis elegans. PLoS Genet. 8.

60. Singh, V., and A. Aballay. 2012. Endoplasmic reticulum stress pathway required for immune homeostasis is neurally controlled by arrestin-1. J. Biol. Chem. 287: 33191–33197.

61. Gray, J.M., J.J. Hill, and C.I. Bargmann. 2005. A circuit for navigation in Caenorhabditis elegans. Proc. Natl. Acad. Sci. U. S. A. 102: 3184–3191.

62. Flavell, S.W., N. Pokala, E.Z. Macosko, D.R. Albrecht, J. Larsch, and C.I. Bargmann. 2013. Serotonin and the neuropeptide PDF initiate and extend opposing behavioral states in C. Elegans. Cell. 154: 1023–1035.

63. Palamiuc, L., T. Noble, E. Witham, H. Ratanpal, M. Vaughan, and S. Srinivasan. 2017. A tachykinin-like neuroendocrine signalling axis couples central serotonin action and nutrient sensing with peripheral lipid metabolism. Nat. Commun. 8.

64. Davis, K.C., Y.I. Choi, J. Kim, and Y.J. You. 2018. Satiety behavior is regulated by ASI/ASH reciprocal antagonism. Sci. Rep. 8: 3–9.

65. Handley, A., and R. Pocock. 2017. Transcriptional control of satiety in Caenorhabditis elegans. Commun. Integr. Biol. 10: e1325978.

66. Murakami, M., M. Koga, and Y. Ohshima. 2001. DAF-7/TGF-β expression required for the normal larval development in C. elegans is controlled by a presumed guanylyl cyclase DAF-11. Mech. Dev. 109: 27–35.

67. Juozaityte, V., D. Pladevall-Morera, A. Podolska, S. Nørgaar, B. Neumann, and R. Pocock. 2017. The ETS-5 transcription factor regulates activity states in Caenorhabditis elegans by controlling satiety. Proc. Natl. Acad. Sci. U. S. A. 114: E1651–E1658.

68. Serrano-Saiz, E., B. Gulez, L. Pereira, M. Gendrel, S.Y. Kerk, B. Vidal, W. Feng, C. Wang, P. Kratsios, J.B. Rand, and O. Hobert. 2020. Modular Organization of Cis-regulatory Control Information of Neurotransmitter Pathway Genes in Caenorhabditis elegans. Genetics. 215: 665–681.

69. Gendrel, M., E.G. Atlas, and O. Hobert. 2016. A cellular and regulatory map of the GABAergic nervous system of C. elegans. Elife. 5: 1–38.

70. Serrano-Saiz, E., L. Pereira, M. Gendrel, U. Aghayeva, A. Battacharya, K. Howell, L.R. Garcia, and O. Hobert. 2017. A neurotransmitter atlas of the Caenorhabditis elegans male nervous

system reveals sexually dimorphic neurotransmitter usage. Genetics. 206: 1251–1269.

71. Speese, S., M. Petrie, K. Schuske, M. Ailion, K. Ann, K. Iwasaki, E.M. Jorgensen, and T.F.J. Martin. 2007. UNC-31 (CAPS) is required for dense-core vesicle but not synaptic vesicle exocytosis in Caenorhabditis elegans. J. Neurosci. 27: 6150–6162.

72. Greene, J.S., M. Dobosiewicz, R.A. Butcher, P.T. McGrath, and C.I. Bargmann. 2016. Regulatory changes in two chemoreceptor genes contribute to a caenorhabditis elegans QTL for foraging behavior. Elife. 5: 1–19.

73. Altun, Z.F., L.A. Herndon, C.A. Wolkow, C. Crocker, R. Lints, and D.H. Hall. WormAtlas. .

74. Serrano-Saiz, E., R.J. Poole, T. Felton, F. Zhang, E.D. De La Cruz, and O. Hobert. 2013. Modular control of glutamatergic neuronal identity in C. elegans by distinct homeodomain proteins. Cell. 155: 659.

75. Jacob, T.C., and J.M. Kaplan. 2003. The EGL-21 carboxypeptidase E facilitates acetylcholine release at Caenorhabditis elegans neuromuscular junctions. J. Neurosci. 23: 2122–2130.

76. Duerr, J.S., D.L. Frisby, J. Gaskin, A. Duke, K. Asermely, D. Huddleston, L.E. Eiden, and J.B. Rand. 1999. The cat-1 gene of Caenorhabditis elegans encodes a vesicular monoamine transporter required for specific monoamine-dependent behaviors. J. Neurosci. 19: 72–84.

77. Richmond, J.E., W.S. Davis, and E.M. Jorgensen. 1999. UNC-13 is required for synaptic vesicle fusion in C . elegans. Nat. Neurosci. 2: 959–964.

78. Smart, T.G., and P. Paoletti. 2012. Synaptic Neurotransmitter-Gated Receptors. Cold Spring Harb. Perspect. Biol. : 1–26.

79. Mckay, J.P., D.M. Raizen, A. Gottschalk, W.R. Schafer, and L. Avery. 2004. eat-2 and eat-18 Are Required for Nicotinic Neurotransmission in the Caenorhabditis elegans Pharynx. Genetics. 166: 161–169.

80. McIntire, S., E. Jorgensen, and H.R. Horvitz. 1993. Genes required for GABA function in C. elegans. Nature. 364: 334–337.

81. Lin, X.G., M. Ming, M.R. Chen, W.P. Niu, Y.D. Zhang, B. Liu, Y.M. Jiu, J.W. Yu, T. Xu, and Z.X. Wu. 2010. UNC-31/CAPS docks and primes dense core vesicles in C. elegans neurons. Biochem. Biophys. Res. Commun. 397: 526–531.

82. Volkow, N.D., G.J. Wang, and R.D. Baler. 2011. Reward, dopamine and the control of food intake: Implications for obesity. Trends Cogn. Sci. 15: 37–46.

83. Alkema, M.J., M. Hunter-Ensor, N. Ringstad, and H.R. Horvitz. 2005. Tyramine functions independently of octopamine in the Caenorhabditis elegans nervous system. Neuron. 46: 247–260.

84. Fernandez, R.W., K. Wei, E.Y. Wang, D. Mikalauskaite, A. Olson, J. Pepper, N. Christie, S. Kim, S. Weissenborn, M. Sarov, and M.R. Koelle. 2020. Cellular Expression and Functional Roles of All 26 Neurotransmitter GPCRs in the C. elegans Egg-Laying Circuit. J. Neurosci. 40: 7475–7488.

85. Sze, J.Y., M. Victor, C. Loer, Y. Shi, and G. Ruvkun. 2000. Food and metabolic signalling defects in a Caenorhabditis elegans serotonin-synthesis mutant. Nature. 403: 560–564.

86. Clark, T., V. Hapiak, M. Oakes, H. Mills, and R. Komuniecki. 2018. Monoamines differentially modulate neuropeptide release from distinct sites within a single neuron pair. PLoS One. 13: 1–22.

87. Wang, J., J. Luo, D.K. Aryal, W.C. Wetsel, R. Nass, and J.L. Benovic. 2017. G protein-coupled receptor kinase-2 (GRK-2) regulates serotonin metabolism through the monoamine oxidase AMX-2 in Caenorhabditis elegans. J. Biol. Chem. 292: 5943–5956.

88. Lee, K.S., S. Iwanir, R.B. Kopito, M. Scholz, J.A. Calarco, D. Biron, and E. Levine. 2017. Serotonin-dependent kinetics of feeding bursts underlie a graded response to food availability in C. elegans. Nat. Commun. 8.

89. Hobson, R.J., V.M. Hapiak, H. Xiao, K.L. Buehrer, P.R. Komuniecki, and R.W. Komuniecki. 2006. SER-7, a Caenorhabditis elegans 5-HT7-like receptor, is essential for the 5-HT stimulation of pharyngeal pumping and egg laying. Genetics. 172: 159–169.

90. Churgin, M.A., R.J. McCloskey, E. Peters, and C. Fang-Yen. 2017. Antagonistic serotonergic and octopaminergic neural circuits mediate food-dependent locomotory behavior in Caenorhabditis elegans. J. Neurosci. 37: 7811–7823.

91. Ringstad, N., N. Abe, and H.R. Horvitz. 2009. Ligand-Gated Chloride Channels Are Receptors for Biogenic Amines in C. elegans. Science (80-.). 325: 96–100.

92. Sulston, J., J. Dew, and S. Brenner. 1975. Dopaminergic neurons in the nematode Caenorhabditis elegans. J. Comp. Neurol. 163: 215–226.

93. Chase, D.L., J.S. Pepper, and M.R. Koelle. 2004. Mechanism of extrasynaptic dopamine signaling in Caenorhabditis elegans. Nat. Neurosci. 7: 1096–1103.

94. Suo, S., J.G. Culotti, and H.H.M. Van Tol. 2009. Dopamine counteracts octopamine signalling in a neural circuit mediating food response in C. elegans. EMBO J. 28: 2437–2448.

95. Nagashima, T., E. Oami, N. Kutsuna, S. Ishiura, and S. Suo. 2016. Dopamine regulates body size in Caenorhabditis elegans. Dev. Biol. 412: 128–138.

96. Sugiura, M., S. Fuke, S. Suo, N. Sasagawa, H.H.M. Van Tol, and S. Ishiura. 2005. Characterization of a novel D2-like dopamine receptor with a truncated splice variant and a D1-like dopamine receptor unique to invertebrates from Caenorhabditis elegans. J. Neurochem. 94: 1146–1157.

97. Bentley, B., R. Branicky, C.L. Barnes, Y.L. Chew, E. Yemini, E.T. Bullmore, P.E. Vértes, and W.R. Schafer. 2016. The Multilayer Connectome of Caenorhabditis elegans. PLoS Comput. Biol. 12: 1–31.

98. Rex, E., S.C. Molitor, V. Hapiak, H. Xiao, M. Henderson, and R. Komuniecki. 2004. Tyramine receptor (SER-2) isoforms are involved in the regulation of pharyngeal pumping and foraging behavior in Caenorhabditis elegans. J. Neurochem. 91: 1104–1115.

99. Tsalik, E.L., T. Niacaris, A.S. Wenick, K. Pau, L. Avery, and O. Hobert. 2003. LIM homeobox gene-dependent expression of biogenic amine receptors in restricted regions of the C. elegans nervous system. Dev. Biol. 263: 81–102.

100. Özbey, N.P., S. Imanikia, C. Krueger, I. Hardege, J. Morud, M. Sheng, W.R. Schafer, M.O. Casanueva, and R.C. Taylor. 2020. Tyramine Acts Downstream of Neuronal XBP-1s to Coordinate Inter-tissue UPRER Activation and Behavior in C. elegans. Dev. Cell. 55: 754-770.e6.

101. Rex, E., V. Hapiak, R. Hobson, K. Smith, H. Xiao, and R. Komuniecki. 2005. TYRA-2 (F01E11.5): A Caenorhabditis elegans tyramine receptor expressed in the MC and NSM pharyngeal neurons. J. Neurochem. 94: 181–191.

102. Chute, C.D., E.M. DiLoreto, Y.K. Zhang, D.K. Reilly, D. Rayes, V.L. Coyle, H.J. Choi, M.J. Alkema,

F.C. Schroeder, and J. Srinivasan. 2019. Co-option of neurotransmitter signaling for inter-organismal communication in C. elegans. Nat. Commun. 10: 1–13.

103. Fu, J., H. Zhang, W. Huang, X. Zhu, Y. Sheng, E. Song, and T. Xu. 2018. AIM interneurons mediate feeding suppression through the TYRA-2 receptor in C. elegans. Biophys. Reports. 4: 17–24.

104. Bendesky, A., M. Tsunozaki, M. V. Rockman, L. Kruglyak, and C.I. Bargmann. 2011. Catecholamine receptor polymorphisms affect decision-making in C. elegans. Nature. 472: 313–318.

105. Hapiak, V., P. Summers, A. Ortega, W.J. Law, A. Stein, and R. Komuniecki. 2013. Neuropeptides amplify and focus the monoaminergic inhibition of nociception in Caenorhabditis elegans. J. Neurosci. 33: 14107–14116.

106. Pirri, J.K., A.D. McPherson, J.L. Donnelly, M.M. Francis, and M.J. Alkema. 2009. A Tyramine-Gated Chloride Channel Coordinates Distinct Motor Programs of a Caenorhabditis elegans Escape Response. Neuron. 62: 526–538.

107. Wragg, R.T., V. Hapiak, S.B. Miller, G.P. Harris, J. Gray, P.R. Komuniecki, and R.W. Komuniecki. 2007. Tyramine and octopamine independently inhibit serotonin-stimulated aversive behaviors in Caenorhabditis elegans through two novel amine receptors. J. Neurosci. 27: 13402–13412.

108. Sun, J., V. Singh, R. Kajino-Sakamoto, and A. Aballay. 2011. Neuronal GPCR controls innate immunity by regulating noncanonical unfolded protein response genes. Science (80-.). 332: 729–732.

109. Yoshida, M., E. Oami, M. Wang, S. Ishiura, and S. Suo. 2014. Nonredundant function of two highly homologous octopamine receptors in food-deprivation-mediated signaling in Caenorhabditis elegans. J. Neurosci. Res. 92: 671–678.

110. Sawin, E.R., R. Ranganathan, and H.R. Horvitz. 2000. C. elegans locomotory rate is modulated by the environment through a dopaminergic pathway and by experience through a serotonergic pathway. Neuron. 26: 619–631.

111. Loer, C.M., and C.J. Kenyon. 1993. Serotonin-deficient mutants and male mating behavior in the nematode Caenorhabditis elegans. J. Neurosci. 13: 5407–5417.

112. Hare, E.E., and C.M. Loer. 2004. Function and evolution of the serotonin-synthetic bas-1 gene and other aromatic amino acid decarboxylase genes in Caenorhabditis. BMC Evol. Biol. 4: 1–20.

113. Ranganathan, R., E.R. Sawin, C. Trent, and H.R. Horvitz. 2001. Mutations in the Caenorhabditis elegans serotonin reuptake transporter MOD-5 reveal serotonin-dependent and -independent activities of fluoxetine. J. Neurosci. 21: 5871–5884.

114. Lints, R., and S.W. Emmons. 1999. Patterning of dopaminergic neurotransmitter identity among Caenorhabditis elegans ray sensory neurons by a TGFβ family signaling pathway and a Hox gene. Development. 126: 5819–5831.

115. Jayanthi, L.D., S. Apparsundaram, M.D. Malone, E. Ward, D.M. Miller, M. Eppler, and R.D. Blakely. 1998. The Caenorhabditis elegans gene T23G5.5 encodes an antidepressant- and cocaine-sensitive dopamine transporter. Mol. Pharmacol. 54: 601–609.

116. Hills, T., P.J. Brockie, and A. V. Maricq. 2004. Dopamine and Glutamate Control Area-Restricted Search Behavior in Caenorhabditis elegans. J. Neurosci. 24: 1217–1225.

117. Li, Y., L. Tiedemann, J. Von Frieling, S. Nolte, S. El-Kholy, F. Stephano, C. Gelhaus, I. Bruchhaus, C. Fink, and T. Roeder. 2017. The role of monoaminergic neurotransmission for metabolic control in the fruit fly drosophila melanogaster. Front. Syst. Neurosci. 11: 1–10.

118. Strome, S. 1986. Fluorescence visualization of the distribution of microfilaments in gonads and early embryos of the nematode caenorhabditis elegans. J. Cell Biol. 103: 2241–2252.

119. Sellegounder, D., C.H. Yuan, P. Wibisono, Y. Liu, and J. Sun. 2018. Octopaminergic signaling mediates neural regulation of innate immunity in caenorhabditis elegans. MBio. 9.

120. Zheng, S., H. Chiu, J. Boudreau, T. Papanicolaou, W. Bendena, and I. Chin-Sang. 2018. A functional study of all 40 Caenorhabditis elegans insulin-like peptides. J. Biol. Chem. 293: 16912–16922.

121. Li, C., and K. Kim. 2014. Family of FLP peptides in caenorhabditis elegans and related nematodes. Front. Endocrinol. (Lausanne). 5: 1–16.

122. Li, C. 2005. The ever-expanding neuropeptide gene families in the nematode Caenorhabditis elegans. Parasitology. 131.

123. Frooninckx, L., L. Van Rompay, L. Temmerman, E. Van Sinay, I. Beets, T. Janssen, S.J. Husson, and L. Schoofs. 2012. Neuropeptide GPCRs in C. Elegans. Front. Endocrinol. (Lausanne). 3: 1–18.

124. Taylor, S.R., G. Santpere, A. Weinreb, A. Barrett, M.B. Reilly, C. Xu, E. Varol, P. Oikonomou, L. Glenwinkel, R. McWhirter, A. Poff, M. Basavaraju, I. Rafi, E. Yemini, S.J. Cook, A. Abrams, B. Vidal, C. Cros, S. Tavazoie, N. Sestan, M. Hammarlund, O. Hobert, and D.M. Miller. 2021. Molecular topography of an entire nervous system. Cell. 184: 4329-4347.e23.

125. Husson, S.J., T. Janssen, G. Baggerman, B. Bogert, A.H. Kahn-Kirby, K. Ashrafi, and L. Schoofs. 2007. Impaired processing of FLP and NLP peptides in carboxypeptidase E (EGL-21)-deficient Caenorhabditis elegans as analyzed by mass spectrometry. J. Neurochem. 102: 246–260.

126. Isaac, R.E., N.D. Bland, and A.D. Shirras. 2009. Neuropeptidases and the metabolic inactivation of insect neuropeptides. Gen. Comp. Endocrinol. 162: 8–17.

127. Yamada, K., T. Hirotsu, M. Matsuki, R.A. Butcher, M. Tomioka, T. Ishihara, J. Clardy, H. Kunitomo, and Y. Iino. 2010. Olfactory plasticity is regulated by pheromonal signaling in Caenorhabditis elegans. Science (80-.). 329: 1647–1650.

128. Nathoo, A.N., R.A. Moeller, B.A. Westlund, and A.C. Hart. 2001. Identification of neuropeptide-like protein gene families in Caenorhabditis elegans and other species. Proc. Natl. Acad. Sci. U. S. A. 98: 14000–14005.

129. Papaioannou, S., L. Holden-Dye, and R.J. Walker. 2008. The actions of Caenorhabditis elegans neuropeptide-like peptides (Nlps) on body wall muscle of Ascaris suum and pharyngeal muscle of C. elegans. Acta Biol. Hung. 59: 189–197.

130. Cheong, M.C., A.B. Artyukhin, Y.J. You, and L. Avery. 2015. An opioid-like system regulating feeding behavior in C. elegans. Elife. 4: 1–19.

131. Bhattacharya, R., D. Touroutine, B. Barbagallo, J. Climer, C.M. Lambert, C.M. Clark, M.J. Alkema, and M.M. Francis. 2014. A Conserved Dopamine-Cholecystokinin Signaling Pathway Shapes Context–Dependent Caenorhabditis elegans Behavior. PLoS Genet. 10.

132. Makino, M., E. Ulzii, R. Shirasaki, J. Kim, and Y.-J. You. 2021. Regulation of Satiety Quiescence by Neuropeptide Signaling in Caenorhabditis elegans. Front. Neurosci. 15: 1–11.

133. Kamath, R.S., and J. Ahringer. 2003. Genome-wide RNAi screening in Caenorhabditis elegans. Methods. 30: 313–321.

134. Rechavi, O., L. Houri-Ze'Evi, S. Anava, W.S.S. Goh, S.Y. Kerk, G.J. Hannon, and O. Hobert. 2014. Starvation-induced transgenerational inheritance of small RNAs in C. elegans. Cell. 158: 277–287.

135. Celniker, S.E., L.A.L. Dillon, M.B. Gerstein, K.C. Gunsalus, S. Henikoff, G.H. Karpen, M. Kellis, E.C. Lai, J.D. Lieb, D.M. MacAlpine, G. Micklem, F. Piano, M. Snyder, L. Stein, K.P. White, and R.H. Waterston. 2009. Unlocking the secrets of the genome. Nature. 459: 927–930.

136. Contrino, S., R.N. Smith, D. Butano, A. Carr, F. Hu, R. Lyne, K. Rutherford, A. Kalderimis, J. Sullivan, S. Carbon, E.T. Kephart, P. Lloyd, E.O. Stinson, N.L. Washington, M.D. Perry, P. Ruzanov, Z. Zha, S.E. Lewis, L.D. Stein, and G. Micklem. 2012. modMine: Flexible access to modENCODE data. Nucleic Acids Res. 40: 1082–1088.

137. Witvliet, D., B. Mulcahy, J.K. Mitchell, Y. Meirovitch, D.R. Berger, Y. Wu, Y. Liu, W.X. Koh, R. Parvathala, D. Holmyard, R.L. Schalek, N. Shavit, A.D. Chisholm, J.W. Lichtman, A.D.T. Samuel, and M. Zhen. 2021. Connectomes across development reveal principles of brain maturation. Nature. 596.

138. Holdorf, A.D., D.P. Higgns, A.C. Hart, P.R. Boag, G.J. Pazour, A.J.M. Walhout, and A.K. Walker. 2020. WormCat: An Online Tool for Annotation and Visualization of Caenorhabditis elegans Genome-Scale Data. Genetics. 214: 279–294.

139. Harris, T.W., V. Arnaboldi, S. Cain, J. Chan, W.J. Chen, J. Cho, P. Davis, S. Gao, C.A. Grove, R. Kishore, R.Y.N. Lee, H.M. Muller, C. Nakamura, P. Nuin, M. Paulini, D. Raciti, F.H. Rodgers, M. Russell, G. Schindelman, K. V. Auken, Q. Wang, G. Williams, A.J. Wright, K. Yook, K.L. Howe, T. Schedl, L. Stein, and P.W. Sternberg. 2020. WormBase: A modern Model Organism Information Resource. Nucleic Acids Res. 48: D762–D767.

140. Szklarczyk, D., A.L. Gable, D. Lyon, A. Junge, S. Wyder, J. Huerta-Cepas, M. Simonovic, N.T. Doncheva, J.H. Morris, P. Bork, L.J. Jensen, and C. von Mering. 2019. STRING v11: protein–protein association networks with increased coverage, supporting functional discovery in genome-wide experimental datasets. Nucleic Acids Res. 47: D607–D613.

141. Meisel, J.D., O. Panda, P. Mahanti, F.C. Schroeder, and D.H. Kim. 2014. Chemosensation of bacterial secondary metabolites modulates neuroendocrine signaling and behavior of C. elegans. Cell. 159: 267–280.

142. Janssen, T., E. Meelkop, M. Lindemans, K. Verstraelen, S.J. Husson, L. Temmerman, R.J. Nachman, and L. Schoofs. 2008. Discovery of a cholecystokinin-gastrin-like signaling system in nematodes. Endocrinology. 149: 2826–2839.

143. Chen, Z., M. Hendricks, A. Cornils, W. Maier, J. Alcedo, and Y. Zhang. 2013. Two Insulin-like Peptides Antagonistically Regulate Aversive Olfactory Learning in C. elegans. Neuron. 77: 572–585.

144. Li, W., S.G. Kennedy, and G. Ruvkun. 2003. daf-28 encodes a C. elegans insulin superfamily member that is regulated by environmental cues and acts in the DAF-2 signaling pathway. Genes Dev. 17: 844–858.

145. Pierce, S.B., M. Costa, R. Wisotzkey, S. Devadhar, S.A. Homburger, A.R. Buchman, K.C. Ferguson, J. Heller, D.M. Platt, A.A. Pasquinelli, L.X. Liu, S.K. Doberstein, and G. Ruvkun. 2001. Regulation of DAF-2 receptor signaling by human insulin and ins-1, a member of the unusually large and diverse C. elegans insulin gene family. Genes Dev. 15: 672–686.

146. Wu, T., F. Duan, W. Yang, H. Liu, A. Caballero, D.A. Fernandes de Abreu, A.R. Dar, J. Alcedo, Q.L. Ch'ng, R.A. Butcher, and Y. Zhang. 2019. Pheromones Modulate Learning by Regulating the Balanced Signals of Two Insulin-like Peptides. Neuron. 104: 1095-1109.e5.

147. Kodama, E., A. Kuhara, A. Mohri-Shiomi, K.D. Kimura, M. Okumura, M. Tomioka, Y. Iino, and I. Mori. 2006. Insulin-like signaling and the neural circuit for integrative behavior in C. elegans. Genes Dev. 20: 2955–2960.

148. Oliveira, R.P., J.P. Abate, K. Dilks, J. Landis, J. Ashraf, C.T. Murphy, and T.K. Blackwell. 2009. Condition-adapted stress and longevity gene regulation by Caenorhabditis elegans SKN-1/Nrf. Aging Cell. 8: 524–541.

149. Kim, K., and C. Li. 2004. Expression and regulation of an FMRFamide-related neuropeptide gene family in Caenorhabditis elegans. J. Comp. Neurol. 475: 540–550.

150. Janssen, T., S.J. Husson, E. Meelkop, L. Temmerman, M. Lindemans, K. Verstraelen, S. Rademakers, I. Mertens, M. Nitabach, G. Jansen, and L. Schoofs. 2009. Discovery and characterization of a conserved pigment dispersing factor-like neuropeptide pathway in Caenorhabditis elegans. J. Neurochem. 111: 228–241.

151. Zhao, T., Y. Hao, and J.M. Kaplan. 2018. Axonal mitochondria modulate neuropeptide secretion through the hypoxic stress response in Caenorhabditis elegans. Genetics. 210: 275–285.

152. Simmer, F., M. Tijsterman, S. Parrish, S.P. Koushika, M.L. Nonet, A. Fire, J. Ahringer, and R.H.A. Plasterk. 2002. Loss of the putative RNA-directed RNA polymerase RRF-3 makes C. Elegans hypersensitive to RNAi. Curr. Biol. 12: 1317–1319.

153. Cermak, N., S.K. Yu, R. Clark, Y.C. Huang, S.N. Baskoylu, and S.W. Flavell. 2020. Whole-organism behavioral profiling reveals a role for dopamine in state-dependent motor program coupling in C. elegans. Elife. 9: 1–34.

154. Zou, W., J. Fu, H. Zhang, K. Du, W. Huang, J. Yu, S. Li, Y. Fan, H.A. Baylis, S. Gao, R. Xiao, W. Ji, L. Kang, and T. Xu. 2018. Decoding the intensity of sensory input by two glutamate receptors in one C. elegans interneuron. Nat. Commun. 9: 1–12.

155. Ghosh, D.D., T. Sanders, S. Hong, L.Y. McCurdy, D.L. Chase, N. Cohen, M.R. Koelle, and M.N. Nitabach. 2016. Neural Architecture of Hunger-Dependent Multisensory Decision Making in C. elegans. Neuron. 92: 1049–1062.

156. Harris, G., H. Mills, R. Wragg, V. Hapiak, M. Castelletto, A. Korchnak, and R.W. Komuniecki. 2010. The monoaminergic modulation of sensory-mediated aversive responses in Caenorhabditis elegans requires glutamatergic/peptidergic cotransmission. J. Neurosci. 30: 7889–7899.

157. Bayer, E.A., and O. Hobert. 2018. Past experience shapes sexually dimorphic neuronal wiring through monoaminergic signalling. Nature. 561: 117–138.

158. Klapper, M., M. Ehmke, D. Palgunow, M. Böhme, C. Matthäus, G. Bergner, B. Dietzek, J. Popp, and F. Döring. 2011. Fluorescence-based fixative and vital staining of lipid droplets in Caenorhabditis elegans reveal fat stores using microscopy and flow cytometry approaches. J. Lipid Res. 52: 1281–1293.

159. Sulston, J.E., and J.G. White. 1980. Regulation and cell autonomy during postembryonic development of Caenorhabditis elegans. Dev. Biol. 78: 577–597.

160. Nguyen, C.Q., D.H. Hall, Y. Yang, and D.H.A. Fitch. 1999. Morphogenesis of the Caenorhabditis

elegans male tail tip. Dev. Biol. 207: 86–106.

161. Tekieli, T., E. Yemini, A. Nejatbakhsh, E. Varol, R.W. Fernandez, N. Masoudi, L. Paninski, and O. Hobert. 2021. Visualizing the organization and differentiation of the male-specific nervous system of C. elegans. bioRxiv. : 2021.04.06.438718.

162. Yemini, E., A. Lin, A. Nejatbakhsh, E. Varol, R. Sun, G.E. Mena, A.D.T. Samuel, L. Paninski, V. Venkatachalam, and O. Hobert. 2020. NeuroPAL: A Multicolor Atlas for Whole-Brain Neuronal Identification in C. elegans. Cell. 184: 272–288.

163. Wexler, L.R., R.M. Miller, and D.S. Portman. 2020. C. elegans Males Integrate Food Signals and Biological Sex to Modulate State-Dependent Chemosensation and Behavioral Prioritization. Curr. Biol. 30: 2695-2706.e4.

164. Barr, M.M., and L.R. Garcia. 2006. Male mating behavior. Wormb. Online Rev. C. elegans Biol. .

165. Haspel, G., M.J. O'Donovan, and A.C. Hart. 2010. Motoneurons dedicated to either forward or backward locomotion in the nematode Caenorhabditis elegans. J. Neurosci. 30: 11151–11156.

166. Hishida, R., T. Ishihara, K. Kondo, and I. Katsura. 1996. hch-1, a gene required for normal hatching and normal migration of a neuroblast in C.elegans, encodes a protein related to TOLLOID and BMP-1. EMBO J. 15: 4111–4122.

167. Pellegrino, M.W., A.M. Nargund, N. V. Kirienko, R. Gillis, C.J. Fiorese, and C.M. Haynes. 2014. Mitochondrial UPR-regulated innate immunity provides resistance to pathogen infection. Nature. 516: 414–417.

168. Papp, D., P. Csermely, and C. Soti. 2012. A role for SKN-1/Nrf in pathogen resistance and immunosenescence in caenorhabditis elegans. PLoS Pathog. 8.

169. Tian, Y., G. Garcia, Q. Bian, K.K. Steffen, L. Joe, S. Wolff, B.J. Meyer, and A. Dillin. 2016. Mitochondrial Stress Induces Chromatin Reorganization to Promote Longevity and UPRmt. Cell. 165: 1197–1208.

170. Yemini, E., T. Jucikas, L.J. Grundy, A.E.X. Brown, and W.R. Schafer. 2013. A database of Caenorhabditis elegans behavioral phenotypes. Nat. Methods. 10: 877–879.

171. Xiao, R., L. Chun, E.A. Ronan, D.I. Friedman, J. Liu, and X.Z. Shawn Xu. 2015. RNAi Interrogation of Dietary Modulation of Development, Metabolism, Behavior, and Aging in C.elegans. Cell Rep. 11: 1123–1133.

172. Russell, J., A.G. Vidal-Gadea, A. Makay, C. Lanam, and J.T. Pierce-Shimomura. 2014. Humidity sensation requires both mechanosensory and thermosensory pathways in Caenorhabditis elegans. Proc. Natl. Acad. Sci. U. S. A. 111: 8269–8274.

173. Goya, M.E., A. Romanowski, C.S. Caldart, C.Y. Bénard, and D.A. Golombek. 2016. Circadian rhythms identified in Caenorhabditis elegans by in vivo long-term monitoring of a bioluminescent reporter. Proc. Natl. Acad. Sci. U. S. A. 113: E7837–E7845.

174. Sandhu, A., D. Badal, R. Sheokand, S. Tyagi, and V. Singh. 2021. Specific collagens maintain the cuticle permeability barrier in Caenorhabditis elegans. Genetics. 217.

175. Sapio, M.R., M.A. Hilliard, M. Cermola, R. Favre, and P. Bazzicalupo. 2005. The Zona Pellucida domain containing proteins, CUT-1, CUT-3 and CUT-5, play essential roles in the development of the larval alae in Caenorhabditis elegans. Dev. Biol. 282: 231–245.

176. Tao, J., Q.Y. Wu, Y.C. Ma, Y.L. Chen, and C.G. Zou. 2017. Antioxidant response is a protective mechanism against nutrient deprivation in C. Elegans. Sci. Rep. 7: 1–8.

177. Bolz, D.D., J.L. Tenor, and A. Aballay. 2010. A conserved PMK-1/p38 MAPK is required in Caenorhabditis elegans tissue-specific immune response to Yersinia pestis infection. J. Biol. Chem. 285: 10832–10840.

178. Troemel, E.R., S.W. Chu, V. Reinke, S.S. Lee, F.M. Ausubel, and D.H. Kim. 2006. p38 MAPK regulates expression of immune response genes and contributes to longevity in C. elegans. PLoS Genet. 2: 1725–1739.

179. Block, D.H.S., K. Twumasi-Boateng, H.S. Kang, J.A. Carlisle, A. Hanganu, T.Y.J. Lai, and M. Shapira. 2015. The Developmental Intestinal Regulator ELT-2 Controls p38-Dependent Immune Responses in Adult C. elegans. PLoS Genet. 11: 1–19.

180. Bakowski, M.A., C.A. Desjardins, M.G. Smelkinson, T.A. Dunbar, I.F. Lopez-Moyado, S.A. Rifkin, C.A. Cuomo, and E.R. Troemel. 2014. Ubiquitin-Mediated Response to Microsporidia and Virus Infection in C. elegans. PLoS Pathog. 10.

181. Haskins, K.A., J.F. Russell, N. Gaddis, H.K. Dressman, and A. Aballay. 2008. Unfolded Protein Response Genes Regulated by CED-1 Are Required for Caenorhabditis elegans Innate Immunity. Dev. Cell. 15: 87–97.

182. Kipreos, E.T., and M. Pagano. 2000. The F-box protein family. Genome Biol. 1: 1–7.

183. Thomas, J.H. 2006. Adaptive evolution in two large families of ubiquitin-ligase adapters in nematodes and plants. Genome Res. 16: 1017–1030.

184. Panek, J., S.S. Gang, K.C. Reddy, R.J. Luallen, A. Fulzele, E.J. Bennett, and E.R. Troemel. 2020. A cullin-RING ubiquitin ligase promotes thermotolerance as part of the intracellular pathogen response in Caenorhabditis elegans. Proc. Natl. Acad. Sci. U. S. A. 117: 7950–7960.

185. Lažetić, V., and E.R. Troemel. 2020. Conservation lost: host-pathogen battles drive diversification and expansion of gene families. FEBS J. 12: 1–11.

186. Sun, Y., Z. Hu, Y. Goeb, and L. Dreier. 2013. The F-Box Protein MEC-15 (FBXW9) Promotes Synaptic Transmission in GABAergic Motor Neurons in C. elegans. PLoS One. 8.

187. Wu, C.W., Y. Wang, and K.P. Choe. 2017. F-box protein XREP-4 is a new regulator of the oxidative stress response in Caenorhabditis elegans. Genetics. 206: 859–871.

188. Aarnio, V., L. Heikkinen, J. Peltonen, G. Goldsteins, M. Lakso, and G. Wong. 2014. Transcriptional profiling reveals differential expression of a neuropeptide-like protein and pseudogenes in aryl hydrocarbon receptor-1 mutant Caenorhabditis elegans. Comp. Biochem. Physiol. - Part D Genomics Proteomics. 9: 40–48.

189. Köhle, C., and K.W. Bock. 2007. Coordinate regulation of Phase I and II xenobiotic metabolisms by the Ah receptor and Nrf2. Biochem. Pharmacol. 73: 1853–1862.

190. Qin, H., Z. Zhai, and J.A. Powell-Coffman. 2006. The Caenorhabditis elegans AHR-1 transcription complex controls expression of soluble guanylate cyclase genes in the URX neurons and regulates aggregation behavior. Dev. Biol. 298: 606–615.

191. Aarnio, V., M. Storvik, M. Lehtonen, S. Asikainen, K. Reisner, J. Callaway, M. Rudgalvyte, M. Lakso, and G. Wong. 2010. Fatty acid composition and gene expression profiles are altered in aryl hydrocarbon receptor-1 mutant Caenorhabditis elegans. Comp. Biochem. Physiol. - C Toxicol. Pharmacol. 151: 318–324.

192. Kamath, R.S., A.G. Fraser, Y. Dong, G. Poulin, R. Durbin, M. Gotta, A. Kanapin, N. Le Bot, S. Moreno, M. Sohrmann, D.P. Welchman, P. Zipperien, and J. Ahringer. 2003. Systematic functional analysis of the Caenorhabditis elegans genome using RNAi. Nature. 421: 231–237.

193. Lercher, M.J., T. Blumenthal, and L.D. Hurst. 2003. Coexpression of Neighboring Genes in Caenorhabditis Elegans Is Mostly Due to Operons and Duplicate Genes. Genome Res. 13: 238–243.

194. Zhou, Z., B. Sun, S. Huang, and L. Zhao. 2019. Roles of circular RNAs in immune regulation and autoimmune diseases. Cell Death Dis. 10.

195. Cortés-López, M., M.R. Gruner, D.A. Cooper, H.N. Gruner, A.I. Voda, A.M. van der Linden, and P. Miura. 2018. Global accumulation of circRNAs during aging in Caenorhabditis elegans. BMC Genomics. 19: 1–12.

196. Blumenthal, T., P. Davis, and A. Garrido-Lecca. 2015. Operon and non-operon gene clusters in the C. elegans genome. WormBook. : 1–20.

197. Mounsey, A., P. Bauer, and I.A. Hope. 2002. Evidence suggesting that a fifth of annotated Caenorhabditis elegans genes may be pseudogenes. Genome Res. 12: 770–775.

198. Tutar, Y. 2012. Pseudogenes. Comp. Funct. Genomics. 2012: 6–9.

199. Ploumi, C., I. Daskalaki, and N. Tavernarakis. 2017. Mitochondrial biogenesis and clearance: a balancing act. FEBS J. 284: 183–195.

200. Zhu, Y.P., Z. Zheng, Y. Xiang, and Y. Zhang. 2020. Glucose Starvation-Induced Rapid Death of Nrf1 α -Deficient, but Not Nrf2-Deficient, Hepatoma Cells Results from Its Fatal Defects in the Redox Metabolism Reprogramming. Oxid. Med. Cell. Longev. 2020.

201. Bartelt, A., S.B. Widenmaier, C. Schlein, K. Johann, R.L.S. Goncalves, K. Eguchi, A.W. Fischer, G. Parlakgül, N.A. Snyder, T.B. Nguyen, O.T. Bruns, D. Franke, M.G. Bawendi, M.D. Lynes, L.O. Leiria, Y.H. Tseng, K.E. Inouye, A.P. Arruda, and G.S. Hotamisligil. 2018. Brown adipose tissue thermogenic adaptation requires Nrf1-mediated proteasomal activity. Nat. Med. 24: 292–303.

202. Wilson, M.A., W.B. Iser, T.G. Son, A. Logie, J. V. Cabral-Costa, M.P. Mattson, and S. Camandola. 2017. Skn-1 is required for interneuron sensory integration and foraging behavior in Caenorhabditis elegans. PLoS One. 12: 1–14.

203. Sykiotis, G.P., and D. Bohmann. 2010. Stress-activated cap'n'collar transcription factors in aging and human disease. Sci. Signal. 3.

Appendices

Supplementary Figures

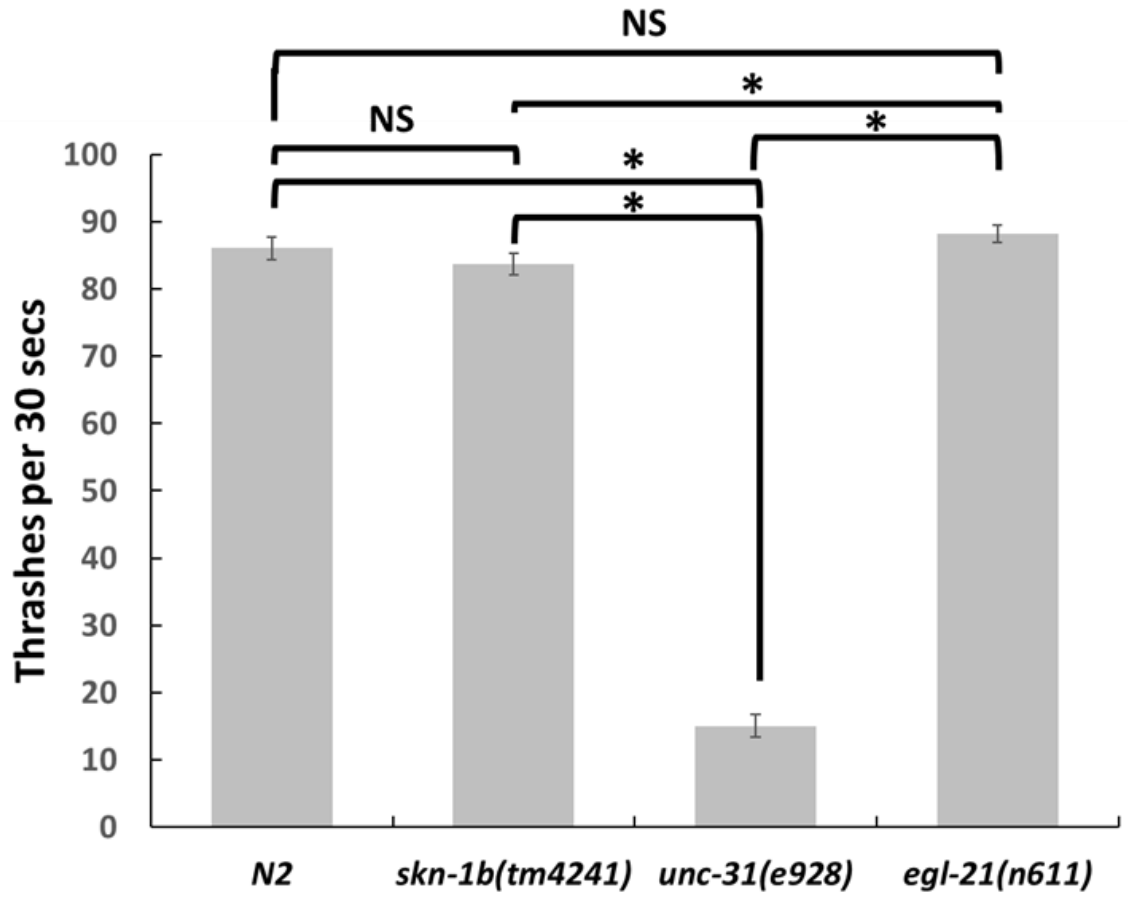

Supplementary Figure 1. The *skn-1b* mutation does not affect body wall muscle movement. Thrashing assay for 30 secs with L4 hermaphrodites. All data points are significantly different (p=<0.012) from each other except N2 compared with *skn-1b* mutants: p=0.199, and *egl-21* mutants: p=0.323. All data points are biological triplicates (12 worms for each repeat, 15 worms for N2 first repeat). Asterisk (*) represents a significant difference using Welch's t-test (p = ≤0.05); NS represents no significant difference. Error bars represent ± SEM. Exact p-values can be found in Supplementary Table 2.

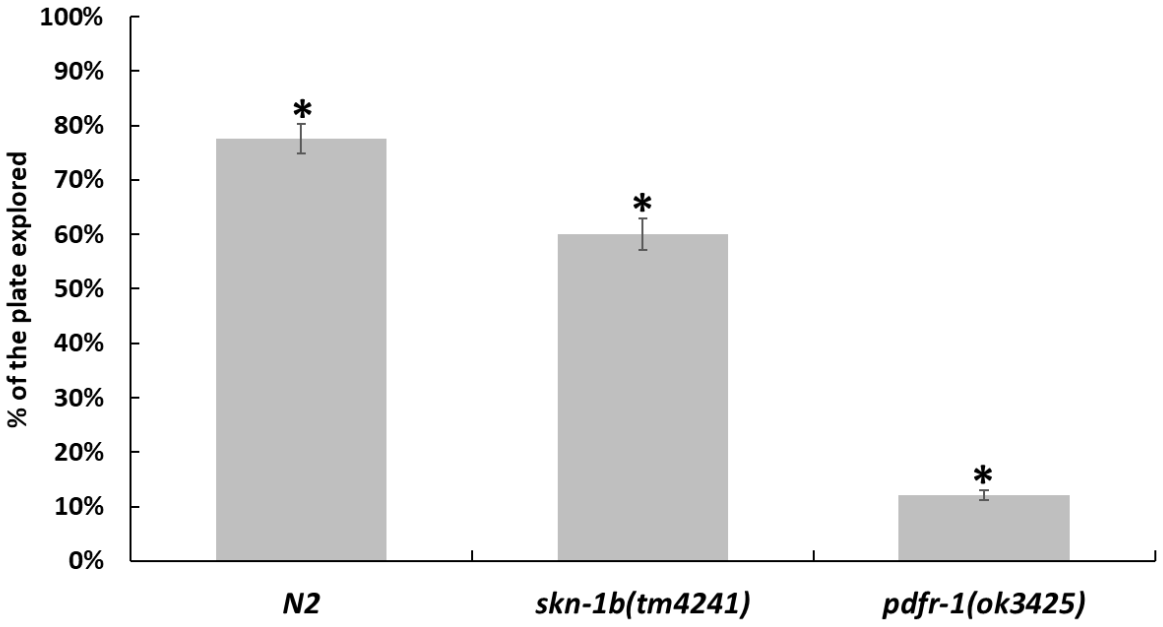

Supplementary Figure 2. *pdfr-1(ok3425)* mutants had significant reduced exploration compared to *skn-1b* mutants. 16 h exploration of L4 hermaphrodites at 25°C. All data points are significantly different (p=<0.031) from each other. Data is the average of 2 biological repeats with repeats one and two used 10 and 14 worms, respectively, for *pdfr-1* mutants. For N2, repeats one and two used 10 and 15 worms, respectively. For *skn-1b* mutants, both trials used 15 worms. Asterisk (*) represents a significant difference using Welch's t-test (p = ≤0.05). Exact p-values can be found in Supplementary Table 2. The PDF neuropeptide receptor *pdfr-1* is needed for roaming [62]. Double mutants were not made due to time constraints.

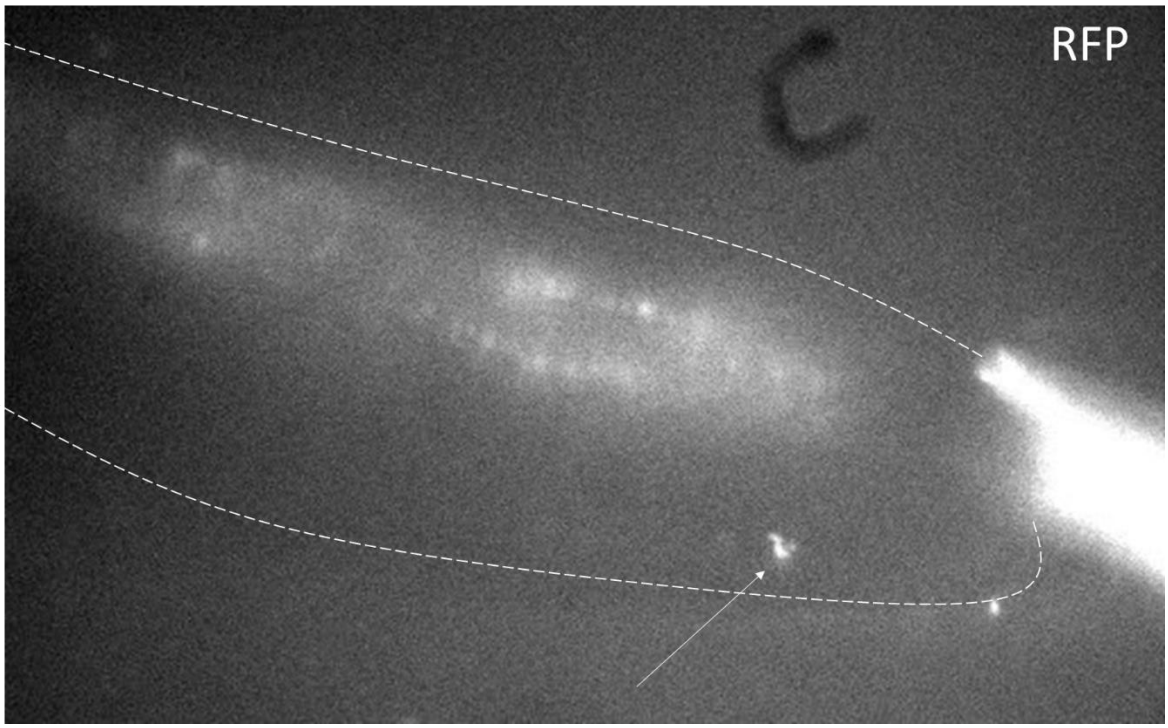

Supplementary Figure 3. In D1 males, SKN-1B is expressed near the tail using endogenous *skn-1b* reporter *knu733[skn-1b::wrmScarlet].* Arrow indicates SKN-1B::mScarlet in the RFP channel is not near the autofluorescence of the gut and spicules. Outline of the worm is represented by dashed lines. Imaged using inverted microscope Olympus IX73 with a PlanApo 100x OTIRFM-SP 1.45 NA lens. Scale could not be determined.

Supplementary Tables

Supplementary Table 1. Primers used for genotyping double mutants. All mutants have a deletion to be identified using PCR. Primer orientation key: F is forward/sense, F IN is a forward/sense sequence located in the deletion of the respective mutant and R is reverse/antisense. PCR band size key: N2 F and R and N2 F IN and R is the band size produced from N2 CGCM strain. Mutant F and R is the band size produced in the respective mutant. No F IN and R is given for mutants as there is no sequence for the primers to attach. PCR protocol is the same for all primers: 1) 94°C (1 min). 2) 94°C (30 sec). 3) 66.5°C (30 sec). 4) 72°C (40 sec). 5) GOTO step 2, 40X. 6) 72°C (7 min). 7) 12°C ∞.

Strain to be genotyped	**Primer orientation**	**Primer sequence**	**PCR band size**
GA1058 *skn-1b(tm4241)*	F	gctgattgaatggaaaacaatcata	N2 F and R: 1207 bp. N2 F IN and R: 400 bp. Mutant F and R: 913 bp.
	F IN	gcttatcctcctttatttgctctc	
	R	tctaggttaacaaccctctgc	
MT14984 *tph-1(n4622)*	F	tctccggatattagattgtgtgg	N2 F and R: 2769 bp. N2 F IN and R: 966 bp. Mutant F and R: 648 bp.
	F IN	cttatcagctcgtgatttcttgg	
	R	actggagaatcaatggtcaactc	
MT15620 *cat-2(n4547)*	F	tccttttacttccgtccgtct	N2 F and R: 1502 bp. N2 F IN and R: 1000 bp. Mutant F and R: 492 bp
	F IN	gaaggaaatgtggtgtctctcttt	
	R	ggagttctcggctactttggt	
MT9455 *tbh-1(n3247)*	F	tgaaatgagtagcttgctgtgtg	N2 F and R: 1747 bp. N2 F IN and R: 677 bp. Mutant F and R: 956 bp.
	F IN	tacgacgcaggaattatggaa	
	R	tctcggttcacgtctccaa	
MT13113 *tdc-1(n3419)*	F	tgcaacttcgttacacttttgg	N2 F and R: 1739 bp. N2 F IN and R: 638 bp. Mutant F and R: 1161 bp.
	F IN	tcactgggcgatcgtttt	
	R	aaaccgaagcaattcacagg	

Supplementary Table 2. *p*-values using Welch's t-test for Chapter 1 Figures 7 and 8. Green highlighted boxes indicate a *p*-value ≤0.05; red highlighted boxes indicate a *p*-value >0.05.

Assay	**Fig. 7A: 16 h exploration assay**		
Genotype	***N2***	***skn-1b(tm4241)***	***unc-31(e928)***
skn-1b(tm4241)	5.10788E-05		
unc-31(e928)	1.4029E-09	0.05858	
skn-1b(tm4241); unc-31(e928)	3.92109E-11	0.031266	0.988926
Assay	**Figure 7B: 16h exploration assay**		
Genotype	***N2***	***skn-1b(tm4241)***	***egl-21(n611)***
skn-1b(tm4241)	1.14977E-08		
egl-21(n611)	6.87275E-13	0.187873961	
skn-1b(tm4241); egl-21(n611)	9.55551E-23	1.01552E-09	1.41E-08
Assay	**Supplementary Figure 1: Thrashing assay (30 secs)**		
Genotype	***N2***	***skn-1b(tm4241)***	***unc-31(e928)***
skn-1b(tm4241)	0.198781213		
unc-31(e928)	2.64046E-42	7.482E-42	
egl-21(n611)	0.323040177	0.01121084	1.35726E-43
Assay	**Supplementary Figure 2. 16 h exploration assay**		
Genotype	***N2***	***skn-1b(tm4241)***	***pdfr-1(ok3425)***
skn-1b(tm4241)	3.06405E-05		
pdfr-1(ok3425)	2.97685E-27	3.84565E-21	
Assay	**Figure 8: 16 h exploration**		

Genotype	*N2*	*skn-1b(tm4241)*	*tdc-1 (n3419)*	*tdc-1(n3419); skn-1b(tm4241)*	*tbh-1 (n3247)*	*skn-1b(tm4241); tbh-1(n3247)*	*cat-2 (n4547)*	*cat-2(n4547); skn-1b(tm4241)*	*tph-1(n4622)*
skn-1b(tm4241)	6.40303E-08								
tdc-1 (n3419)	3.73348E-09	0.844193257							
tdc-1(n3419); skn-1b(tm4241)	1.30763E-07	0.991273189	0.858055715						
tbh-1 (n3247)	0.881158669	9.81808E-09	3.04025E-10	2.40489E-08					
skn-1b(tm4241); tbh-1(n3247)	2.18387E-08	0.802578777	0.943803668	0.816298972	3.18007E-09				
cat-2 (n4547)	0.682514985	2.56647E-09	6.09209E-11	6.84653E-09	0.783550716	8.22344E-10			
cat-2(n4547); skn-1b(tm4241)	0.000685118	0.197643414	0.133160187	0.202899148	0.000326029	0.135729797	0.000154038		
tph-1(n4622)	3.02902E-08	6.75241E-20	1.34594E-23	8.05601E-19	5.36611E-09	3.51295E-20	1.28355E-08	1.11351E-11	
tph-1(n4622); skn-1b(tm4241)	0.095133236	0.008444597	0.004298814	0.009235314	0.069501226	0.004962171	0.045752034	0.18060683	2.40964E-07

Supplementary Table 3: RNA-Seq log2 fold changes of gene expression in *skn-1b(tm4241)* mutants compared to N2. RNA-Seq analysis (processing and expression change) performed by Isabel Gonçalves Silva. 22 genes not tested with RNAi. **dve-1* RNAi was tested, but no exploration was measured due to developmental defects.

Gene ID	Gene Name	Log2 fold change	*p*-value	Tested with RNAi?
WBGene00010212	*fbxa-192*	1.8	1.26E-16	Y
WBGene00010209	*fbxa-191*	1.3	9.25E-07	Y
WBGene00044213	*Y102A5C.36*	1.3	1.35E-06	N
WBGene00014955	*Y102A5C.6*	1.3	5.30E-05	N
WBGene00020859	*bath-25*	1.3	0.022063	Y
WBGene00021338	*Y34F4.3*	1.2	0.022063	N
WBGene00021055	*W06A11.4*	1.1	1.06E-05	N
WBGene00014954	*Y102A5C.5*	1.1	0.001645	N
WBGene00015456	*C04G6.6*	0.9	5.61E-04	Y
WBGene00017726	*F22H10.2*	0.9	0.02118	Y
WBGene00008998	*ncs-4*	0.9	0.047029	Y
WBGene00001758	*gst-10*	0.8	0.005279	N
WBGene00010295	*fbxa-193*	0.8	0.009804	Y
WBGene00015236	*B0511.11*	0.8	0.022063	Y
WBGene00020408	*T10D4.6*	0.7	0.001557	Y
WBGene00011498	*T05G5.1*	0.7	0.033058	Y
WBGene00022564	*ZC204.14*	0.6	0.009804	Y
WBGene00010128	*F55G11.8*	-0.7	6.82E-04	Y
WBGene00022861	*dve-1*	-0.7	0.022362	Y*
WBGene00000298	*cat-4*	-0.8	8.72E-04	N
WBGene00010123	*F55G11.2*	-0.8	0.009804	Y
WBGene00006365	*syg-1*	-0.8	0.017596	Y
WBGene00006321	*sup-12*	-0.8	0.034489	Y
WBGene00007193	*B0491.6*	-0.9	2.20E-13	Y
WBGene00017576	*cdh-8*	-0.9	0.013536	Y
WBGene00001123	*dyf-7*	-1	0.009804	N
WBGene00010189	*F57B1.6*	-1	0.041687	N
WBGene00018335	*F42A9.6*	-1.1	3.08E-11	Y
WBGene00009304	*eva-1*	-1.1	0.011529	Y
WBGene00018304	*agr-1*	-1.1	0.015114	Y
WBGene00001824	*hbl-1*	-1.1	0.022063	Y
WBGene00004048	*plx-2*	-1.1	0.022362	N
WBGene00022396	*Y97E10AR.1*	-1.1	0.039968	N
WBGene00004233	*ptr-19*	-1.1	0.041687	Y
WBGene00000853	*cut-6*	-1.2	0.013536	Y
WBGene00010039	*F54C8.6*	-1.2	0.017596	Y
WBGene00008760	*F13E9.11*	-1.2	0.0185	N
WBGene00002983	*lgx-1*	-1.2	0.022063	Y
WBGene00006666	*twk-11*	-1.2	0.034489	N
WBGene00021805	*Y53G8AM.5*	-1.2	0.039968	N

WBGene00011508	*T05H10.3*	-1.2	0.041687	Y
WBGene00021525	*Y41D4B.26*	-1.2	0.045629	N
WBGene00044024	*C35A5.11*	-1.2	0.049026	Y
WBGene00007229	*C01G6.9*	-1.3	0.003695	Y
WBGene00011175	*R09E10.5*	-1.3	0.008834	Y
WBGene00010830	*M02G9.1*	-1.3	0.011479	Y
WBGene00001828	*hch-1*	-1.3	0.011659	Y
WBGene00006538	*tbb-4*	-1.3	0.012644	Y
WBGene00007800	*C29A12.6*	-1.3	0.019417	Y
WBGene00020626	*T20F5.4*	-1.3	0.02118	Y
WBGene00019906	*R05G9R.1*	-1.4	0.001645	Y
WBGene00006643	*tsp-17*	-1.4	0.003521	Y
WBGene00011345	*dma-1*	-1.4	0.005924	Y
WBGene00001858	*hil-7*	-1.4	0.007341	Y
WBGene00009041	*cut-3*	-1.4	0.007341	Y
WBGene00004155	*pqn-73*	-1.5	0.001913	Y
WBGene00011104	*cut-5*	-1.6	6.17E-04	Y
WBGene00019704	*fbxb-40*	-1.7	2.70E-05	Y
WBGene00018452	*F45D11.5*	-1.7	2.84E-05	N
WBGene00019699	*math-34*	-1.8	8.91E-06	N
WBGene00018456	*fbxc-39*	-2	3.46E-07	N
WBGene00009008	*F21D5.3*	-2.1	9.84E-18	Y
WBGene00018448	*F45D11.1*	-2.2	8.85E-09	N
WBGene00019703	*fbxb-41*	-2.3	2.81E-09	Y
WBGene00019705	*fbxb-45*	-2.4	4.28E-11	N
WBGene00019700	*btb-11*	-2.5	3.08E-11	Y
WBGene00019619	*asp-14*	-2.7	0	Y
WBGene00016295	*fbxc-40*	-3.6	3.91E-28	N
WBGene00018455	*fbxc-42*	-4.5	4.81E-48	N

Supplementary Table 4. Expression of *skn-1b(tm4241)* differentially expressed genes in non-neuronal cells. 68 of 69 genes were analysed (*F45D11.5* not detected by CeNGEN) using 'All cells unfiltered' data. Glia were grouped into 10 categories (AMsh, AMso, CEPsh, Glia_1-5, PMsh and PMso), muscle into 5 categories (anal, body wall, body wall anterior, pharyngeal and vulval) and intestine in 1 category. Y denotes gene expression; N denotes no expression. Genes were separated into 3 groups: 42 genes expressed in neurons (grey); 15 genes not expressed in neurons (green) and 11 genes not expressed in neurons and only detected in the 'All cells unfiltered' data set (blue). The latter set means that the genes in green were registered by CeNGEN in neurons, but with expression of 0 (see Methods: Bioinformatics for more detail), whereas the genes in blue were not registered.

Gene	Glia	Muscle	Intestine	Gene	Glia	Muscle	Intestine
agr-1	Y	Y	Y	*asp-14*	Y	N	Y
B0491.6	Y	Y	Y	*bath-25*	N	N	N
B0511.11	N	Y	Y	*C01G6.9*	Y	Y	N
C04G6.6	N	Y	Y	*C29A12.6*	Y	N	N
C35A5.11	Y	Y	N	*cut-6*	Y	Y	N
cat-4	Y	Y	Y	*F21D5.3*	N	Y	Y
cdh-8	Y	Y	N	*F55G11.8*	N	N	Y
cut-3	N	Y	N	*fbxa-191*	N	N	N
cut-5	Y	N	N	*fbxb-45*	N	N	N
dma-1	Y	Y	N	*R05G9R.1*	Y	N	N
dve-1	Y	Y	Y	*R09E10.5*	N	N	N
dyf-7	Y	Y	Y	*T05H10.3*	N	Y	N
eva-1	Y	Y	Y	*Y102A5C.36*	N	Y	Y
F13E9.11	Y	Y	Y	*Y102A5C.6*	N	Y	N
F22H10.2	N	Y	Y	*Y53G8AM.5*	N	N	N
F42A9.6	Y	Y	Y	*btb-11*	N	N	N
F54C8.6	Y	Y	N	*F45D11.1*	Y	N	N
F57B1.6	N	N	N	*F55G11.2*	N	N	Y
fbxa-192	Y	Y	N	*fbxb-40*	N	N	N
fbxa-193	Y	N	N	*fbxb-41*	Y	N	N
gst-10	Y	Y	Y	*fbxc-39*	N	N	N
hbl-1	Y	Y	Y	*fbxc-40*	Y	Y	N
hil-7	Y	Y	Y	*fbxc-42*	N	N	N
lgx-1	Y	Y	N	*hch-1*	N	N	N
M02G9.1	Y	Y	N	*math-34*	N	N	Y
ncs-4	N	Y	N	*ptr-19*	Y	N	N
plx-2	Y	Y	Y				
pqn-73	N	Y	N				
sup-12	Y	Y	Y				
syg-1	Y	Y	Y				
T05G5.1	Y	Y	Y				
T10D4.6	Y	Y	N				
T20F5.4	Y	Y	Y				
tbb-4	Y	Y	Y				
tsp-17	N	Y	N				
twk-11	N	Y	N				
W06A11.4	Y	Y	N				
Y102A5C.5	N	N	N				
Y34F4.3	N	N	N				
Y41D4B.26	Y	Y	N				
Y97E10AR.1	Y	Y	Y				
ZC204.14	Y	Y	Y				

Supplementary Table 5. RNAi screen from 37 genes P values and raw data for Fig. 18. 'Expression' shows the log2fold expression of the gene in *skn-1b* mutants compared to N2. 'Genotype and RNAi gene' shows the genotype of the worm used first: N2 or *skn-1b* mutants followed by the gene that RNAi was performed on e.g. *F55G11.8*. 'vs own control' shows Welch's t-test used to understand if any significant difference between the genotype and its own genotype control has occurred e.g. N2 *F55G11.8* has N2 as its genotype, so the following control it was compared to would be N2 EV, whereas 'vs opposite control' would use *skn-1b* mutants EV for its comparison. *p*-values >0.05 are labelled as red representing not statistically significant, whereas *p*-values ≤0.05 are labelled green to represent statistical significance. Red highlighting indicates no significant difference between either N2 or *skn-1b* EV control. Orange highlighting indicates no significant difference between own control, but a significant difference between the opposite control. Green highlighting indicates significant difference between both EV controls. Blue highlighting indicates significant difference between own control, but no significant difference between opposite control.

Expression (log2fold)	Genotype and RNAi gene	Average exploration	SEM	vs own control	vs opposite control
-0.7	N2 *F55G11.8*	0.75	0.08	0.649987609	0.051847149
-0.7	*skn-1b(tm4241) F55G11.8*	0.56	0.11	0.796348409	0.097037378
-0.8	*skn-1b(tm4241) sup-12*	0.63	0.09	0.320033309	0.132150718
-0.9	N2 *B0491.6*	0.73	0.15	0.697136753	0.244987447
-1.1	N2 *F42A9.6*	0.72	0.12	0.571629792	0.180512136
-1.1	N2 *hbl-1*	0.69	0.10	0.346386731	0.186058471
-1.2	*skn-1b(tm4241) C35A5.11*	0.59	0.11	0.622344568	0.116746112
-1.3	*skn-1b(tm4241) R09E10.5*	0.73	0.09	0.076238539	0.520757901
-1.3	*skn-1b(tm4241) hch-1*	0.60	0.09	0.477873359	0.096892064
-1.3	*skn-1b(tm4241) tbb-4*	0.63	0.10	0.393069155	0.195177986
-1.3	*skn-1b(tm4241) C29A12.6*	0.73	0.08	0.05935115	0.473281995
-1.3	*skn-1b(tm4241) T20F5.4*	0.73	0.08	0.051895562	0.472634014
-1.4	*skn-1b(tm4241) tsp-17*	0.69	0.08	0.117098297	0.279723433
-1.4	*skn-1b(tm4241) dma-1*	0.72	0.12	0.181773062	0.585532713
-1.5	*skn-1b(tm4241) pqn-73*	0.56	0.11	0.768839495	0.09404872
-1.6	*skn-1b(tm4241) cut-5*	0.63	0.06	0.223609587	0.050986406
-1.7	*skn-1b(tm4241) fbxb-40*	0.59	0.12	0.619981267	0.165508053
-2.1	*skn-1b(tm4241) F21D5.3*	0.70	0.13	0.254569164	0.485837812
-2.3	*skn-1b(tm4241) fbxb-41*	0.66	0.09	0.245293093	0.198921741
0.9	N2 *C04G6.6*	0.91	0.06	0.149463741	0.001164977
0.9	*skn-1b(tm4241) C04G6.6*	0.64	0.03	0.058819023	0.007138323
0.9	N2 *F22H10.2*	0.83	0.08	0.694123976	0.010150822
0.9	*skn-1b(tm4241) F22H10.2*	0.65	0.05	0.094782821	0.029133936
0.7	N2 *TO5G5.1*	0.83	0.04	0.509944556	0.000202607
0.7	*skn-1b(tm4241) TO5G5.1*	0.58	0.05	0.421293828	0.003998021
-0.8	*skn-1b(tm4241) F55G11.2*	0.56	0.08	0.719035085	0.045957015
-0.8	N2 *syg-1*	0.88	0.06	0.236293403	0.000698376
-0.8	N2 *sup-12*	0.85	0.07	0.542788582	0.006915047
-0.9	*skn-1b(tm4241) B0491.6*	0.50	0.05	0.693942569	0.001218451
-1.3	N2 *C01G6.9*	0.88	0.05	0.19343041	0.000248898
-1.3	N2 *R09E10.5*	0.88	0.05	0.174235542	0.00014634

-1.3	N2 *M02G9.1*	0.85	0.08	0.577160751	0.009811952
-1.3	N2 *hch-1*	0.89	0.04	0.095576513	2.01059E-05
-1.4	N2 *tsp-17*	0.90	0.04	0.059597305	6.95247E-06
-1.4	*skn-1b(tm4241) hil-7*	0.32	0.10	0.125636224	0.008047917
-1.4	*skn-1b(tm4241) cut-3*	0.44	0.12	0.524040562	0.034243937
-2.3	N2 *fbxb-41*	0.90	0.06	0.187333179	0.000727489
0.6	N2 *ZC2041.1*	0.98	0.01	2.09883E-05	9.38765E-09
-0.9	N2 *cdh-8*	0.91	0.03	0.029697187	2.10186E-06
-1.1	N2 *eva-1*	0.92	0.02	0.00418933	1.43109E-07
-1.1	N2 *agr-1*	0.99	0.01	5.6974E-06	7.69431E-09
-1.1	N2 *ptr-19*	0.98	0.01	1.29525E-05	1.04382E-08
-1.2	N2 *cut-6*	0.96	0.01	0.000107164	2.01264E-08
-1.2	N2 *F54C8.6*	0.95	0.01	0.000127912	3.32964E-08
-1.2	*skn-1b(tm4241) F54C8.6*	0.91	0.01	1.42655E-07	0.002563379
-1.2	N2 lgx-1	0.92	0.03	0.008754961	4.03976E-07
-1.2	N2 *T05H10.3*	0.92	0.03	0.01004324	5.13395E-07
-1.2	N2 *C35A5.11*	0.92	0.04	0.035668334	5.96005E-06
-1.3	N2 *tbb-4*	0.95	0.02	0.000533101	3.72077E-08
-1.3	N2 *C29A12.6*	0.97	0.02	0.00014697	1.62413E-08
-1.3	N2 *T20F5.4*	0.97	0.01	5.40267E-05	1.48801E-08
-1.4	N2 *R05G9R.1*	0.93	0.02	0.002201909	9.07575E-08
-1.4	*skn-1b(tm4241) R05G9R.1*	0.63	0.01	0.049206141	6.30124E-05
-1.4	N2 *dma-1*	0.98	0.02	3.45116E-05	9.82401E-09
-1.4	N2 hil-7	0.28	0.08	0.001739606	0.035125757
-1.4	N2 *cut-3*	0.94	0.02	0.001232811	6.18688E-08
-1.5	N2 *pqn-73*	0.94	0.03	0.002277903	1.10147E-07
-1.6	N2 *cut-5*	0.95	0.01	0.000108753	2.40272E-08
-1.7	N2 *fbxb-40*	0.96	0.02	0.00017372	2.11121E-08
-2.1	N2 *F21D5.3*	0.96	0.02	0.000279785	2.35796E-08
0.6	*skn-1b(tm4241) ZC2041.1*	0.75	0.06	0.01926096	0.548383261
-0.8	*skn-1b(tm4241) syg-1*	0.72	0.04	0.005664773	0.12846713
-0.9	*skn-1b(tm4241) cdh-8*	0.79	0.07	0.015973237	0.901104543
-1.1	*skn-1b(tm4241) F42A9.6*	0.81	0.03	9.16952E-05	0.825204644
-1.1	*skn-1b(tm4241) eva-1*	0.82	0.04	0.00011728	0.641608839
-1.1	*skn-1b(tm4241) agr-1*	0.74	0.07	0.031038517	0.448602223
-1.1	*skn-1b(tm4241) hbl-1*	0.75	0.07	0.031756071	0.589836534
-1.1	*skn-1b(tm4241) ptr-19*	0.74	0.05	0.0129051	0.402264017
-1.2	*skn-1b(tm4241) cut-6*	0.83	0.09	0.021582696	0.75915781
-1.2	*skn-1b(tm4241) lgx-1*	0.81	0.07	0.008733517	0.878965045
-1.2	*skn-1b(tm4241) T05H10.3*	0.75	0.06	0.018814979	0.565476164
-1.3	*skn-1b(tm4241) C01G6.9*	0.74	0.05	0.009803085	0.379421899
-1.3	*skn-1b(tm4241) M02G9.1*	0.72	0.05	0.016364029	0.269901982